 doi:10.20944/preprints202205.0043.v1

Benefits of an integrated power and hydrogen offshore grid in a net-zero North Sea energy system

Martínez-Gordón, R[1,*]; Gusatu, L.F[1]; Morales-España, G[2]; Sijm, J[2]; Faaij, A.P.C[1,2]

[1] *Integrated Research on Energy, Environment, and Society, University of Groningen, Nijenborgh 6, 9747 AG, Groningen, the Netherlands*
[2] *TNO Energy Transition Studies, P.O. Box 37154, 1030 AD, Amsterdam, the Netherlands*

Abstract:
The North Sea Offshore Grid concept has been envisioned as a promising alternative to: 1) ease the integration of offshore wind and onshore energy systems, and 2) increase the cross-border capacity between the North Sea region countries at low cost. In this paper we explore the techno-economic benefits of the North Sea Offshore Grid using two case studies: a power-based offshore grid, where only investments in power assets are allowed (i.e. offshore wind, HVDC/HVAC interconnectors); and a power-and-hydrogen offshore grid, where investments in offshore hydrogen assets are also permitted (i.e. offshore electrolysers, new hydrogen pipelines and retrofitted natural gas pipelines). We compare these scenario results with a business as usual scenario, in which offshore wind is connected radially to the shore and no offshore grid is deployed. All scenarios are run with the IESA-NS model, without any specific technology ban and under open optimization. This paper also presents a novel methodology, combining Geographic Information Systems and Energy System Models, to cluster offshore spatial data and define meaningful offshore regions and offshore hub locations. This novel methodology is applied to the North Sea region to define nine offshore clusters taking into account offshore spatial claims, and identifying suitable areas for single-use and multi-use of space for renewable energy purposes. The scenario results show that the deployment of an offshore grid provides relevant cost savings, ranging from 1% to 4.1% of relative cost decrease (2.3 bn € to 8.7 bn €) in the power-based, and ranging from 2.8% to 7% of relative cost decrease (6 bn € to 14.9 bn €) in the power-and-hydrogen based. In the most extreme scenario (**H2**) an offshore grid permits to integrate 283 GW of HVDC connected offshore wind and 196 GW of HVDC meshed interconnectors. Even in the most conservative scenario (**P1**) the offshore grid integrates 59 GW of HVDC connected offshore wind capacity and 92 GW of HVDC meshed interconnectors. When allowed, the deployment of offshore electrolysis is considerable, ranging from 61 GW to 96 GW, with capacity factors of around 30%. Finally, we also find that, when imported hydrogen is available at 2 €/kg (including production and transport costs), large investments in an offshore grid are not optimal anymore. In contrast, at import costs over 4 €/kg imported hydrogen is not competitive.

Keywords: North Sea region, offshore grid, offshore hydrogen, offshore wind, system integration, IESA-NS
Word count: 11000

1. Introduction and knowledge gaps

The North Sea region (NSR) countries[1] have committed to drastically reduce their greenhouse gas (GHG) emissions in the following decades. In line with the Paris Agreement [1], the NSR aims to "limit the increase in the global average temperature to at least 2°C above the pre-industrial level". Some NSR countries have already set a net-zero target by 2050 in their national mitigation plans (i.e. Germany [2], Denmark [3], Sweden [4] and the United Kingdom [5]). From the European Union perspective, the European Green Deal, presented in 2020,

* Corresponding author: R.Martinez.Gordon@rug.nl
[1] NSR countries include Belgium, Denmark, Germany, the Netherlands, Norway, Sweden and the United Kingdom

Preprints (www.preprints.org) | NOT PEER-REVIEWED | Posted: 5 May 2022 doi:10.20944/preprints202205.0043.v1

proposed a 55% reduction of GHG emissions compared to 1990 by 2030, and a net-zero emission target by 2050.

Offshore wind has been identified as a key element to decarbonize the energy system of the NSR. In 2020 the cumulative installed capacity of offshore wind in the NSR reached 20 GW [6]. Different studies conclude that this installed capacity should be multiplied in order to meet the 2050 mitigation targets. To name a few, WindEurope estimates around 212 GW deployed by 2050 [7]. Ruijgrok et al. [8] rises that estimate to 180 GW of offshore wind.

However, integrating this large amount of offshore wind capacity is not straightforward. First, the North Sea region is an extremely busy area, with multiple coexisting activities (e.g. sand extraction, military use, protected areas or oil and gas (O&G) extraction [9]). Therefore, finding suitable areas and enough space to accommodate over 200 GW of offshore wind requires cautious spatial planning. Second, integrating offshore wind requires a large deployment of infrastructure, including HVDC and HVAC interconnectors, transformers and offshore hubs. Third, offshore wind electricity production is highly intermittent and variable, and therefore enough flexible resources should be present in the system in order to properly integrate it.

In the NSR context, one of the most promising alternatives to ease the integration of large offshore wind capacity is the North Sea Offshore Grid concept (NSOG). The NSOG concept can be exemplified in *Figure 1*. In a 'business as usual scenario' offshore wind power plants (OWPPs) are usually connected radially to the onshore energy systems (*Figure 1* left). With the NSOG concept (*Figure 1* right), OWPPs far from the shore[2] are connected to offshore hubs, and these offshore hubs can be connected to each other, in order to minimise investments in interconnectors. Thus, the NSOG, as mentioned in [10], provides two main functionalities: connecting offshore generation to onshore energy systems; and interconnecting different energy systems (i.e. increase cross-border interconnectivity).

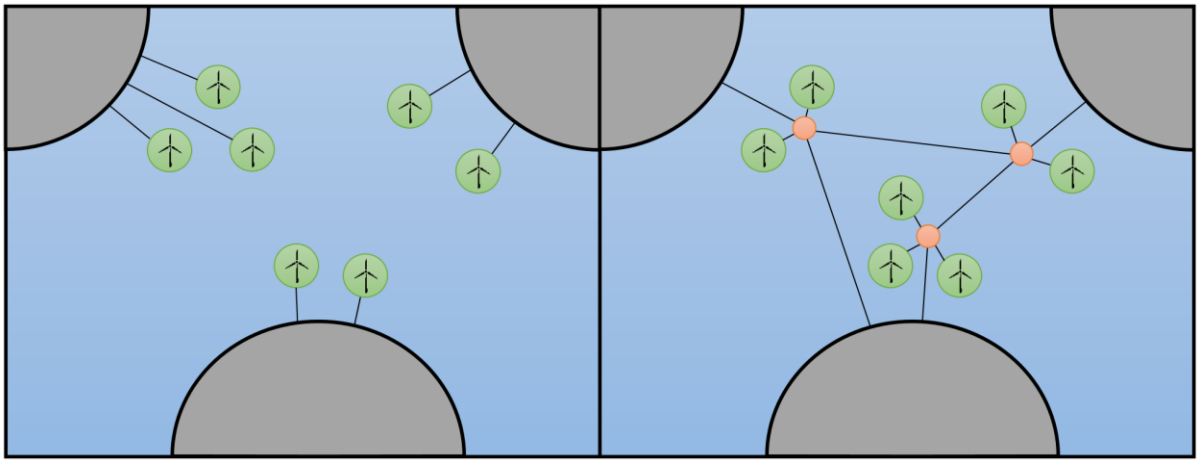

Figure 1: comparison between radial connection of OWPPs (left) and the NSOG concept (right)

[2] For OWPPs close enough to the shore it is in general cost-effective to use radial HVAC interconnectors. The NSOG concept is intended for far from shore HVDC connected OWPPs.

Preprints (www.preprints.org) | NOT PEER-REVIEWED | Posted: 5 May 2022 doi:10.20944/preprints202205.0043.v1

The NSOG concept has been envisioned by the European Commission as a realistic alternative for the medium (2030) and long (2050) term. Different transmission system operators (TSO) have also analysed the potential benefits of the NSOG (e.g. Energinet and Tennet in the North Sea Wind Power Hub[3]). The NSOG has also been discussed in the political sphere. For example, in 2020, the minister of Economic Affairs and Climate Policy of the Netherlands and the minister of Climate, Energy and Utilities of Denmark signed a memorandum of understanding (MoU) in order to "initiate cooperation on the planning of possibly one or more offshore energy hubs with one or more interconnectors for mutual benefit of the two countries". Additionally, in 2021 the Danish parliament approved the construction of an artificial island in the North Sea, with a capacity of 3 GW by 2030 and with a potential increase to 10 GW in the long term.

There is a large body of literature analysing the implications of the NSOG, for example, in [10] Dedecca et al. reviewed NSOG related studies from 2010 to 2016, while in [11] Martinez-Gordón et al. included an analysis of NSOG studies up to 2021. These two review efforts identified more than 40 studies evaluating the NSOG from different perspectives.

In general, NSOG studies available in the literature share some common trends:

- A vast majority of the studies focus solely on the power sector, either using power system models, or using multi-sector models with high level of detail in the power sector and simplistic representations of other sectors, such as heat, transport or industry.
- The use of space is not considered in most of the studies. In general, offshore wind potentials are defined exogenously, and the implications in terms of spatial needs and space availability are not discussed.
- The definition of offshore hub locations is in general arbitrary. Most of the studies do not use clustering methods to define their optimal location, nor assess their viability from a technical and environmental point of view. Additionally, most of the studies consider independent hubs per country, and therefore the possibility of offshore hubs shared among different countries is barely explored.

Considering these trends in the literature, we identify the first knowledge gap that this paper intends to fill:

- There is a lack of studies in which the NSOG concept is analysed by covering all the sectors of the energy system, and therefore endogenously capturing the interactions between different energy sectors, and by paying attention to the multiple spatial constraints of the North Sea, which affect the maximum offshore wind potentials and the suitable locations of offshore infrastructure.

Another trend that has been analysed in the literature is the role that hydrogen can play in the NSOG development. Previous studies indicate that large amounts of hydrogen might be relevant in order to decarbonise the NSR (up to 7.3 EJ in [12]). The production of part of this hydrogen offshore has recently emerged as an attractive alternative. Some of the potential

[3] https://northseawindpowerhub.eu/

Preprints (www.preprints.org) | NOT PEER-REVIEWED | Posted: 5 May 2022 doi:10.20944/preprints202205.0043.v1

benefits of the production of hydrogen offshore are: 1) due to the fact that electricity is used in-situ near the OWPP, the interconnector capacity needed to connect OWPP to shore is reduced, thus lowering the required investments. 2) in scenarios with high penetration of offshore wind in the NSR, there is a considerable amount of curtailment during some periods of high wind availability (e.g. in [12] it is cost-effective to curtail 30 TWh of offshore wind in 2050). Offshore electrolysers might provide enough flexible capacity in order to integrate this curtailed energy. 3) certain existing offshore assets, such as O&G platforms or pipelines, might be repurposed for hydrogen uses (e.g. by placing of electrolysers on platforms, or transport of hydrogen via natural gas pipelines). Thus, certain investments in new infrastructure might be alleviated by reusing and repurposing existing assets.

However, most of the studies in the literature have evaluated the feasibility of offshore hydrogen production focusing solely on techno-economic aspects, ignoring its integration in the energy system. For example, in [13] Singlitico et al. analysed the levelised cost of (offshore) electricity and hydrogen production with different types of electrolyser placements, technologies and locations. Jiang et al. [14], performed a techno-economic analysis and electrolyser size optimization of a far offshore wind-hydrogen project, where hydrogen is produced from offshore wind far from shore (200 km) and transported via cargo boats. Yan et al. [15], presented a techno-economic analysis of different system configurations for offshore wind system integration, including offshore hydrogen production and transport via pipelines or cargo boats. Other studies, such as [16][17] also evaluated the viability of offshore hydrogen production.

One of the only comprehensive studies that has analysed the role of offshore hydrogen focusing on its integration in the energy system is [18], where Gea-Bermudez et al. used the Balmorel model to analyse different scenarios where offshore hydrogen production pathways were available in 2035 and 2045. The study uses a sector-coupled version of Balmorel, including certain details of the heat and transport sectors, and provides a comprehensive analysis with in depth results and insights. However, the study does not consider all the GHG emissions of the energy system, and some parts of the energy system, such as industry or transport volumes are not defined endogenously by the model. Additionally, the study does not explore the spatial implications of the projected deployed offshore wind, nor considers these spatial constraints to define the best locations of the offshore hubs.

Thus, the second knowledge gap that this paper aims to cover is identified:

- There is a lack of studies in which the role of offshore hydrogen production within the NSOG concept is covered including all the sectors of the energy system, hence accounting endogenously for all the interactions between different energy sectors.

Considering the aforementioned knowledge gaps, this paper aims to provide new insights on both the NSOG optimal design and the offshore hydrogen production. The main contributions are threefold:

1) We analyse the benefits of an NSOG design in the NSR in 2050, using an enhanced version of the IESA-NS optimization energy system model [12]. For this analysis, we model different scenarios in which all the sectors of the energy system are included.

Preprints (www.preprints.org) | NOT PEER-REVIEWED | Posted: 5 May 2022 doi:10.20944/preprints202205.0043.v1

Future potentials of wind energy production are estimated based on space availability including competing activities. In this paper, we obtain the locations of the offshore hubs of the NSOG using spatial data clustering and considering space use.

2) We study the benefits of producing hydrogen offshore, by analysing scenarios where investments in offshore electrolysers and hydrogen infrastructure are allowed.
3) We develop a methodology to link the IESA-NS model with Geographic Information System (GIS) data, in order to integrate the spatial analysis of the North Sea (including space availability, co-existence of offshore activities and multi-use of space). This methodology is applied in this paper to the particular case of the NSR, but it can be applied to any offshore region of the world.

The rest of the paper is organised as follows: section 2 provides a summary of the methodology used in the paper, including the methods for spatial data analysis and a description of the IESA-NS energy system model. Section 3 provides a description of the different scenarios evaluated in the paper. Section 4 presents the results of the spatial data analysis, including the clusters used in our NSOG concept and the resulting OWPP potentials. Section 5 shows the results of the IESA-NS model optimization for the NSOG scenarios. Section 6 provides insights about different sensitivity analyses performed to the base scenarios. Section 7 shows a concise system cost overview. Finally, section 8 provides some conclusions, remarks and limitations of the study.

2. Methodology

The methodological framework to be used in this paper, described in *Figure 2*, is divided in the following three steps.

The first component is the geographic information system (GIS) and spatial analysis step. This step comprises the analysis and the mapping of the different activities taking place in the North Sea basin. These activities (e.g. military use, fisheries, sand extraction or shipping) demand large amounts of space, limiting the available space for renewable energy uses, such as OWPPs. Therefore, in this methodological step we identify the maximum potential of OWPP deployment under different future spatial planning strategies. Additionally, the North Sea contains a considerable existing energy infrastructure (e.g. power cables, platforms or natural gas pipelines). In this step we also map this infrastructure (which could be eventually retrofitted in the NSOG).

Subsequently, the second component defines the NSOG nodes. As mentioned in the introduction, the NSOG concept requires the definition of 'offshore hubs' which can be connected to multiple OWPPs. In this step, spatial data from the GIS analysis are used to define a proper location for the NSOG offshore nodes (i.e. 'offshore hubs') via spatial data clustering. Thus, this step comprises data treatment and curation, input to the clustering algorithm, use of heuristics to define the number of clusters (i.e. 'offshore hubs') and the regionalization of the North Sea according to the resulting clusters.

Finally, the last component integrates the compiled spatial data and offshore nodes in the IESA-NS energy system model, The IESA-NS model, described in detail in [12], permits to

Preprints (www.preprints.org) | NOT PEER-REVIEWED | Posted: 5 May 2022 doi:10.20944/preprints202205.0043.v1

include a tailor made offshore representation, thus allowing us to directly implement the findings and results from the data clustering step.

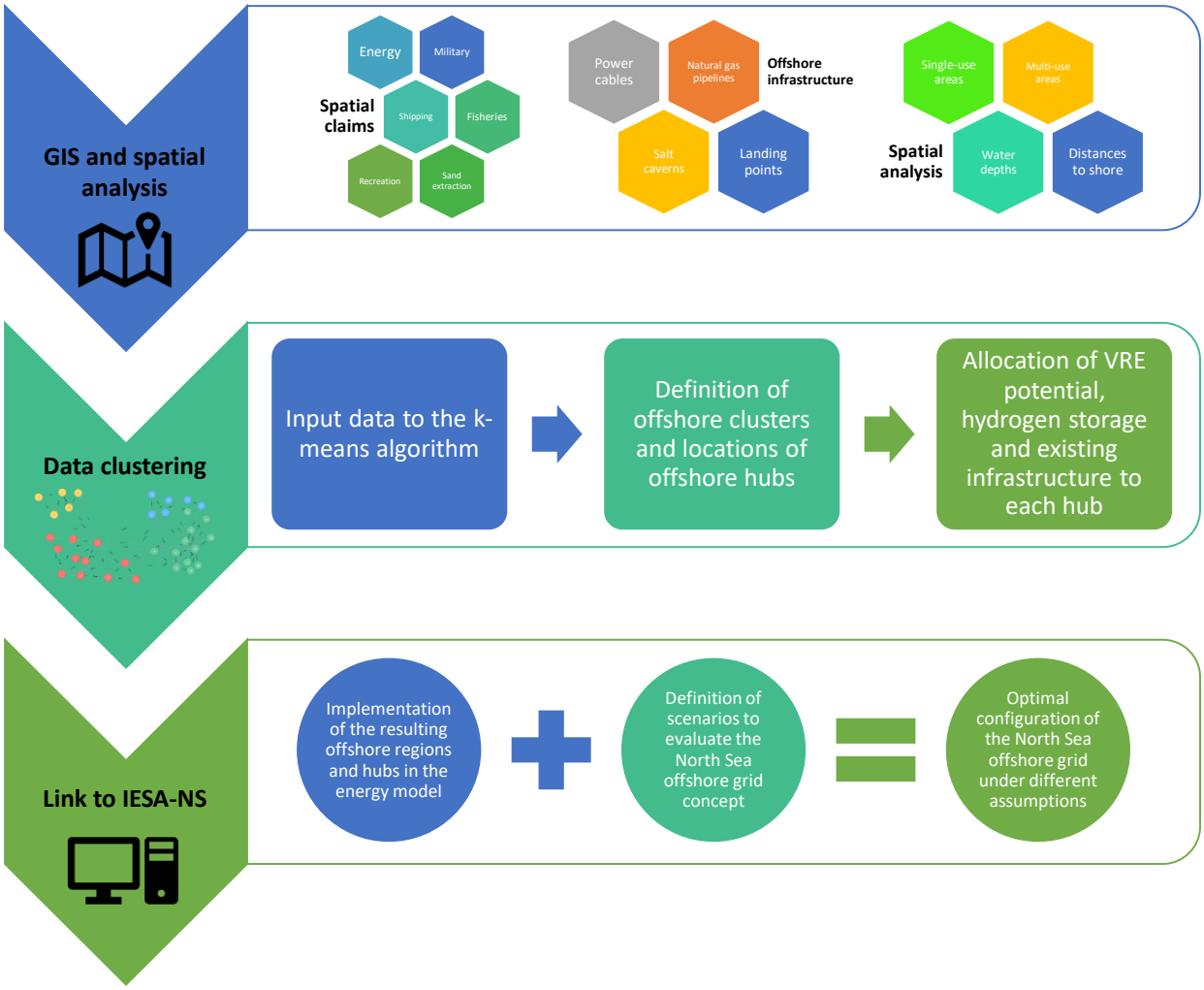

Figure 2: spatial clustering data, methdology and link to IESA-NS

2.1. Spatial claims analyses

The main objective of the GIS analysis is to identify the space available in the North Sea for OWPP deployment. This space is calculated 1) by identifying the areas where OWPPs can be directly deployed because there are no competing activities, and 2) by identifying the areas where OWPPs could eventually share space with other existing activities.

The activities considered for the GIS analyses of space use are: shipping routes, sand and gravel extraction, O&G installations (platforms and pipelines), marine protected areas (Natura 2000), other valuable and vulnerable areas, fishing areas, areas with OWPPs operational or authorised, and OWPP scoping areas. Details about the data sources and the geographical coverage of them are presented in **Appendix A** (see *Table 9*).

Preprints (www.preprints.org) | NOT PEER-REVIEWED | Posted: 5 May 2022 doi:10.20944/preprints202205.0043.v1

2.2. Spatial data clustering and regionalization of the North Sea

The role of spatial resolution and spatial data clustering in energy system models has gained momentum in recent research, due to (among other reasons) the relevance of spatial granularity in systems with large amounts of variable renewable energy sources (VRES) (see e.g. [19][11]). There are multiple algorithms that can be used for spatial clustering purposes. Some of the most popular ones are summarized in **Appendix A** (see *Table 11*).

In the case of the NSOG, we define the 'best offshore hub' configuration as the one in which 1) all potential OWPP deployment areas are connected to a hub nearby, and 2) the number of hubs is as low as possible, so we can integrate as many OWPPs as possible with the least infrastructure needs. As those two requirements are based on purely geographical data (e.g. OWPP locations and distances to centroids) k-means is the preferred algorithm (See more details in **Appendix A**), and thus the one that will be used in this paper.

2.3. Spatial clustering methodology steps

A relevant decision of the clustering methodology is to decide which data sets need to be input to the k-means algorithm. As we mentioned, the primary goal of the 'best offshore hub configuration' is to find the setup in which all OWPPs can be connected to a hub with the minimum dispersion. In this study, we decide to define the clusters using as input data the areas suitable for OWPPs deployment in the short and medium term.

There are different reasons to justify the use of this data for the k-means algorithm. First, there is high certainty that these areas will eventually harbour OWPPs[4]. Therefore, it is likely that the offshore hubs will be primarily located around these areas in order to minimize infrastructure costs. Additionally, the current political discussion (e.g. the case of Denmark and the offshore island concept approved by the Danish parliament and to be finished by 2030) is focused on infrastructure development in the 2020 and 2030 decades. Thus, it seems likely that the first hub developments will be located around areas where the deployment of OWPPs is certain. It is true that this is a myopic approach, and therefore the planning of offshore hubs using longer time horizons (e.g. candidate areas for OWPP deployment in 2050) might provide alternative solutions. But with this approach there are higher risks, as it might happen that offshore hubs are developed in areas where, in the long term, OWPPs are not deployed (e.g. because of environmental or financial reasons).

It is also important to remark that, in the case of areas suitable for OWPP deployment near the shore, radial HVAC interconnectors are always preferred over hub-connected HVDC interconnectors. In the literature, the range 80-120 km is a usual tipping point where HVDC becomes competitive versus HVAC [20]. Therefore, for this paper, we will include as input data for the clustering only data farther than 80 km from the shore, as we assume that OWPPs deployments closer than 80 km from the shore will always be connected radially via HVAC cables and will not be part of the NSOG infrastructure.

All in all, the sequential steps of the proposed spatial clustering methodology are:

[4] In the selected areas either there are already OWPPs deployed, they are commissioned for short-term OWPP deployment, or there are explorations with high political ambitions to develop OWPPs in medium-future term.

Preprints (www.preprints.org) | NOT PEER-REVIEWED | Posted: 5 May 2022 doi:10.20944/preprints202205.0043.v1

1) Harmonize the size of the input data, so that all data points have equal weights

As mentioned, input data points to be used in the k-means algorithm include 'high certainty' OWPPs deployment areas. However, these areas are not necessarily similar in size, and they might differ significantly to each other. Therefore, in this step, all the areas are divided (or merged) so that each of them covers an area of (approximately) 600 km^2. Subsequently, the centroid of each area is identified, as the k-means algorithm (in general) requires discrete data points as input data, and not continuous areas.

2) Apply heuristics to find the number of clusters to be used in the NSOG

As explained in **Appendix A**, in k-means the number of nodes is an input to the algorithm. Therefore, before applying the k-means algorithm we need to decide how many nodes are sufficient to properly represent the NSOG concept. There are multiple heuristics available in the literature to find the 'optimal' number of clusters. In this case, as explained in **Appendix A**, we decide to use two: the 'elbow method' and the '80 km heuristic'.

Regarding the elbow method, different GIS software (e.g. QGIS) permit to directly plot the elbow graph without running multiple times k-means and manually calculating the deviations. Regarding the 80 km heuristic, as it is a tailor-made heuristic for this paper, it should be manually calculated.

3) Apply the k-means algorithm with the chosen number of clusters

Once the number of clusters using both heuristics has been calculated, the k-means algorithm can be run for the last time in order to find the final offshore node configuration.

4) Apply a density-based function to each cluster to determine the area covered by each cluster

In our NSOG 'best configuration' we assume that OWPPs are connected via HVAC to the hubs, and that the hubs are (can) be interconnected via HVDC. Therefore, in this step we identify the area around the offshore hubs that is suitable for OWPP taking into account only the geographical distance. In geometrical terms, that means drawing a circle of 80 km of radius, which as stated before, is the limit where HVAC is cost-effective compared to HVDC. If any of these areas is closer than 80 km to the nearest shore, they will not be allocated to the hub, because as mentioned we assume that these areas can be directly connected via HVAC interconnectors to a shore landing point, and therefore will not be hub-connected.

5) Add (if necessary) nodes in unallocated areas

After finding the best hub locations, and adding the suitable available space to each hub, it might happen that certain areas of the North Sea remain unallocated. Therefore, in this stage additional nodes can be manually added.

6) Overlap the use of space maps to quantify the total space available (technically) for OWPP deployment

With the density based function we identify the HVAC connectable areas around the offshore hubs, but not all these areas are necessarily available for OWPPs deployment, as some of it might be reserved for other uses (e.g. sand extraction, military use or restricted

Preprints (www.preprints.org) | NOT PEER-REVIEWED | Posted: 5 May 2022 doi:10.20944/preprints202205.0043.v1

Natura 2000 areas), as analysed in **Section 2.1**. Therefore, the unsuitable portions of space have to be deducted.

7) Calculate the OWPP potential (in GW) and divide between fixed-bottom and floating

Once we know the area available for OWPP deployment, we need to quantify how much GW of OWPPs can be deployed. In order to do so, we need to use a power density value (MW/km^2), which will vary depending on the scenario. To finalize the process, we need to consider the water depth in different areas in the North Sea, in order to divide the calculated potential in the clusters between fixed-bottom offshore wind (above -55 meters of depth) and floating wind (below -55 meters of depth).

8) Link of the resulting clusters with existing infrastructure

The final step is to link the resulting clusters with the existing infrastructure. There are two types of infrastructure that we aim to identify and link. First, the existing onshore DC connection points, which will be used to connect the offshore hubs to the onshore energy demand areas. The location of these connection points are relevant, because the geographical distance to the offshore hubs will affect the HVDC connection costs. The second infrastructure that we aim to identify are existing natural gas pipelines that could be connected to the offshore hubs and retrofitted to transport hydrogen. This existing infrastructure will be relevant to analyse the feasibility of offshore hydrogen production.

2.4. IESA-NS, new improvements and modifications

The IESA-NS model (standing for **I**ntegrated **E**nergy **S**ystem **A**nalysis for the **N**orth **S**ea region) is an integrated energy system model, firstly introduced in [12] and based on the IESA-Opt model [21][22]. The IESA-Opt model was initially developed to cover the energy system of the Netherlands in detail, filling multiple knowledge gaps that most integrated ESMs have [23].

The IESA-NS model is a cost-optimization model, formulated as an LP, that optimizes the long term investment planning and short term operation of the NSR energy system. The model can optimize multiple years simultaneously, accounts for all the national GHG emissions and includes a thorough representation of all the sectors of the energy system.

Appendix B presents a detailed explanation of the energy system representation in IESA-NS, the technologies included, the spatial, temporal and technological resolution, and many other assumptions and relevant information. **Appendix C** shows the mathematical formulation used in the IESA-NS model.

Even though the IESA-NS model is focused on the NSR, it also permits to analyse the interactions with the European power and gas grids. In order to do so, the IESA-NS model optimizes also the European power dispatch, and therefore electricity imports and exports, between the NSR and the surrounding countries, are completely endogenous. As shown in *Figure 3* left, the European power dispatch includes 14 additional nodes to represent the other EU countries. The European capacities and transmission interconnectors outside of the NSR are fixed according to the Ten Year Network Development Plan of ENTSOE [24], hence

Preprints (www.preprints.org) | NOT PEER-REVIEWED | Posted: 5 May 2022 doi:10.20944/preprints202205.0043.v1

the model does not invest in capacity expansion outside of the NSR[5]. Regarding the gas network (*Figure 3* right), there are two main external sources of natural gas: Russia (RU) and northern Africa (AF). These natural gas hubs are connected to Europe and to the NSR via the clustered regions of eastern Europe (EE) and southern Europe (SO). Additionally, LNG can be imported in countries that have an LNG terminal and a decompression station. Naturally, NSR countries with natural gas fields under their domain (like Norway) have access to a national natural gas source, which can also be traded across Europe to minimize the total system costs.

Another key aspect of the IESA-NS model is its modularity to represent the offshore part of the region with as many different offshore nodes as required by the user. The importance of properly representing the spatial components of the NSR in energy modelling approaches has already been evaluated in the literature [11][9]. This modularity allows that the offshore design can be adapted to any case study: analyses of particular regions of the NSR can be evaluated adding new nodes with different wind profiles; offshore grid case studies with different hub locations and meshed interconnectors can also be implemented; interactions between wind and hydrogen in certain areas; and, in general, any analysis that requires a high level of spatial resolution.

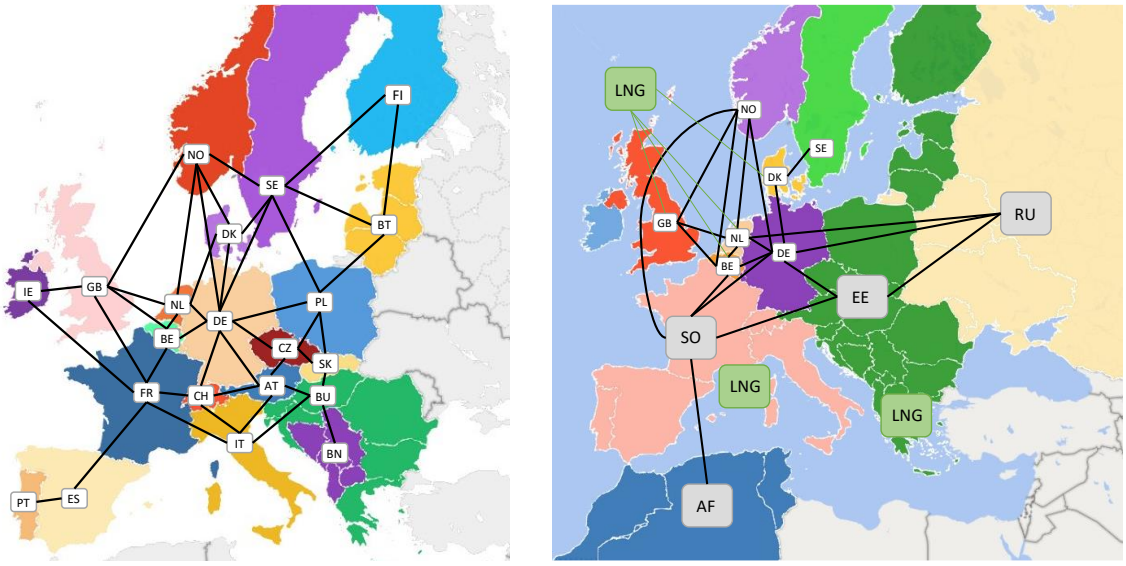

Figure 3: European nodes and international interconnectors considered for the European power dispatch in IESA-NS (left) and European natural gas and LNG network considered in IESA-NS (right)

3. Scenarios

The scenarios in the IESA-NS model are defined by providing six different types of data inputs, as shown in *Figure 4*: the projected demand of energy drivers (e.g. production volumes of different industries); the cost of input resources (e.g. cost of natural gas in 2050); the potentials for decarbonization technologies (e.g. solar PV potential); the policy regulations assumed for the transition (e.g. mitigation targets for 2050, ban of CCUS); the projected costs and operational parameters of the technologies (e.g. CAPEX of an electrolyser in 2050); and

[5] Interconnector capacity between NSR countries is optimised, interconnector capacity between countries outside of the NSR is fixed according to the TYNDP.

Preprints (www.preprints.org) | NOT PEER-REVIEWED | Posted: 5 May 2022 doi:10.20944/preprints202205.0043.v1

the power capacities of EU countries outside of the NSR (because, as mentioned before, in extra NSR countries power dispatch is optimised but capacity expansion is not).

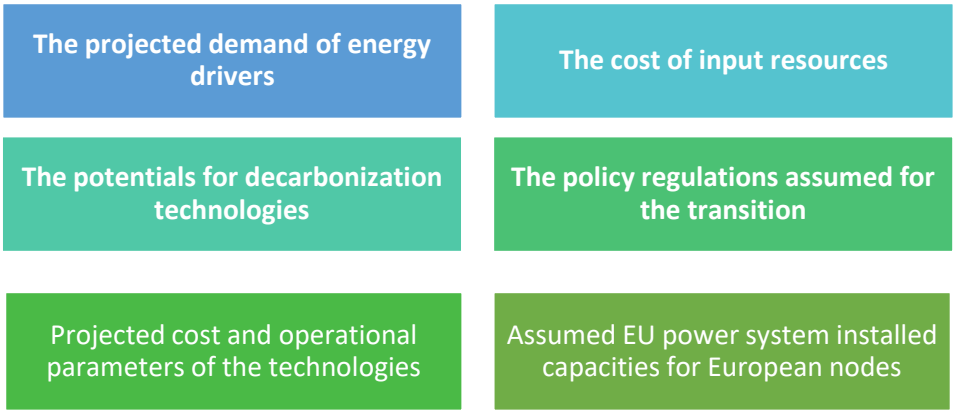

Figure 4: inputs required for scenario definition in IESA-NS

The scenarios used in this paper are mainly focused on offshore parameters, as the ultimate goal of this research is to evaluate the techno-economic benefits of the NSOG concept. A complete description of the onshore assumptions of all the scenarios, providing details, data sources and more details on the onshore configuration of the scenarios is provided in **Appendix D**. As a summary, most of the onshore energy drivers and cost assumptions are derived from the the JRC POTEnCIA Central scenario for all the NSR countries [25]. The POTEnCIA Central scenario assumes a business as usual economic development, with the European GDP growing accordingly to the '2018 Ageing report' (i.e., around 1.38% growth per year until 2050) [26], a growth of population and households based on EUROSTAT data, and projections of industry based on the sectoral Gross Value Added (GVA) values (see [25]). Additional details of the data used and scenario configuration can also be consulted online in [27] together with the whole database of the model.

Regarding mitigation targets, in all scenarios it is assumed that all NSR countries aim to reach net-zero emissions by 2050. We assume that these emission targets also cover the international transport and industry feedstock[6].

Regarding commodities, in all the scenarios all NSR countries can import natural gas, a certain amount of biomass and biofuels (variable per scenario), coal and crude oil. In all the scenarios NSR countries can produce hydrogen nationally, and hydrogen trades are allowed only within the NSR countries via investments in hydrogen pipelines. Therefore, the trade and imports/exports of hydrogen with other countries or regions outside of the NSR (e.g. Middle East or northern Africa) are not allowed. Due to the fact that imports of low-cost green hydrogen from external countries can have a large impact on the system costs, system configuration and VRE needs; and because the production of hydrogen offshore might be

[6] Current mitigation targets do not include most of the emissions related to international aviation and navigation. Therefore, NSR countries might reach net-zero targets while emitting considerable amounts of CO_2 in the international space. Regarding the use of oil as feedstock in the chemical industry, due to the fact that the oil is embedded in the final product, no direct emissions are accounted in the process. These two areas are not covered in current mitigation targets, but will most likely be part of long term mitigation policies.

Preprints (www.preprints.org) | NOT PEER-REVIEWED | Posted: 5 May 2022 doi:10.20944/preprints202205.0043.v1

heavily affected by these import/export dynamics, a set of dedicated 'hydrogen trade' scenarios will be evaluated separately in a sensitivity analysis in **Section 6.**

Table 1 provides a summary of the 5 scenarios included in the core of this paper. In the reference scenario neither offshore grid investments nor offshore hydrogen production pathways are allowed. Offshore developments follow a 'business as usual' trend, so that each country can invest in OWPPs in their own North Sea shelf. A power density of **3.6 MW/km^2** is assumed for all the countries[7]. The multi-use of space is constrained to a small fraction of marine protected areas and fisheries, in line with the findings in [9]. Values range from 2% to 10% of the available space, as shown in *Table 2*.

The NSOG concept is evaluated with four scenarios. In two of them only investments in power (OWPPs plus interconnectors) are allowed, and therefore offshore hydrogen production is not included. The first of these two scenarios assumes a power density of **3.6 MW/km^2** and no multi-use of space, and therefore is comparable to the reference scenario. In the second scenario the power density is increased to **6.4 MW/km^2**, and the multi-use of space for marine protected areas and fisheries is increased to 50% (*Table 2*).

The two last scenarios of this paper are the ones in which the NSOG concept is complemented with offshore hydrogen production. These two scenarios with a NSOG and offshore hydrogen are defined identically to the two previous ones, but allowing investments in offshore electrolysers in the offshore hubs, and allowing investments in H_2 pipelines.

Table 1: scenarios used in this paper

Scenario	Explanation	Key values	Code
Reference – no offshore grid, no hydrogen offshore	Investments in the NSOG are not allowed. NSR countries develop their offshore energy system independently	Power density: 3.6 MW/km^2. Multi-use of space: reference	**REF**
NOSG – no hydrogen offshore	Investments in a power-based NSOG are allowed. Investment in an offshore hydrogen infrastructure are not allowed.	Power density: 3.6 MW/km^2. Multi-use of space: reference	**P1**
NOSG with high wind density – no hydrogen offshore		Power density: 6.4 MW/km^2. Multi-use of space: optimistic	**P2**
NOSG – hydrogen offshore	Investments in a power and hydrogen NSOG are allowed. Investment in an offshore hydrogen infrastructure are allowed.	Power density: 3.6 MW/km^2. Multi-use of space: reference	**H1**
NOSG with high wind density – hydrogen offshore		Power density: 6.4 MW/km^2. Multi-use of space: optimistic	**H2**

[7] Note that the km^2 represents the area available for OWPP deployment, and **not** the total area of the North Sea for each country or cluster.

Preprints (www.preprints.org) | NOT PEER-REVIEWED | Posted: 5 May 2022 doi:10.20944/preprints202205.0043.v1

Table 2: share of available space in the multi use areas (fisheries combined with marine protected areas) per scenario, derived from [9]

% of available areas for multi-use	**Reference scenarios**	**Optimistic scenarios**
Netherlands	2%	50%
Germany	2%	50%
Denmark	2%	50%
Norway	2%	50%
Scotland	2%	50%
England	10%	50%

4. Spatial clustering results

This section presents the results of the spatial analysis and spatial clustering. These results define the 'best offshore hub' configuration and the geometry of the NSOG. This configuration will be used as an input in the IESA-NS model to evaluate the feasibility of the NSOG in different scenarios.

As mentioned in **Section 2.4**, the first step is the data gathering of 'high certainty' OWPP deployment sites, and the harmonization of these data so that all the areas have equal size. In order to ease the clustering stage, the centroid of each area is calculated. Results of this stage are shown in *Figure 5*. Note that these data points include only 'high certainty' areas that are further than 80 km from the shore, we assume that OWPPs deployments within 80 km to shore will be directly connected via HVAC connectors to the shore, and thus will not be part of any NSOG infrastructure.

Preprints (www.preprints.org) | NOT PEER-REVIEWED | Posted: 5 May 2022 doi:10.20944/preprints202205.0043.v1

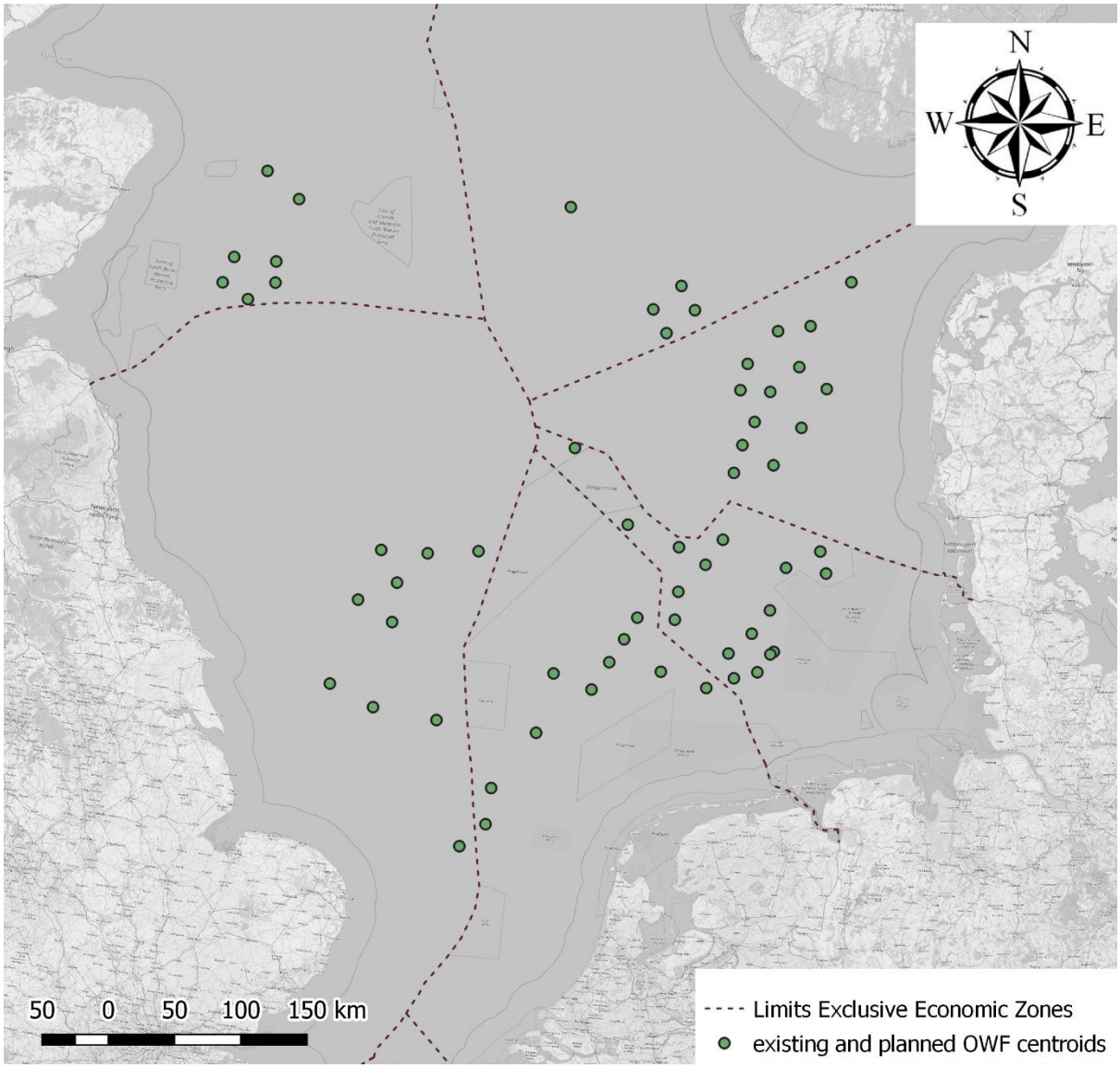

Figure 5: input data to the k-means algorithm: planned OWF and exploration areas

The following step is to find the 'best offshore hub' configuration using the heuristics described in the methodological section: the elbow method, and the 80 km heuristic. The results of both heuristics can be seen in *Figure 6*. The left axis indicates the number of wind farms further than 80 km from the nearest centroid for a different number of clusters, while the right axis indicates the sum of squared errors[8].

It is clear than the inflection point lays between 4 and 6 nodes in both heuristics. From these numbers, increasing the system resolution (e.g. using 7 or more nodes) entails only a marginal reduction of the sum of squared errors (i.e. the average dispersion of the clusters, right axis of *Figure 6*) and the number of OWPP sites further than 80 km (left axis of *Figure 6*). For this paper, we decide to use the higher resolution of this range (i.e. 6 nodes), because from 4 to

[8] In the k-means algorithm, the squared errors are related to the distance of the OWPPs to the nearest centroid (e.g. offshore hubs)

Preprints (www.preprints.org) | NOT PEER-REVIEWED | Posted: 5 May 2022 doi:10.20944/preprints202205.0043.v1

6 nodes there is not a significant difference in computational performance while running the IESA-NS model.

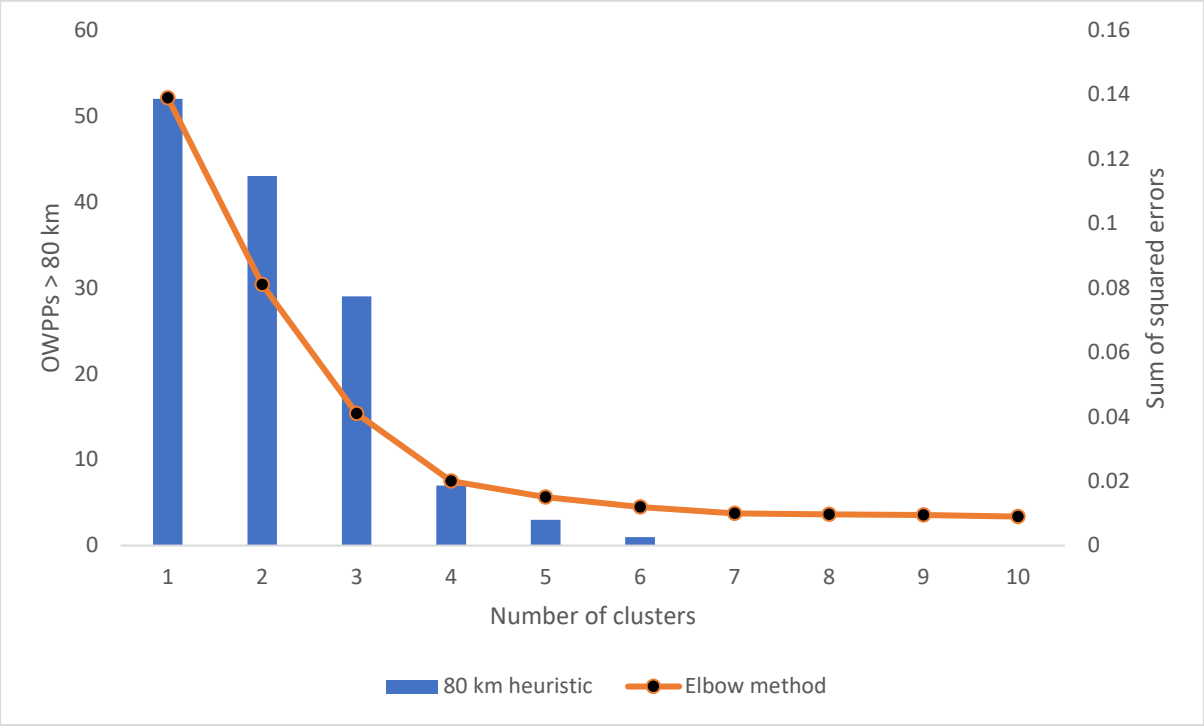

Figure 6: elbow method and 80 km heuristic results

Once the number of clusters is defined, the following step is to run the k-means algorithm and find the 'best offshore hub' configuration. *Figure 7* shows the resulting configuration, with the six resulting clusters and the centroid of each cluster (i.e. the optimal geographical location of the hub).

Preprints (www.preprints.org) | NOT PEER-REVIEWED | Posted: 5 May 2022 doi:10.20944/preprints202205.0043.v1

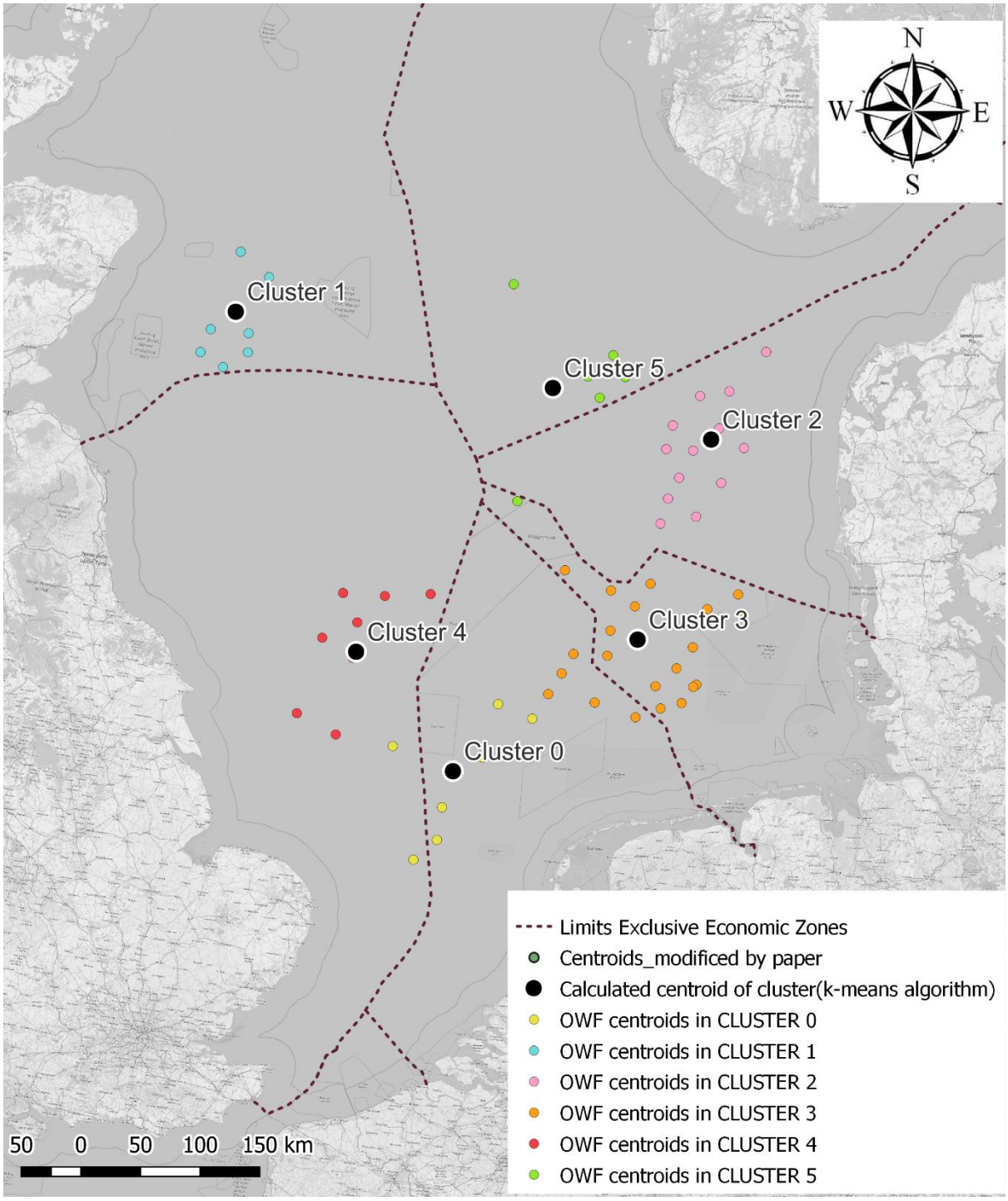

Figure 7: output of the k-means algorithm with 6 clusters

With the centroids of the clusters defined, the next step is to apply a density function to allocate an area of 80 km of radius to each cluster, and to add (if needed) additional clusters exogenously to unallocated areas. The results of this step can be seen in *Figure 8*. With the buffers of the optimal locations of the centroids, there are two large areas in the Dogger Bank and in the English shelf that remain unallocated. These areas are relatively close to the defined clusters and include considerable space for OWPP deployment. Thus, we decide to add two more clusters in these two areas.

Preprints (www.preprints.org) | NOT PEER-REVIEWED | Posted: 5 May 2022 doi:10.20944/preprints202205.0043.v1

Naturally, the buffers calculated in *Figure 8* do not represent the areas suitable for OWPP deployment within each cluster. As explained above, the North Sea is an extremely busy area, and certain spaces are occupied by different activities. The analysis of space available, considering all the activities mentioned in *Table 9* can be consulted in *Figure 9*. Observe that the space is divided in available areas for single-use (i.e. exclusively for OWPPs deployment), available areas for multi-use (i.e. OWPPs can share space with other activities to a certain extent, depending on the scenario), and areas unavailable for OWPPs deployment (i.e. areas used exclusively by other activities, where OWPPs cannot be deployed in any case). There is also a division between the space located under and over 80 km from the nearest shore. The reason is that, as previously explained, we assume that the OWPPs located closer than 80 km to the shore can be directly connected via HVAC cables, hence not being part of the NSOG infrastructure.

All things considered, *Figure 10* shows the overlap between the buffers of each cluster and the space available. With this overlap we 1) quantify the space available (single-use or multi-use) and unavailable within each cluster, and 2) subtract the areas within the original clusters that are closer than 80 km to the nearest shore.

Subsequently, we need to quantify the space available in each of the clusters. *Table 3* shows the area (in km^2) of single-use and multi-use allocated to each cluster. *Table 4* translate these areas into OWPPs capacity potentials for the reference scenario, using the reference density of 3.6 GW/ km^2 and the reference multi-use of space values shown in *Table 2*. The same calculation is presented in *Table 5* for the optimistic scenario (i.e. 6.4 GW/ km^2 and 50% of the multi-use areas, as shown in *Table 2*).

Finally, another important calculation which can be consulted in **Appendix E** is the physical distance from each cluster centroid to each other, and to the nearest onshore connection point. These values are needed to calculate different HVDC and hydrogen pipeline infrastructure costs, which are naturally dependent on the distance. These calculations of power interconnector and pipeline infrastructure costs are also shown in **Appendix E**.

Preprints (www.preprints.org) | NOT PEER-REVIEWED | Posted: 5 May 2022 doi:10.20944/preprints202205.0043.v1

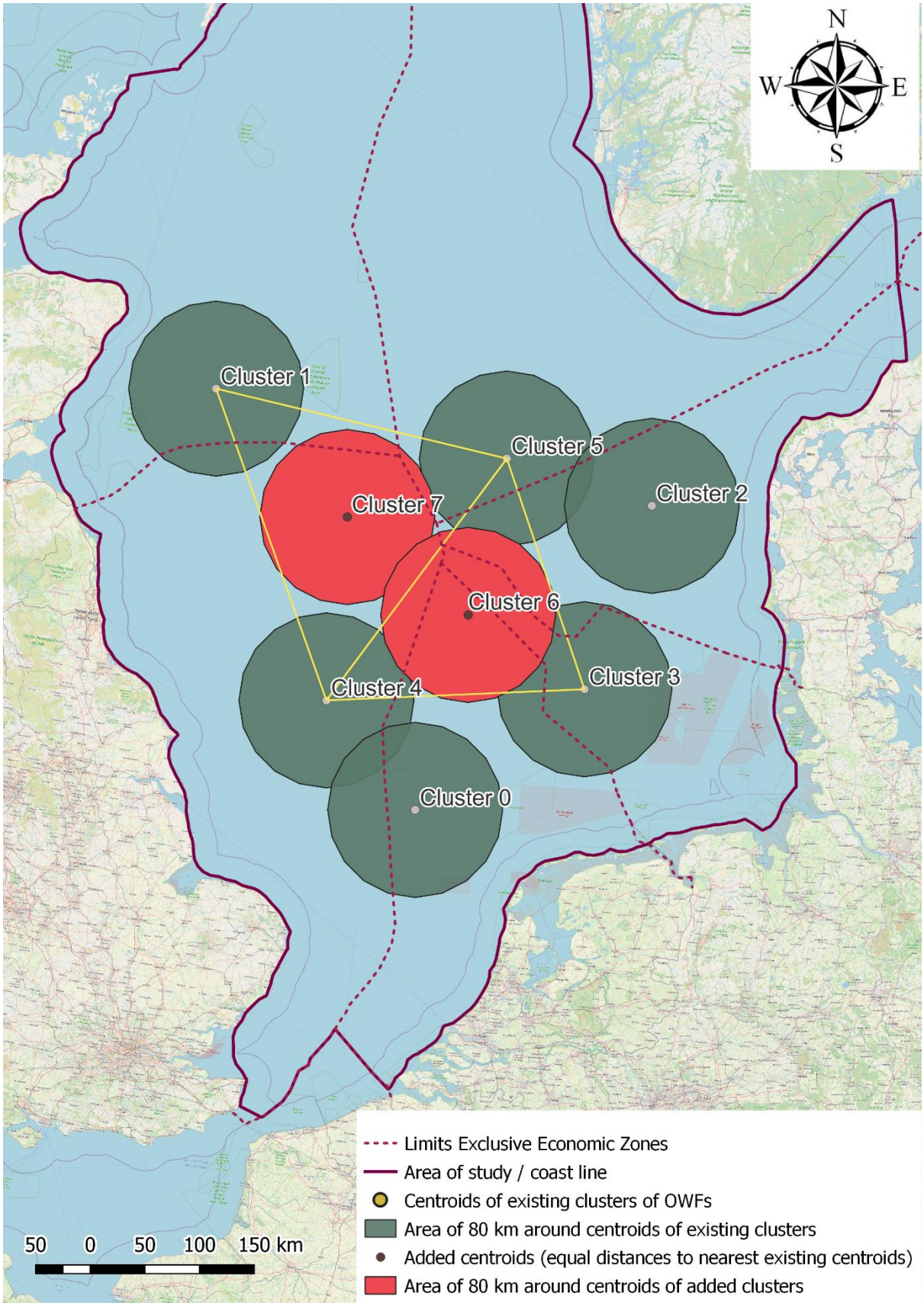

Figure 8: density function applied to the defined clusters

Preprints (www.preprints.org) | NOT PEER-REVIEWED | Posted: 5 May 2022 doi:10.20944/preprints202205.0043.v1

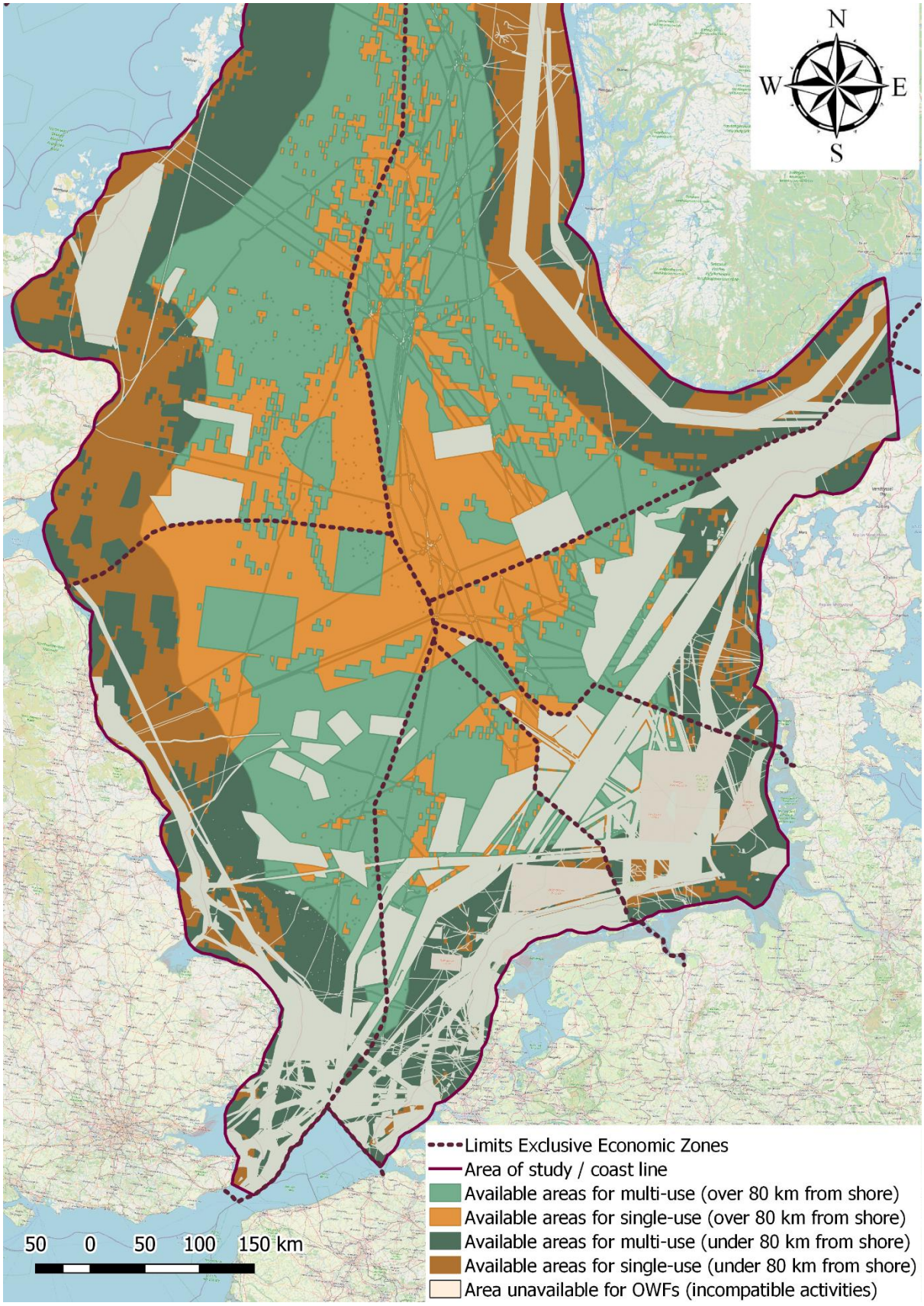

Figure 9: map of available areas for single-use and multi-use in the North Sea considered for this study

Preprints (www.preprints.org) | NOT PEER-REVIEWED | Posted: 5 May 2022 doi:10.20944/preprints202205.0043.v1

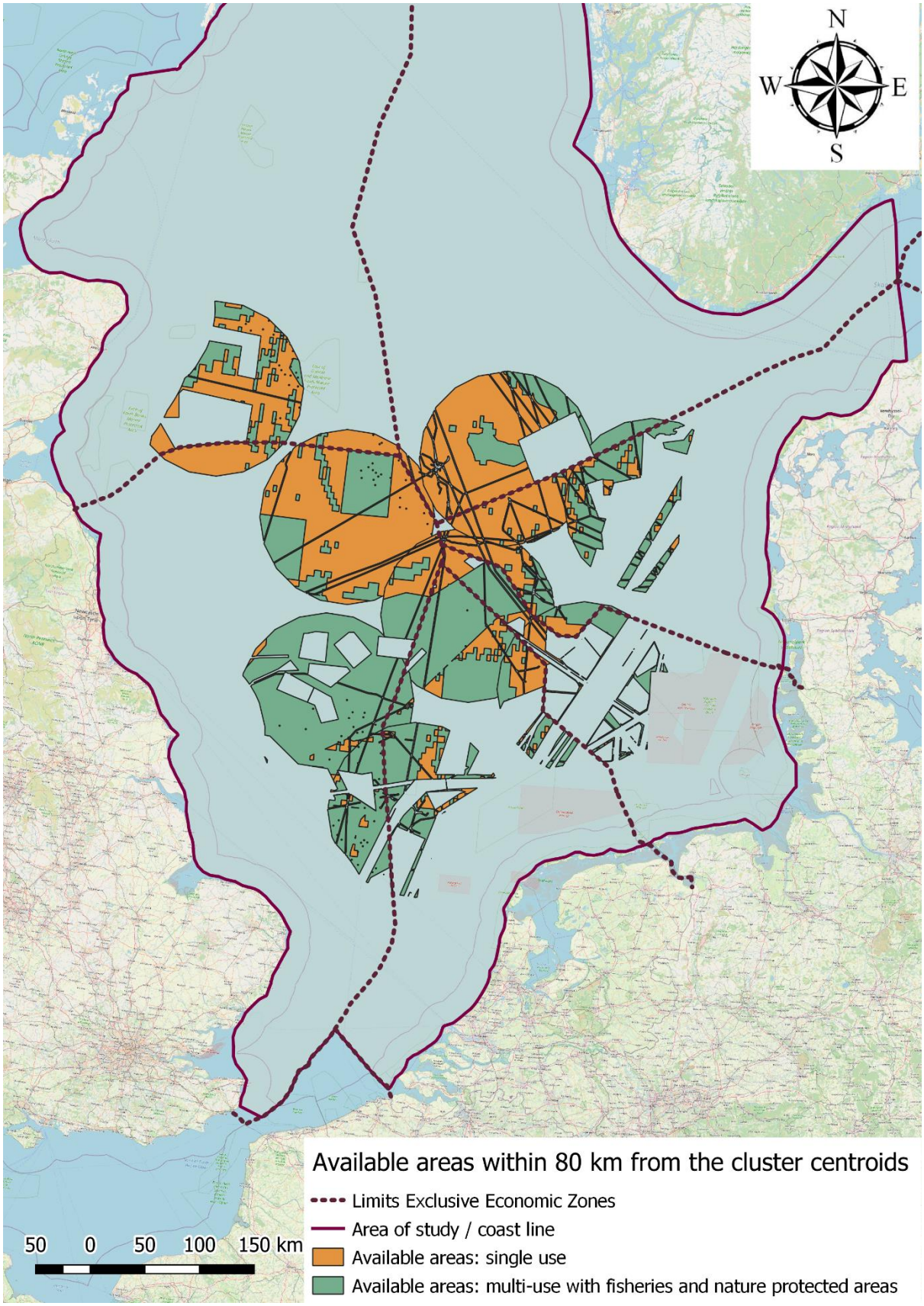

Figure 10: map of area available for single-use and multi-use in each of the clusters

Preprints (www.preprints.org) | NOT PEER-REVIEWED | Posted: 5 May 2022 doi:10.20944/preprints202205.0043.v1

Table 3: available single-use and multi-use area in the defined clusters

	Cluster 0		Cluster 1		Cluster 2		Cluster 3		Cluster 4		Cluster 5		Cluster 6		Cluster 7	
	Area single-use (km2)	Area multi-use (km2)	Area single-use (km2)	Area multi-use (km2)	Area single-use (km2)	Area multi-use (km2)	Area single-use (km2)	Area multi-use (km2)	Area single-use (km2)	Area multi-use (km2)	Area single-use (km2)	Area multi-use (km2)	Area single-use (km2)	Area multi-use (km2)	Area single-use (km2)	Area multi-use (km2)
Netherlands	824	3451	0	0	0	0	1180	1194	66	1168	0	0	1862	6740	0	0
Germany	0	0	0	0	0	0	608	1216	0	0	0	0	1072	1567	0	0
Denmark	0	0	0	0	988	3934	436	767	0	0	4040	618	2089	895	0	0
Norway	0	0	0	0	0	866	0	0	0	0	8585	2507	0	0	463	0
Scotland	0	0	5336	2478	0	0	0	0	0	0	0	0	0	0	1153	82
England	222	3733	2135	173	0	0	0	0	326	12068	0	0	1418	1899	11783	5704

Table 4: maximum potential of OWPP deployment in the different clusters for the reference scenario: power density of 3.6 GW/km², and low deployment in multi-use areas (Table 2)

	Cluster 0		Cluster 1		Cluster 2		Cluster 3		Cluster 4		Cluster 5		Cluster 6		Cluster 7	
	Single-use (GW)	Multi-use (GW)	Single-use (GW)	Multi-use (GW)	Single-use (GW)	Multi-use (GW)	Single-use (GW)	Multi-use (GW)	Single-use (GW)	Multi-use (GW)	Single-use (GW)	Multi-use (GW)	Single-use (GW)	Multi-use (GW)	Single-use (GW)	Multi-use (GW)
Netherlands	3	0.3	0	0	0	0	4.2	0.1	0.2	0.1	0	0	6.7	0.5	0	0
Germany	0	0	0	0	0	0	2.2	0.1	0	0	0	0	3.9	0.1	0	0
Denmark	0	0	0	0	3.5	0.3	1.6	0.1	0	0	14.5	0	7.5	0.1	0	0
Norway	0	0	0	0	0	0.1	0	0	0	0	30.9	0.2	0	0	1.7	0
Scotland	0	0	19	0.2	0	0	0	0	0	0	0	0	0	0	4.2	0
England	0.8	1.3	7.7	0.1	0	0	0	0	1.2	4.3	0	0	5.1	0.7	42.4	2

Table 5: maximum potential of OWPP deployment in the different clusters for the optimistic scenario: power density of 6.4 GW/km², and high deployment in multi-use areas (Table 2)

	Cluster 0		Cluster 1		Cluster 2		Cluster 3		Cluster 4		Cluster 5		Cluster 6		Cluster 7	
	Single-use (GW)	Multi-use (GW)	Single-use (GW)	Multi-use (GW)	Single-use (GW)	Multi-use (GW)	Single-use (GW)	Multi-use (GW)	Single-use (GW)	Multi-use (GW)	Single-use (GW)	Multi-use (GW)	Single-use (GW)	Multi-use (GW)	Single-use (GW)	Multi-use (GW)
Netherlands	5.3	11	0	0	0	0	7.6	3.8	0.4	3.7	0	0	11.9	21.6	0	0
Germany	0	0	0	0	0	0	3.9	3.9	0	0	0	0	6.9	5	0	0
Denmark	0	0	0	0	6.3	12.6	2.8	2.5	0	0	25.9	2	13.4	2.9	0	0
Norway	0	0	0	0	0	2.8	0	0	0	0	54.9	8	0	0	3	0
Scotland	0	0	34.2	7.9	0	0	0	0	0	0	0	0	0	0	7.4	0.3
England	1.4	11.9	13.7	0.6	0	0	0	0	2	38.6	0	0	9	6	75	18.2

Preprints (www.preprints.org) | NOT PEER-REVIEWED | Posted: 5 May 2022 doi:10.20944/preprints202205.0043.v1

Once the offshore wind locations are defined, and the OWPP deployment potential is allocated to each of them, it is then necessary to link this setup to the existing power and natural gas infrastructure.

Regarding the power infrastructure, we proceed to identify existing and planned onshore HVDC connection points because: 1) they are well connected to existing energy demand clusters, and 2) it is more likely that future offshore grid developments are connected to existing onshore infrastructure, in order to minimise investments and unnecessary costs.

Suitable onshore HVDC connection points are identified by using the ENTSO-E Transmission System Map [24] and the EMODnet database of the North Sea activities [28]. In the United Kingdom two relevant connection points are identified: one in Blyth, where currently the converter of the North Sea link is located (1.4 GW HVDC interconnector between Norway and the UK). The other in Bicker Fen, where the converter of the Viking Link will be placed (1.4 GW HVDC interconnector between Denmark and the UK, expected for 2023). In Norway we identify two onshore connecting points: one in Kvilldal (the Norwegian connecting point of the aforementioned North Sea link), and another one in Feda, where the NordNed cable is connected (0.7 GW HVDC interconnector between Norway and the Netherlands). In Denmark we identify one connecting point, located in Revsing (connecting point of the aforementioned Viking link). In Germany we identify Büsum as a candidate connecting point, as it already harbours the converter of the NordLink interconnector (1.4 GW HVDC between Norway and Germany). Finally, in the Netherlands, two onshore connecting points are used: Maasvlakte (connecting point of the BritNed cable, an 1 GW interconnector between the UK and the Netherland), and Eemshaven, which harbours the converter of the aforementioned NorNed cable. All the candidate links between the offshore hubs and the connection points can be seen in *Figure 11*, together with the suitable hub-to-hub interconnectors. The cost of all the HVDC interconnectors of *Figure 11*, which are naturally dependent on the distances, are also calculated in **Appendix E**.

Regarding natural gas infrastructure, we proceed to identify existing natural gas pipelines in the North Sea, using the Global Fossil Infrastructure Tracker, developed by the Global Energy Monitor [29] and the ENTSOG natural gas maps [30]. We select the candidate pipelines that 1) were in operation in 2021 and 2) cross any of the buffer areas of the offshore hub locations (i.e. *Figure 10*). We assume that the pipelines falling within these criteria can be retrofitted to transport hydrogen, and can be connected to the nearest offshore hub where electrolysers can be located. **Appendix E** identifies the suitable pipelines and their estimated size and capacity.

Finally, in order to quantify how much hydrogen storage could be deployed in each of the resulting clusters, it is also desirable to identify suitable hydrogen storage locations in the North Sea. To this end, we use the technical potential of salt caverns for hydrogen storage in the NSR countries quantified in [31]. Overlapping the available salt caverns in the North Sea and the resulting clusters (*Figure 10*), we identify that the buffer areas of clusters 0, 2, 3, 4, 5 and 6 contain salt caverns suitable for hydrogen storage.

Preprints (www.preprints.org) | NOT PEER-REVIEWED | Posted: 5 May 2022 doi:10.20944/preprints202205.0043.v1

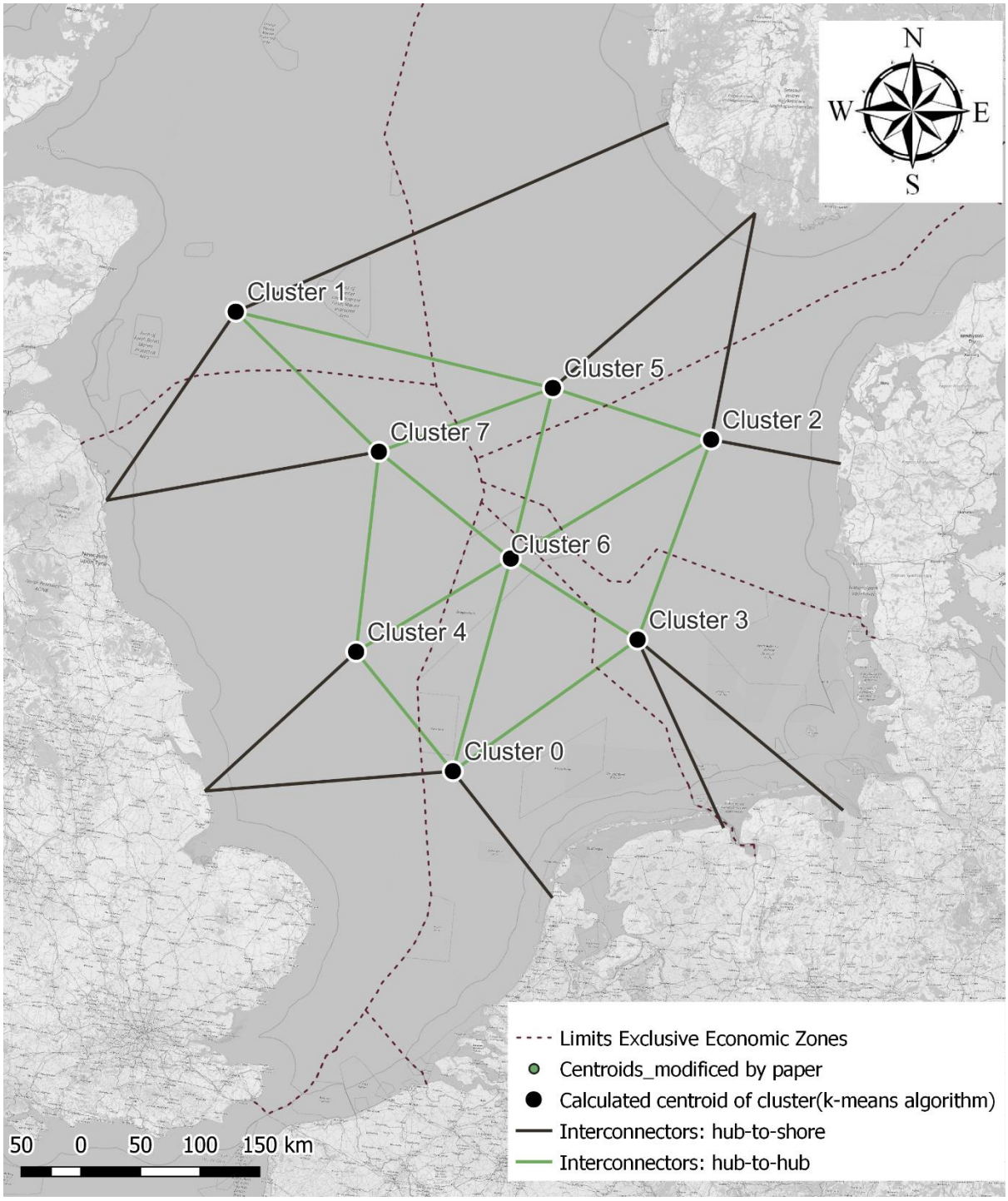

Figure 11: NSOG interconnectors allowed, divided in hub-to-hub interconnectors (green) and hub-to-shore interconnectors (black)

5. Scenario modelling results

In this section, we provide the main results of the five scenarios described in **Section 3**. We first provide an overview of the main insights of the reference scenario, then we analyse the results of the NSOG with and without hydrogen scenarios. To conclude, we briefly compare all the scenarios in terms of system costs, and we analyse these results. All the outcomes of the scenarios, with further disaggregation per country and per technology, can be openly consulted in [27].

Preprints (www.preprints.org) | NOT PEER-REVIEWED | Posted: 5 May 2022 doi:10.20944/preprints202205.0043.v1

The results for this paper have been obtained by running the scenarios outlined above by means of the IESA-NS model in a laptop with 32 GB of RAM and an Intel i8750-H processor, using the Gurobi 9.01 solver via the barrier method. The IESA-NS model is implemented in AIMMS. The computational time required to run the scenarios ranges from 2 hours (single year, optimization of the energy system in 2050) to 30 hours (3 years, simultaneous optimization of 2030, 2040 and 2050). Since the objective of this paper is to analyse decarbonisation scenarios in 2050, not the pathway towards these scenarios (e.g., intermediate targets), and to reduce the computational load, only the year 2050 is optimized.

5.1. Insights reference scenario (REF)

The reference scenario (**REF**) achieves net-zero emissions primarily by using large amounts of RES. In all countries, the share of RES in the total primary energy ranges between 70% and 95%, while the share of RES in final electricity lays between 93% and 98%. Natural gas is the largest fossil fuel contributor (13% of the primary energy of the whole NSR), while the contributions of crude oil and coal are negligible (less than 1% of the total primary energy).

Figure 12 gives more details about the electricity generation across the NSR. As it can be seen in *Figure* 12, solar PV and onshore wind are dominant in all the countries. There are also large contributions of flexible CCGT generation, except in Norway and Sweden, due to their abundant dispatchable hydropower potential.

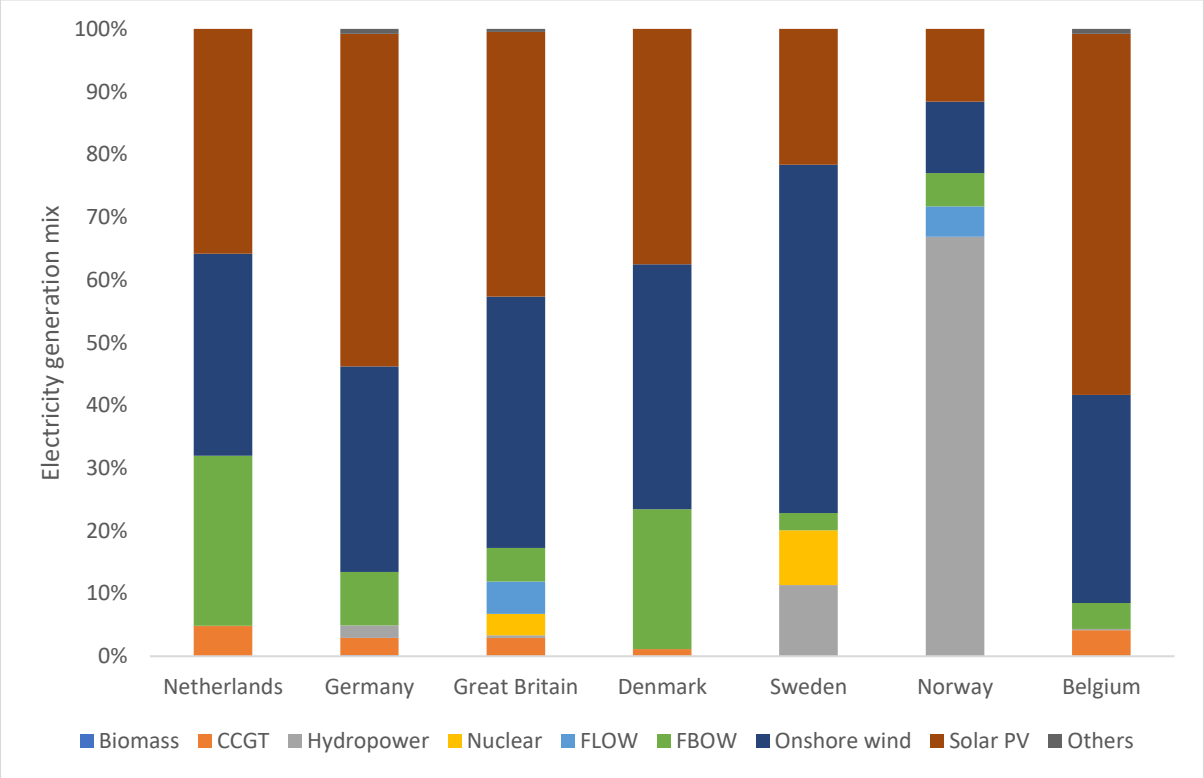

Figure 12: breakdown of the power generation in the reference scenario in the NSR countries in 2050

In the specific case of offshore wind, it is interesting to compare the total deployment of hub-connected OWPPs for the NSR (99 GW) with the technical potential used as input in the reference scenario (171 GW). This difference hints that it is not optimal to invest in OWPPs in

Preprints (www.preprints.org) | NOT PEER-REVIEWED | Posted: 5 May 2022 doi:10.20944/preprints202205.0043.v1

certain areas, thus justifying the analysis of the NSOG concept, to evaluate if larger amounts of OWPPs could be optimally integrated by building a more interconnected infrastructure.

It is also interesting to analyse the imports and exports dynamics within the NSR countries. Regarding power, in the absence of the NSOG, country-to-country interconnectors are the only source of international power trade. *Figure 13* shows the net power trade balance between countries, while *Table 6* shows the total cross border capacity between countries in 2050. Note that none of the scenarios constrains the interconnector capacity expansion, and therefore the values of *Table 6* represent the cost-optimal values of cross border capacity. It is interesting to see that the United Kingdom, Belgium, the Netherlands and (especially) Germany import a considerable amount of electricity, while Scandinavian countries (especially Sweden) are net exporters. The reason is that the former countries have higher population densities and contain larger industrial clusters, and therefore their energy demand is considerably higher. Additionally, partly due to this high population density, the space available for VREs deployment is limited. In contrast, Scandinavian countries have a lower energy demand, enough space for large scale VRE deployment and, on top of that, a large amount of dispatchable hydropower capacity.

This same conclusion can also be derived from the interconnector capacity expansion (*Table 6*), where we can see that the links between Scandinavia and the rest of the NSR are strengthened (notably the links between Sweden, Germany and the Netherlands).

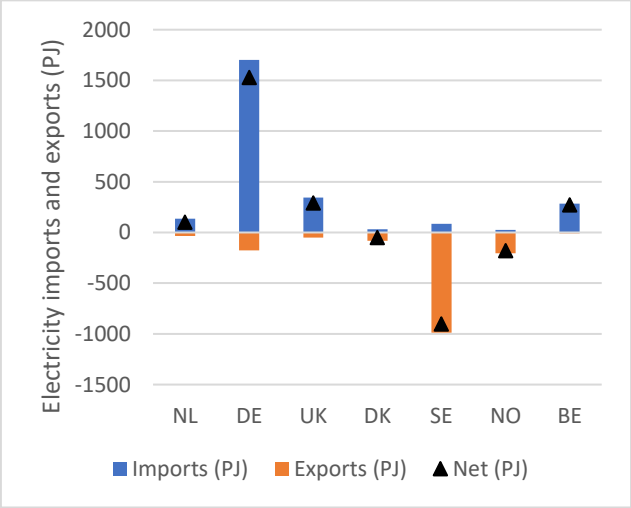

Figure 13: power imports, exports and net balance for the NSR countries in 2050 (PJ)

Table 6: cross border capacity expansion between NSR countries in 2050 (GW) in the reference scenario

	Netherlands	Germany	Great Britain	Denmark	Sweden	Norway	Belgium
Netherlands	-	8.73	3.82	1.75	0	4.84	1.4
Germany	xx	-	0	9	61	1.4	1
Great Britain	xx	xx	-	0	0	10	2.49
Denmark	xx	xx	xx	-	2.44	1.64	0
Sweden	xx	xx	xx	xx	-	4	0
Norway	xx	xx	xx	xx	xx	-	0
Belgium	xx	xx	xx	xx	xx	xx	-

Preprints (www.preprints.org) | NOT PEER-REVIEWED | Posted: 5 May 2022 doi:10.20944/preprints202205.0043.v1

Another key insight of the reference scenario is the large use of hydrogen in the NSR. In 2050, around 6 EJ of hydrogen are used, mainly to decarbonise the international transport and some industrial sectors. As hydrogen can be traded within the NSR (but not with extra NSR countries), it is also interesting to analyse the hydrogen imports and exports dynamics between the NSR countries. Scandinavian countries are net exporters, while the Netherlands and Germany are net importers. Great Britain, Belgium and Norway remain self-sufficient, with almost no trades with surrounding countries. It is interesting to see that Denmark and Germany play a 'trading hub' role, with large amounts of imports and exports, due to their location and good connectivity with multiple NSR countries.

In general, most of the results of the reference scenario (additional results can be consulted in [27]) justify the analysis of the NSOG concept. From the power generation perspective, it can help to integrate more OWPPs offshore and improve the connectivity between Scandinavia and the rest of the NSR. From the hydrogen perspective, due to the massive use and trade of hydrogen in the NSR, allowing its production offshore might help to find a better optimal configuration.

5.2. Insights NSOG without hydrogen (P1 and P2)

The following two scenarios (**P1** and **P2**), described in **Section 3**, include an electricity based NSOG concept (i.e. no investments in offshore hydrogen and pipelines). *Figure 14* shows the optimal investments in floating and fixed-bottom OWPPs (bold numbers near the nodes, in GW), and in HVDC interconnectors (italic numbers near the lines, in GW). It is important to remark that the numbers shown in *Figure 14* include only HVDC connected wind deployments (i.e. hub-connected OWPPs further than 80 km from shore). OWPPs deployed within 80 km to the nearest shore are connected via HVAC cables and not shown.

In both cases it is clear that investments in the NSOG architecture are cost-effective. In the scenario with the reference offshore wind density (**P1**, top of *Figure 14*) 59.4 GW of hub-connected OWPPs are deployed, while in the high density scenario (**P2**, bottom of *Figure 14*) this number increases to 162 GW. Investments in HVDC interconnectors are also abundant in both scenarios. In **P1** there is an investment in 92.1 GW of HVDC interconnectors. In **P2** this number rises to 212.8 GW.

Preprints (www.preprints.org) | NOT PEER-REVIEWED | Posted: 5 May 2022 doi:10.20944/preprints202205.0043.v1

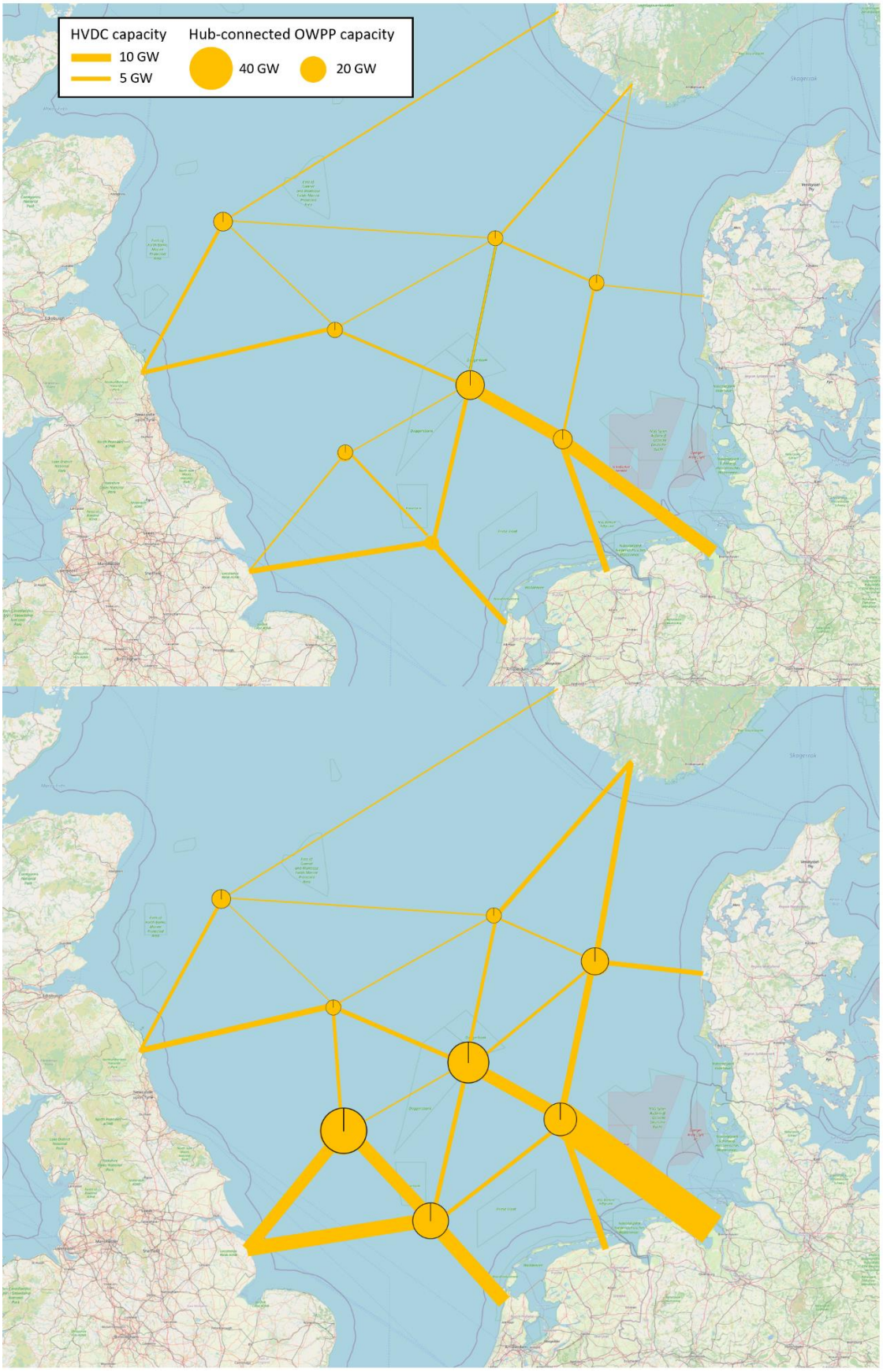

Figure 14: optimal investments in HVDC interconnectors and OWPP capacity. Data in GW. The diagram on top represents the scenario with reference OWPP density (P1), the diagram on the bottom represents the scenario with high OWPP density (P2).

Preprints (www.preprints.org) | NOT PEER-REVIEWED | Posted: 5 May 2022 doi:10.20944/preprints202205.0043.v1

The deployment of fixed-bottom OWPPs is dominant compared to floating wind, as shown in *Figure 15*. As expected, the dominance of fixed-bottom is purely economical, since its CAPEX is substantially lower than the one of floating OWPPs. Additionally, most of the areas suitable for hub-connected floating OWPPs are located near the United Kingdom and Norway (i.e. clusters 7, 1 and 5). As we inferred from the reference scenario, these three countries have a large amount of onshore VRE potential, and therefore the system does not find optimal to invest in all the offshore potential. In any case, all the scenarios in this section assume a reference projection of floating wind CAPEX (2700 €/kW) and reference values of offshore VRE potential. Additional scenario analysis should be performed with more optimistic projections of floating CAPEX, and a more constrained onshore potential (e.g. low social acceptability of onshore wind).

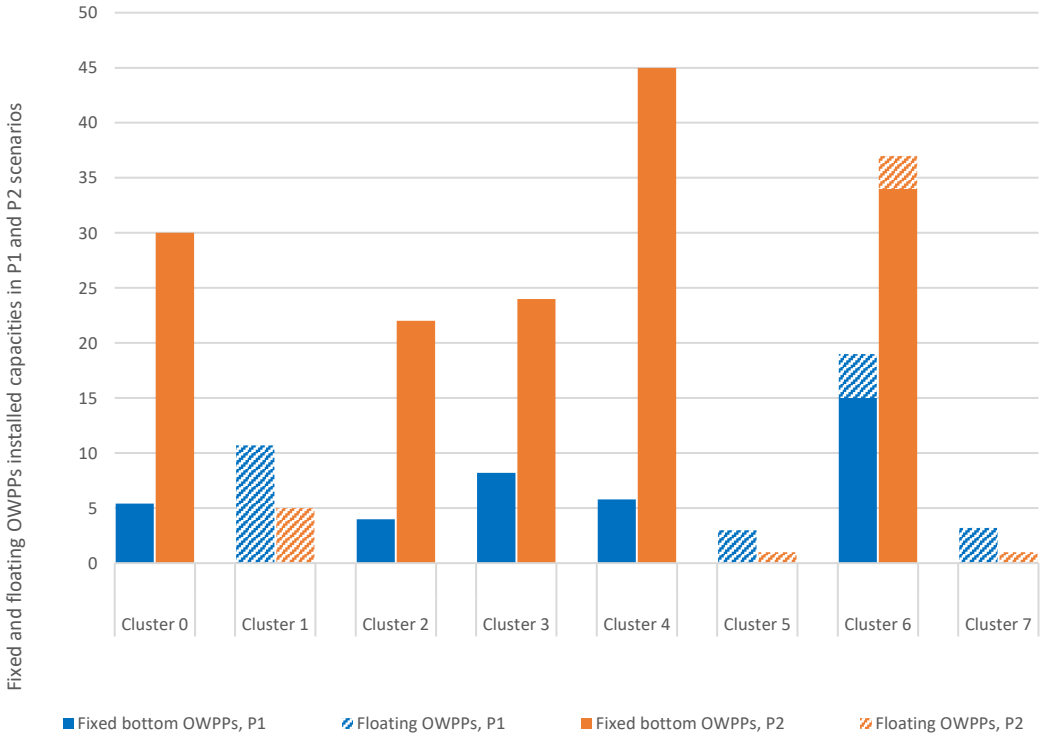

Figure 15: fixed-bottom and floating OWPPs installed capacities in the power NSOG scenarios

As mentioned through the paper, the role of the interconnectors of the NSOG concept is not only to connect OWPPs to onshore energy systems, but also to interconnect countries. Therefore, it is expected that the large deployment of the hub-to-hub and hub-to-shore HVDC interconnectors (i.e. *Figure 14*) alleviates the need for country to country interconnectors (i.e. *Table 6*). *Table 7* shows the capacity expansion of country to country interconnectors in the scenarios where the power based NSOG concept is evaluated. As it was expected, when the NSOG is deployed the need for country-to-country interconnectors is alleviated, as NSOG interconnectors can be used to connect countries as well. If we aggregate the numbers, in the **REF** scenario (*Table 6*) the total country-to-country interconnection between NSR countries reaches 115 GW. This number is reduced to 94 GW and 73 GW for **P1** and **P2**, respectively (*Table 7*).

Preprints (www.preprints.org) | NOT PEER-REVIEWED | Posted: 5 May 2022 doi:10.20944/preprints202205.0043.v1

Table 7: cross border onshore capacity expansion between NSR countries in 2050 (GW) in the power based NSOG scenarios. Numbers represent country-to-country interconnectors, and therefore NSOG interconnectors are not included

		Netherlands	Germany	Great Britain	Denmark	Sweden	Norway	Belgium
P1	Netherlands	-	4.25	1	0.7	0	6.2	1.4
	Germany	xx	-	0	8.5	52	1.4	1
	Great Britain	xx	xx	-	0	0	7.5	2
	Denmark	xx	xx	xx	-	2.4	1.6	0
	Sweden	xx	xx	xx	xx	-	4	0
	Norway	xx	xx	xx	xx	xx	-	0
	Belgium	xx	xx	xx	xx	xx	xx	-
P2	Netherlands	-	4.25	1	0.7	0	3	2.4
	Germany	xx	-	0	5.75	39	2.6	1.9
	Great Britain	xx	xx	-	0	0	3.9	1.5
	Denmark	xx	xx	xx	-	2	1.7	0
	Sweden	xx	xx	xx	xx	-	3.7	0
	Norway	xx	xx	xx	xx	xx	-	0
	Belgium	xx	xx	xx	xx	xx	xx	-

5.3. Insights NSOG with hydrogen (H1 and H2)

The last two scenarios allow investments of both power and hydrogen offshore assets, i.e. OWPPs, HVDC interconnectors, offshore electrolysers placed on the offshore hubs, and hydrogen pipelines. Retrofitting of certain natural gas pipelines is allowed as explained in **Appendix E**.

Power and hydrogen reference density (H1)

Figure 16 shows the outcomes of the scenario with power and hydrogen investments and the reference value of OWPP deployment density (**H1**). Regarding power investments (top of *Figure 16*), it is cost-effective to deploy 172 GW of hub-connected OWPPs and 143 GW of HVDC interconnectors. These are considerably higher numbers than the ones of **P1** (top of *Figure 14*), i.e. additional 113 GW of hub-connected OWPPs and additional 49 GW of HVDC interconnectors. Therefore, it can be inferred that allowing the system to invest in an offshore hydrogen infrastructure is beneficial to integrate OWPPs in the system. As observed in *Figure 18*, this additional OWPP deployment corresponds to floating wind turbines, notably in clusters 5 and 7.

Regarding hydrogen infrastructure (bottom of *Figure 16*), one can observe that the United Kingdom, Germany and especially the Netherlands benefit substantially from the offshore hydrogen production. The system finds optimal to invest in 61 GW of offshore electrolysers, 49.4 GW of new hydrogen pipelines, and 22 GW of retrofitted natural gas pipelines. Note that the Netherlands is the only country that finds cost-effective to invest in new pipelines to import hydrogen from offshore hubs. This is in line with the results of the reference scenario,

Preprints (www.preprints.org) | NOT PEER-REVIEWED | Posted: 5 May 2022 doi:10.20944/preprints202205.0043.v1

as we saw that the Netherlands is the country with higher dependency on hydrogen trades across the NSR.

It is also interesting to analyse the capacity factors of both offshore electrolysers and hydrogen pipelines. Regarding electrolysers, they have an average capacity factor of 32%, which is lower than the average capacity factor of OWPPs (i.e. between 40% and 45%). This evidences that the system finds optimal to slightly oversize the electrolyser capacity, in order to provide additional flexibility to the system. Regarding hydrogen pipelines, the retrofitted ones present a capacity factor of around 10% for Germany, 20% for the UK and 87% for the Netherlands, while the new hydrogen pipeline connecting the Netherlands to the cluster 3 presents a capacity factor of 85%. This also justifies the trend shown in the reference scenario: Germany and the UK are not heavily dependent on imported hydrogen, and therefore invest in retrofitted pipelines due to their low CAPEX, in order to benefit from cheap hydrogen imports from offshore hubs when required. In contrast, the Netherlands imports a large amount of hydrogen from other NSR countries, thus importing offshore hydrogen production at a constant rate appears to be a cost-effective alternative.

Power and hydrogen high density (H2)

Regarding the scenario with high OWPP deployment density (**H2**), *Figure 17* shows the optimal investments in power (top) and hydrogen (bottom) infrastructure. Likewise in **H1**, it is clear that allowing hydrogen investments permit to integrate additional amounts of OWPPs. In this case, the total hub-connected OWPP capacity deployed adds up to 283 GW, compared to the 162 GW of **P2**. This additional OPWW deployment is mostly provided by floating wind in clusters 1, 6 and 7, as seen in *Figure 18*. Regarding HVDC interconnectors, in this scenario there is a deployment of 195.8 GW. This number is slightly lower than in **P2** (212.8 GW of HVDC). The main trigger of this reduction is the deployment of offshore electrolysers, which alleviates the need for investments in HVDC interconnectors.

Offshore hydrogen investments are considerable in this scenario, as shown at the bottom of *Figure 17*. We can see a deployment of 96 GW of offshore electrolysers, 73.8 GW of newly built hydrogen pipelines and 32.4 GW of retrofitted natural gas pipelines. The Netherlands is, again, the country with more investments in hydrogen infrastructure and imported hydrogen from the NSOG, and again, it does not seem cost-optimal for Denmark and Norway to be connected to the offshore hydrogen infrastructure. Likewise in **H1**, electrolysers work with relatively low capacity factors (33 %) providing flexibility to the energy system. Similarly, retrofitted gas pipelines present a capacity factor of around a 10 % in Germany, 20 % in the UK and 84 % in the Netherlands, while newly built hydrogen pipelines show a capacity factor of 87 % in the Netherlands.

Preprints (www.preprints.org) | NOT PEER-REVIEWED | Posted: 5 May 2022 doi:10.20944/preprints202205.0043.v1

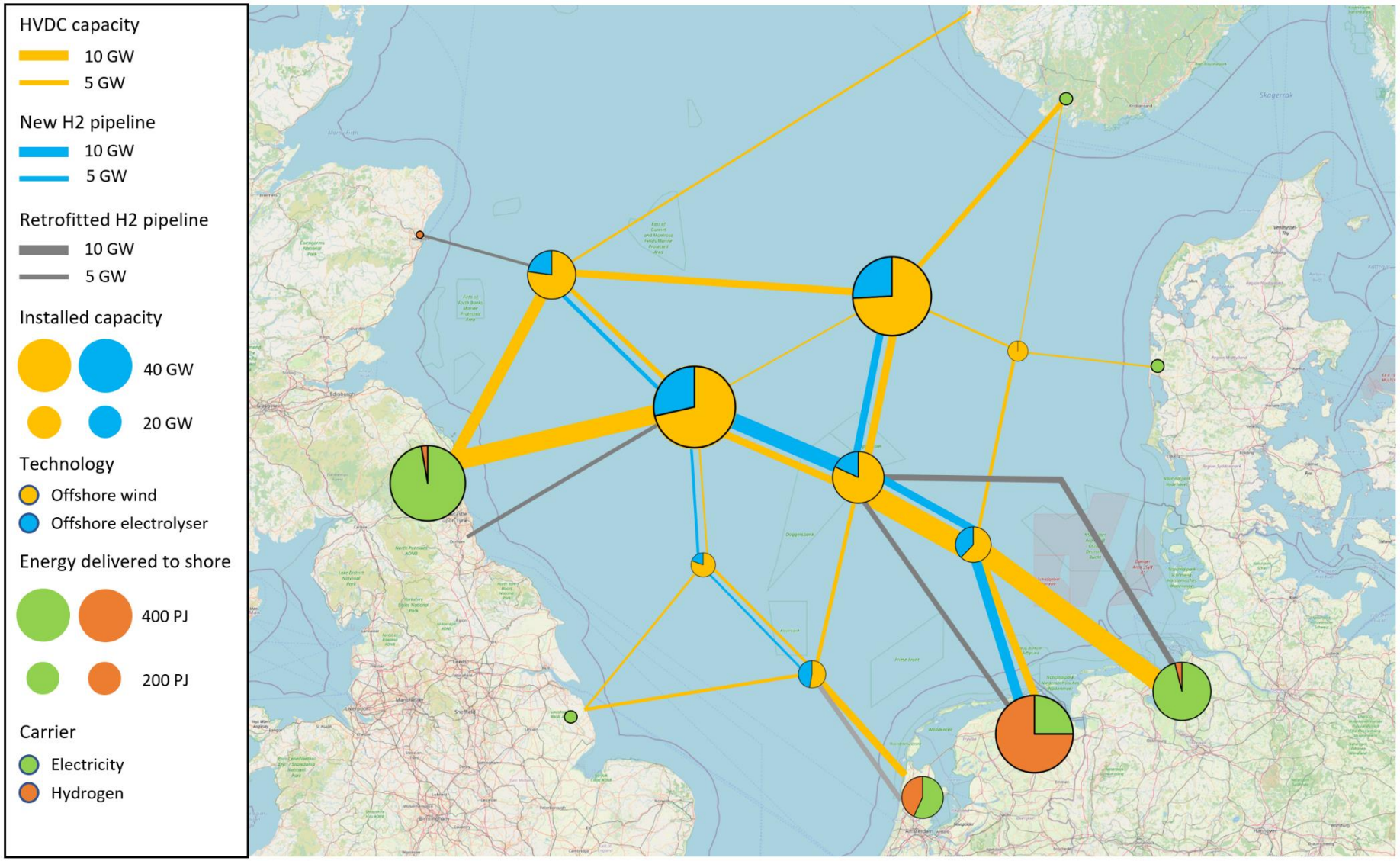

Figure 16: optimal investments in HVDC interconnectors and OWPP capacity and in electrolysers and hydrogen pipelines in H1.

Preprints (www.preprints.org) | NOT PEER-REVIEWED | Posted: 5 May 2022 doi:10.20944/preprints202205.0043.v1

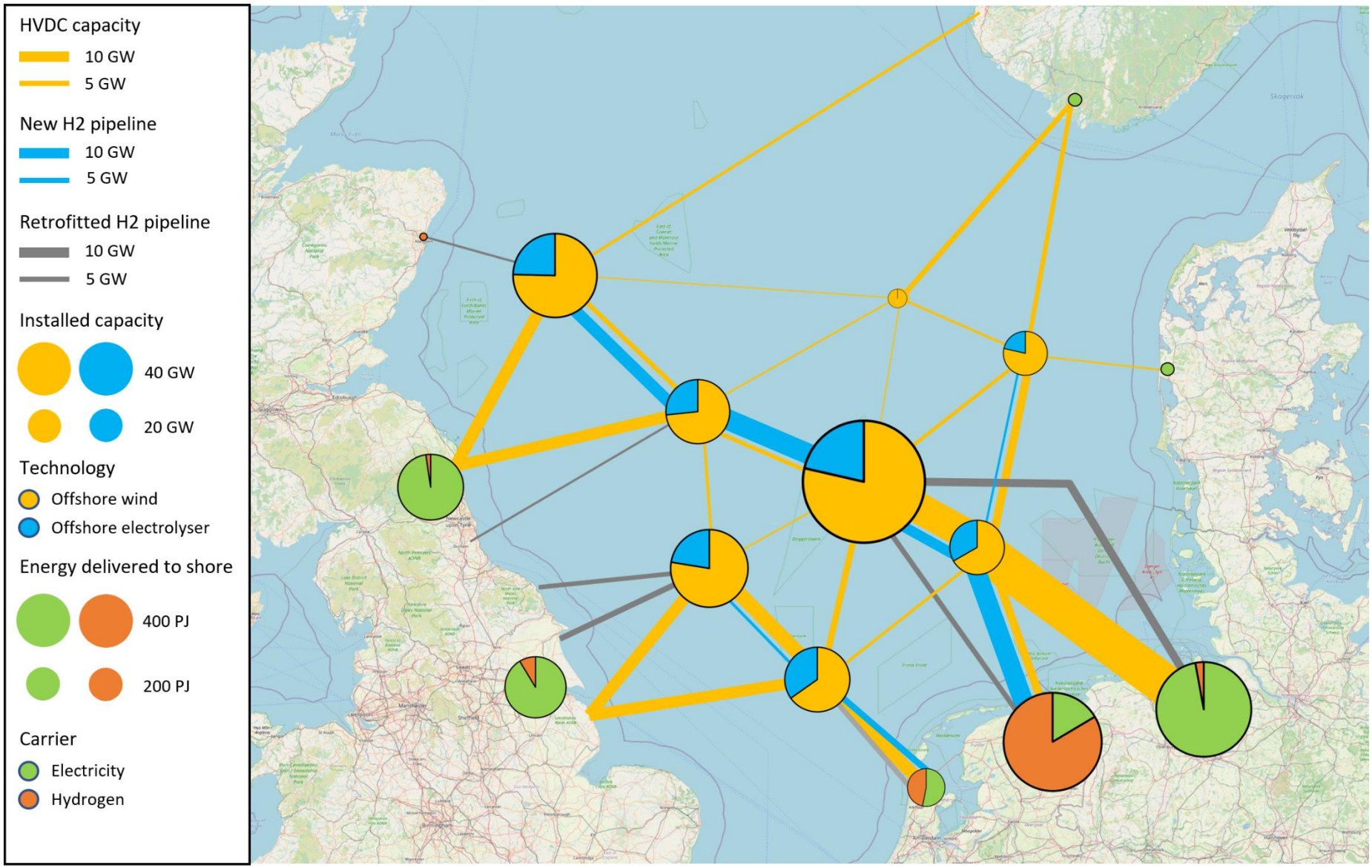

Figure 17:optimal investments in HVDC interconnectors and OWPP capacity and in electrolysers and hydrogen pipelines in H2.

Preprints (www.preprints.org) | NOT PEER-REVIEWED | Posted: 5 May 2022 doi:10.20944/preprints202205.0043.v1

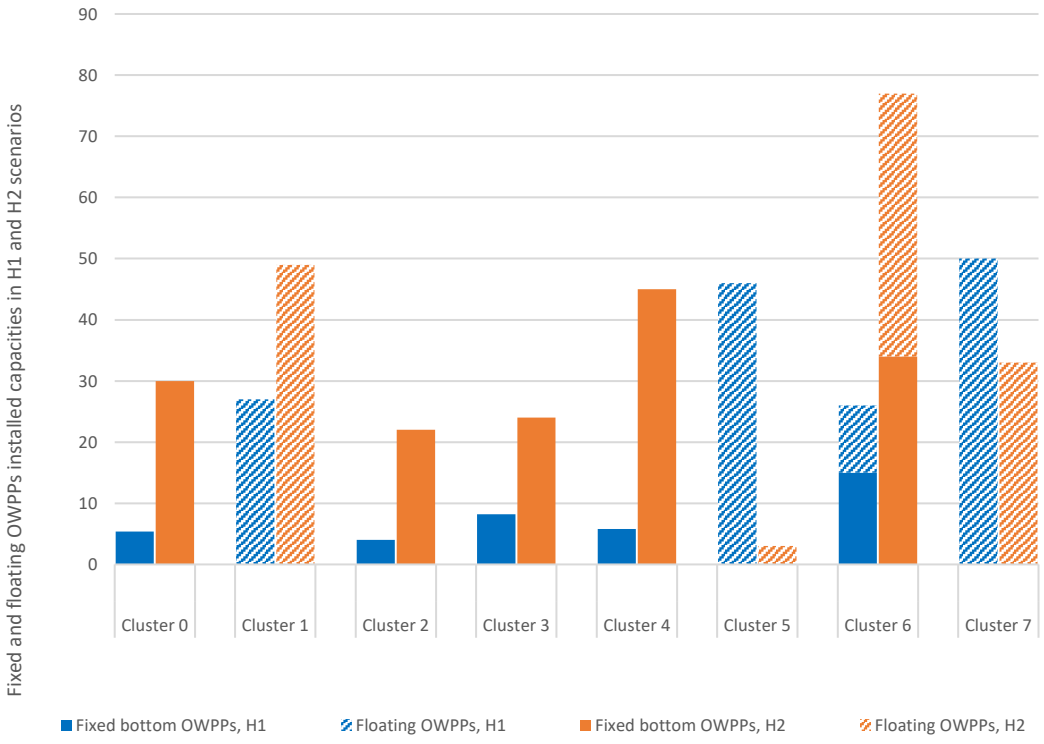

Figure 18: fixed-bottom and floating OWPPs installed capacities in the power and hydrogen NSOG scenarios

Even though in both scenarios there is a substantial deployment of offshore hydrogen infrastructure (i.e. offshore electrolysers and pipelines), it is relevant to put these numbers into context. *Figure 19* shows the total onshore and offshore hydrogen production volumes across the NSOG scenarios. When offshore electrolysers are allowed, the share of offshore hydrogen in the total hydrogen production ranges from 10% (**H1**) to 15% (**H2**). This outcome hints that, even though the contribution of offshore hydrogen can be beneficial to minimize the total system costs, the system still requires a large contribution of onshore hydrogen production (either via electrolysers or via natural gas reforming) to reach the net-zero mitigation target. Another relevant insight that can be derived from *Figure 19* is that hydrogen production offshore does not necessarily substitute the hydrogen production onshore, but it complements it.

Preprints (www.preprints.org) | NOT PEER-REVIEWED | Posted: 5 May 2022 doi:10.20944/preprints202205.0043.v1

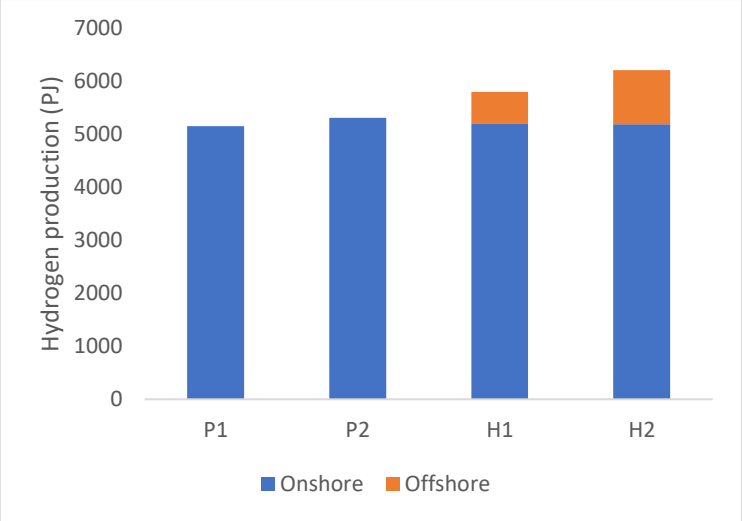

Figure 19: total onshore and offshore hydrogen production across the NSOG scenarios

Hydrogen storage needs onshore and offshore (short term and long term)

It is also relevant to quantify how much hydrogen storage is needed in 2050 to guarantee the hydrogen supply in all NSR countries. As shown in *Figure 19*, a highly decarbonised NSR energy system requires large amounts of hydrogen production (over 5 EJ). A part of this hydrogen is produced in-situ and directly used, and does not require storage. But a large part of the total hydrogen is produced in centralized facilities and distributed via a hydrogen network, requiring hydrogen storage to balance supply and demand.

As mentioned in the scenario definition and in the methodology, in the NSOG scenarios with offshore hydrogen production hydrogen can be stored either offshore (i.e. salt caverns within the buffer areas of the clusters) or onshore. *Figure 20* shows the size of the storage deployed in the offshore nodes while *Figure 21* shows the storage deployed onshore in all NSR countries.

The storage in offshore salt caverns is in both scenarios lower than the onshore hydrogen storage alternatives. In **H1**, the offshore storage volumes add up to 34 PJ, while this number increases to 59 PJ in **H2**. These numbers are marginal compared to the total hydrogen storage potential in the North Sea calculated in [31]. For example, in [31] the estimated hydrogen storage potential for the Netherlands is over 3000 PJ.

Preprints (www.preprints.org) | NOT PEER-REVIEWED | Posted: 5 May 2022 doi:10.20944/preprints202205.0043.v1

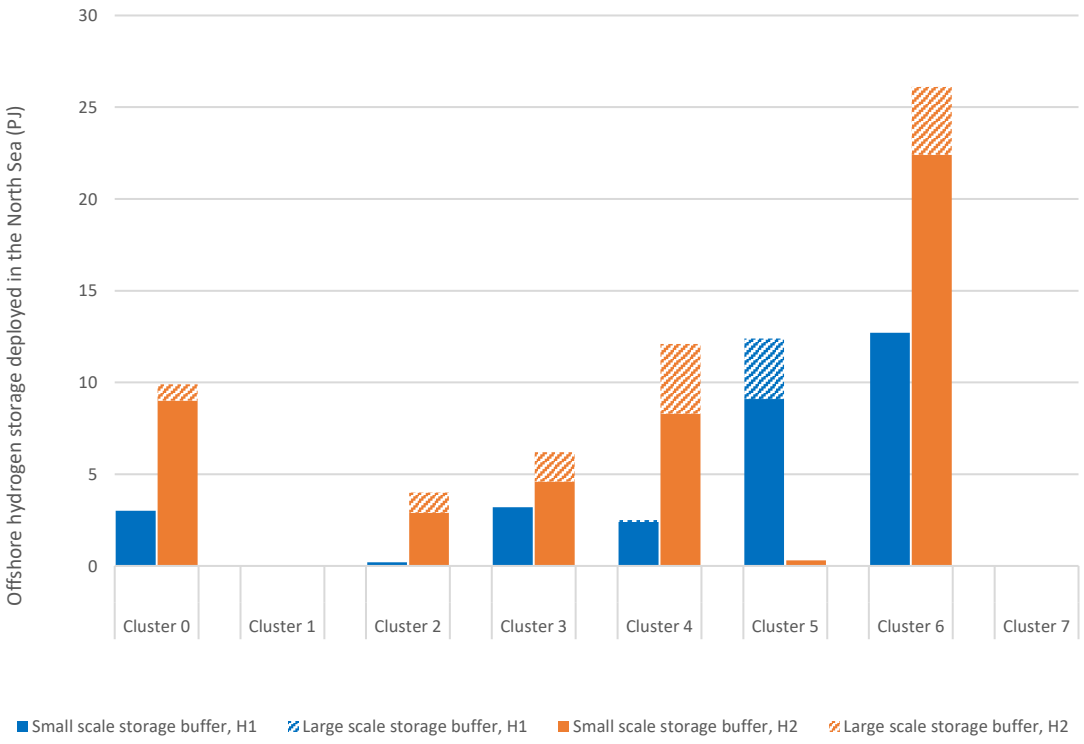

Figure 20: size (PJ) of the optimal hydrogen storage deployed in each of the offshore clusters

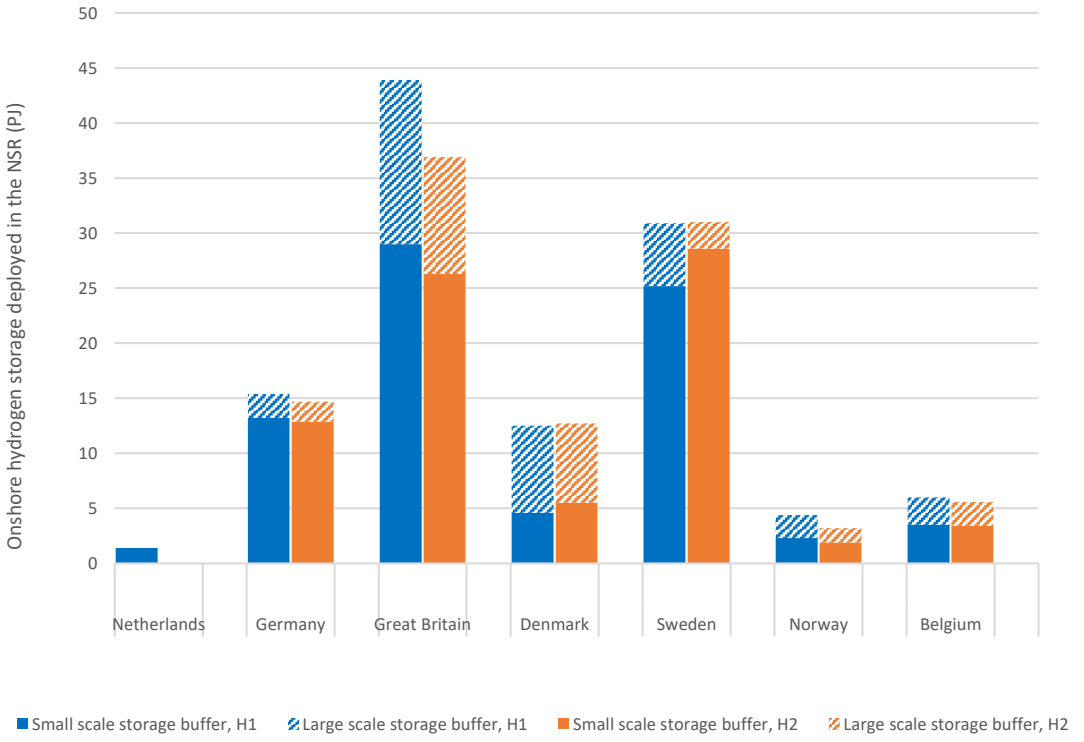

Figure 21: size (PJ) of the optimal hydrogen storage deployed in each NSR countries (onshore)

Preprints (www.preprints.org) | NOT PEER-REVIEWED | Posted: 5 May 2022 doi:10.20944/preprints202205.0043.v1

6. Sensitivity analyses

This section aims to explore different sensitivity analyses around selected key parameters, in order to complement the findings of the NSOG scenarios. The explanation, rationale and details about the sensitivities performed in this section are shown in *Table 8*.

Table 8: sensitivity analysis evaluated

Sensitivity analysis	Explanation	Rationale	Scenario modified
Different onshore wind social acceptance levels	The technical potential of onshore wind is varied from 20% of the maximum potential to 100% of the maximum potential.	Reaching the maximum technical potential of onshore wind entails a large use of onshore space. It is unclear that this large use of space will be socially accepted. In this context of low onshore wind deployment, the benefits of the NSOG might be multiplied because of the need of more offshore wind.	**H2**
Imports of hydrogen from regions outside the NSR are allowed	Imports of hydrogen from regions outside the NSR (e.g. North Africa or Middle East) are allowed at certain prices, ranging from 2 €/kg to 5 €/kg	As shown in previous scenarios, large amounts of hydrogen are necessary to reach the net-zero target by 2050 (see *Figure 19*). In these scenarios, hydrogen can only be produced and traded within the NSR. Thus, if hydrogen can be imported at a cheap price from external regions, the need for hydrogen production (and to some extent the need for renewable power) might be reduced.	**H2**

For the sake of simplicity, the results from the sensitivity analyses can be found in the supplementary material [27]. In this section we will briefly summarize the main findings and insights of each one of the sensitivities considered. The system cost implications are not covered in this section, as they are included in **Section 7**.

6.1. Different onshore wind social acceptance levels

- As expected, the lower the onshore acceptability of onshore wind is, the higher the deployment of offshore wind in the NSOG. In the base case, i.e., maximum potential of onshore wind, the total deployment of hub-connected OWPPs is 283 GW (128 GW of floating and 155 GW of fixed bottom). In the most constrained onshore scenario, i.e., 20% of the maximum onshore wind potential, the total deployment of hub-connected OWPPs is 449 GW (294 GW of floating and 155 GW of fixed bottom). Thus, it is observed that the lower availability of onshore wind is substituted by floating wind.

Preprints (www.preprints.org) | NOT PEER-REVIEWED | Posted: 5 May 2022 doi:10.20944/preprints202205.0043.v1

- The reduction of the onshore wind potential also entails an increase of offshore hydrogen production. This is quite intuitive: since onshore wind is one of the main low-carbon technologies used for green hydrogen production, when its availability is reduced, the system decides to invest in extra offshore wind, and either import electricity to the shore via the NSOG to feed onshore electrolysers, or produce hydrogen offshore. In the base case, i.e., maximum potential of onshore wind, the total offshore electrolyser capacity is 96 GW, while in the most constrained scenario, i.e., 20% of the maximum onshore wind potential, this capacity is increased to 150 GW. In terms of offshore hydrogen production, in the base case 890 PJ of offshore hydrogen are produced, while in the most constrained scenario this figure is increased to 1407 PJ.
- Another key consequence of the onshore potentials is the expansion of NSOG interconnectors. When the onshore wind acceptability is low (i.e. 20%), the optimal configuration deploys 340 GW of HVDC interconnectors in the NSOG, compared to the 200 GW of the base case. The reason is that, due to the reduction of onshore OWPPs deployed, additional NSOG interconnectors allow to integrate more floating OWPPs in the system, and increase the interconnection between Scandinavian countries (net importers in most of the scenarios) and the rest.

6.2. Hydrogen extra NSR imports allowed

- The availability of imports from outside of the NSR affects the cost-effectiveness of the NSOG. With the cheapest estimate for imported hydrogen (2 €/kg, including transport cost) the total deployment of OWPPs amounts to 53 GW (considerably lower than the 294 GW of the base scenario without hydrogen imports). This outcome is reasonable: as hydrogen can be imported directly from external countries, the need for low-carbon electricity is reduced, and therefore the investments in offshore wind are decreased. When the total import cost is fixed to 4 €/kg and above, imports of hydrogen from outside the NSR are marginal, and therefore the investments in the NSOG are similar to the base case.
- When cheap imports of hydrogen are available (i.e. 2 €/kg) the use of hydrogen in the NSR is considerably increased (9 EJ compared to the 6.2 EJ of the base scenario without hydrogen imports).
- Lastly, when hydrogen can be imported at cheap costs the production of hydrogen offshore is reduced substantially. In the scenario with imports of hydrogen available at 2 €/kg, only 78 PJ of offshore hydrogen are produced, and only retrofitted natural gas pipelines are used for offshore hydrogen transport (i.e. no investments in new hydrogen pipelines).

7. System cost analysis

The scenario analysis and sensitivities performed throughout the paper showed that it is cost-effective to invest in an NSOG architecture, either power-based or power-and-hydrogen

Preprints (www.preprints.org) | NOT PEER-REVIEWED | Posted: 5 May 2022 doi:10.20944/preprints202205.0043.v1

based. Thus, here we aim to identify the total system costs of all scenarios, in order to quantify the potential economic benefits of deploying the NSOG in different contexts.

As we mentioned in the model description, the IESA-NS model covers all the energy sectors of the NSR. Therefore, the total system costs that the IESA-NS model provides also cover all the sectors of the energy system. Thus, when evaluating cost differences between scenarios, very large figures (e.g. hundreds of millions of €) translate into small percentages in relative terms. As a consequence, with the total values it is difficult to quantify the benefits of changes in specific sectors (e.g. impact of the NSOG).

As the NSOG mainly affects the power sector, one alternative might be to compare the system costs solely of the power sector across different scenarios. However, this comparison could guide us to misleading conclusions. For example, in some scenarios, the NSOG might enable additional investments (hence costs) in offshore wind deployment, which could be used to decarbonise other sectors. In this case, the overall system costs might be smaller while the specific power system costs might be larger.

In order to solve this issue and find meaningful cost comparison across scenarios we propose to calculate a corrected system cost value. To this end, we evaluate the technological stocks that are constant across all the scenarios, and we subtract the system costs associated from these stocks. For example, it might happen that across all the scenarios the stocks related to the transport sector (e.g. road vehicles, airplanes and ships) are identical. Therefore, a considerable fraction of the total system cost might be baseline to all scenarios and remain unaffected by the NSOG. Thus, subtracting these 'static system cost' we can find a more meaningful relative increase/decrease in system costs across scenarios.

Base scenarios: REF vs P1 vs P2 vs H1 vs H2

First, we compare in *Figure 22* the total system cost of the four NSOG scenarios compared to the base case (i.e. the scenario without NSOG investments, **REF**). The benefits of **P1** are quite modest, i.e. 2.3 bn € savings (1% relative cost decrease). In the case of **P2**, the savings compared to the base case are multiplied, i.e. 8.7 bn € (4.1% relative cost decrease).

Investments in offshore hydrogen entail relevant reductions in system costs. In **H1** the system costs are reduced by 6 bn € (2.8% relative cost decrease), while costs are reduced by 14.9 bn € (7% relative cost decrease) in **H2**.

Preprints (www.preprints.org) | NOT PEER-REVIEWED | Posted: 5 May 2022 doi:10.20944/preprints202205.0043.v1

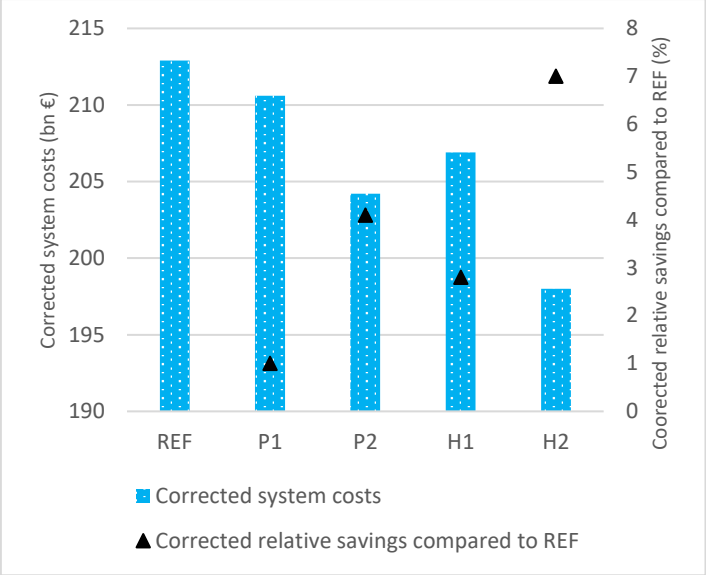

Figure 22: Difference in total system cost across the NSOG scenarios compared to the base case

Sensitivity analysis: onshore wind social acceptance

Regarding the onshore wind social acceptance sensitivity analysis, and in order to provide a meaningful system cost comparison, *Figure 23* provides the system cost values of each scenario with and without NSOG investments. Note that if we directly compare the system costs of different onshore acceptance levels (e.g. 20% vs 100% of maximum potential) we do not quantify the system cost benefits of the NSOG, which is the main focus of this paper.

As expected, the cost benefit of the NSOG concept is increased with lower onshore wind societal acceptance. In the most constrained scenario (onshore wind constrained to 20% of the base case) implementing the NSOG entails 29.2 bn € of system cost savings (11.6% relative cost decrease).

Sensitivity analysis: imports of extra NSR hydrogen

The system cost impacts of allowing imports of hydrogen from outside the NSR are shown in *Figure 23*. In absolute terms, the availability of hydrogen imports at 2 €/kg alleviates the system costs by around 78 bn €, due to its large penetration in the energy system (as mentioned in **Section 6**, at this price 9 EJ of hydrogen are used in the NSR). In relative terms, if this import price is available, the benefits of the NSOG are marginal (i.e. 0.9 bn €, which corresponds to a 0.7% of relative savings). The reason is that, at this price, the local hydrogen production via electrolysis is reduced, and therefore the need for low-carbon electricity is alleviated. Thus, less investments in offshore wind are optimal, and the benefits of a NSOG are almost negligible.

In line with the findings of **Section 6**, it can also be seen that, at prices over 4 €/kg, imported hydrogen is not competitive, and it does not affect the system costs. In other words, at prices over 4 €/kg the system prefers either to produce the hydrogen within the NSR, or to avoid its use in different sectors.

Preprints (www.preprints.org) | NOT PEER-REVIEWED | Posted: 5 May 2022 doi:10.20944/preprints202205.0043.v1

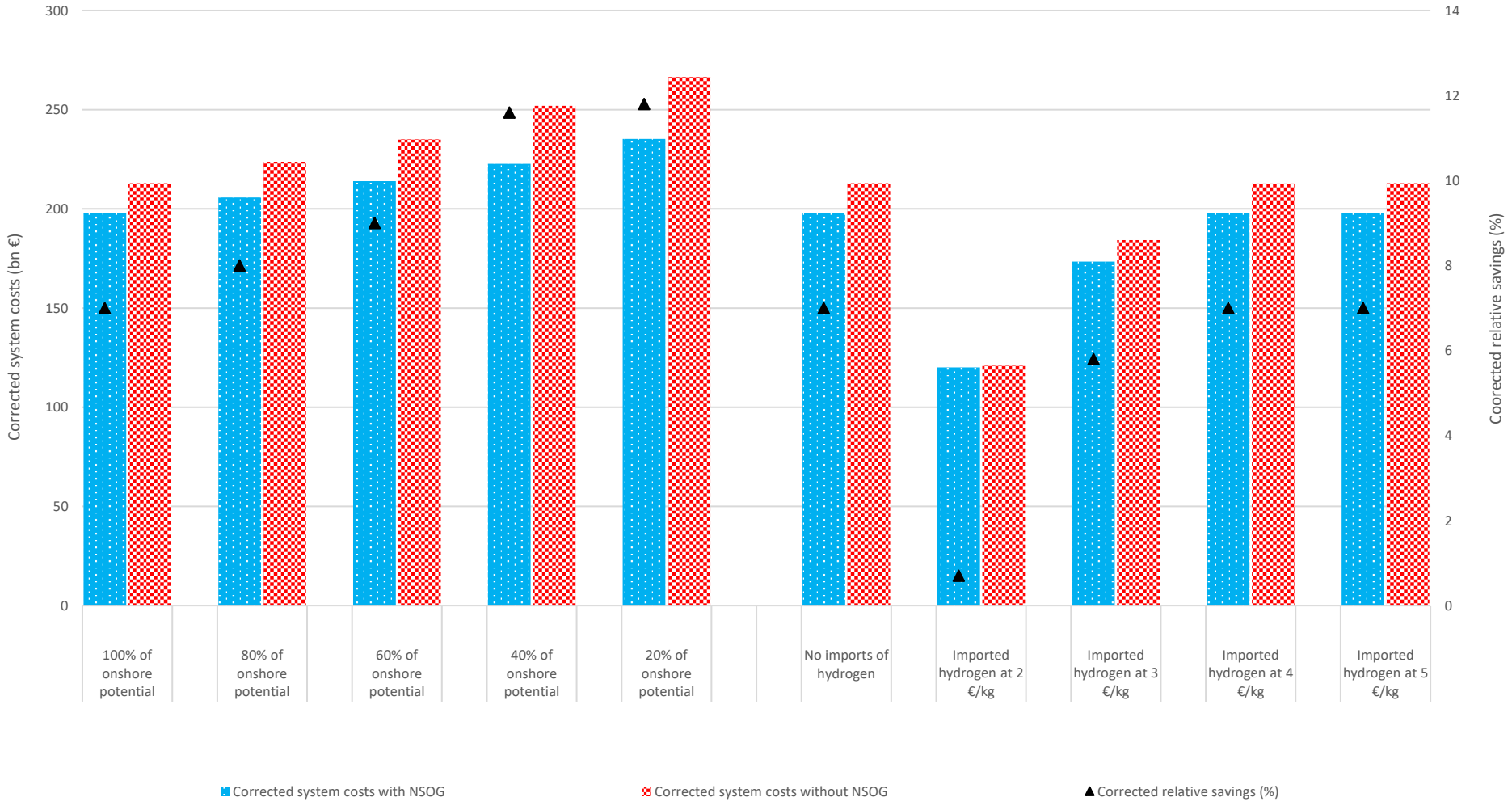

Figure 23: corrected system cost of the sensitivity analyses evaluated in this study

Preprints (www.preprints.org) | NOT PEER-REVIEWED | Posted: 5 May 2022 doi:10.20944/preprints202205.0043.v1

8. Conclusions

Overall, the outcomes of this paper show that the deployment of an NSOG is cost-effective and beneficial from a system perspective. We analysed five different scenarios: a base case, without investments in an offshore grid infrastructure (**REF**); two scenarios with investments in power assets, i.e. OWPPs and HVDC interconnectors (**P1** and **P2**); and two scenarios with investments in both power and hydrogen assets, i.e. offshore electrolysis and new/retrofitted hydrogen pipelines (**H1** and **H2**). In general, the NSOG concept permits to integrate larger amounts of OWPPs (up to 283 GW of HVDC connected OWPPs), increase the cross-border interconnectivity between NSR countries (up to 196 GW of HVDC interconnectors within the NSOG), and substantially reduce the total system costs (up to 14.9 bn €, 7% relative cost decrease).

Additionally, we presented in this paper a novel methodology to integrate Geographic Information Systems data and energy system models. We applied this methodology to the North Sea in order to identify nine offshore nodes, representing offshore hub locations, using high resolution spatial data of different offshore activities. This methodology could be implemented in other offshore areas in order to analyse in detail offshore energy system developments, for example in the Baltic Sea, the Gulf of Mexico or the Mediterranean Sea.

It is important to highlight the limitations of this study. First, the ecological impacts of the deployment of offshore hubs and energy infrastructure (e.g., HVDC cables or hydrogen pipelines) is not taken into account in the different NSOG scenarios. The impacts of these deployments in the ecosystem can be serious (see e.g., [32]). Further research should be carried on to assess the best layout of offshore infrastructure considering not only techno-economic parameters, but also potential ecological impacts. It is also important to mention that in this study we solely analyse optimal system configurations in 2050, and therefore transition pathways, progressive infrastructure developments and investment decisions in intermediate periods (e.g., 2030 or 2040) are not part of this study. Certain offshore technologies, such as wave energy, tidal energy or biomass from algae are not included in any of the scenarios. Additionally, we did not evaluate the space needs for offshore electrolyser deployment. In some scenarios there are large (up to 20 GW) deployments of electrolysers in offshore hubs. Additional research should evaluate how to properly integrate such large capacities in offshore hubs, and to evaluate whether this could entail additional offshore electrolysis costs. On top of that, even though the IESA-NS model captures to some extent interactions with the European power system, only the energy system of the NSR is optimized (e.g. power capacity expansion or decarbonisation of industry). The main consequence of this is that there is no external competition to the investments in the NSOG. For example, it might be the case that, in 2050, imports of electricity or hydrogen from neighbouring regions are cost-effective compared to produce them locally in the NSR. Additional research should be conducted at EU level to analyse these potential synergies at continental scale. Additionally, the need for hydrogen in the NSR in our scenarios is relatively high compared to reference EU level scenarios. The main driver for this high hydrogen use is that our scenarios include very ambitious decarbonisation targets, i.e. net-zero in 2050 including international transport and

Preprints (www.preprints.org) | NOT PEER-REVIEWED | Posted: 5 May 2022 doi:10.20944/preprints202205.0043.v1

industrial feedstock, and hydrogen is therefore heavily used to produce e-fuels and low-carbon feedstocks.

In terms of results, we first explored the benefits of a power-based NSOG (i.e. without investments in offshore hydrogen). Results show that a power-based NSOG can help to integrate 59.4-162 GW of hub-connected OWPPs (114.4-217 GW including the near shore, HVAC connected OWPPs), while increasing the HVDC interconnectors by 92.1-212.8 GW (scenarios **P1** and **P2**). Regarding system cost, the power-based NSOG concept can potentially reduce the NSR system costs by 2.3-8.7 bn €, representing a 1-4.1% corrected reduction of system costs, compared to the business as usual scenario (**REF**), where no NSOG is deployed. This range stresses the importance of a proper spatial planning and collaboration between NSR countries. While the **P1** scenario (i.e. low multi-use of space and reference OWPP deployment density) provides a modest reduction of system costs, in **P2** (i.e. increased multi-use of space and higher deployment density) the savings are multiplied.

We also evaluated the benefits of a power and hydrogen NSOG concept. Results show that a combined power and hydrogen NSOG permits to integrate 172-283 GW of hub-connected OWPPs (227-338 GW including the near shore, HVAC connected OWPPs), while increasing the HVDC interconnectors by 143-195.8 GW (scenarios **H1** and **H2**). Regarding system costs, the power and hydrogen NSOG concept can potentially reduce the NSR system costs by 6-14.9 bn €, representing a 2.8-7% corrected reduction of system costs. In line with the insights from **P1** and **P2**, this range exemplifies the need for a coordinated spatial planning in the NSR. Additionally, the system costs savings of **H1** and **H2** are considerably higher than the ones of **P1** and **P2**, pointing out that offshore hydrogen production can be beneficial from a system perspective, providing flexibility offshore (and therefore helping to integrate the variability of OWPPs), delivering hydrogen to onshore demand points via new and retrofitted infrastructure, and reducing the need for expensive HVDC interconnectors.

In relative terms, the share of offshore energy generation compared to primary energy use in the NSR ranges from 5% in **P1** to 14% in **H2**. Additionally, in **P1** the deployed OWPPs generate the 12% of all the renewable electricity in the NSR, while this number reaches 28% in **H2**. These numbers hint that the NSOG can produce a considerable amount of the low-carbon electricity required to meet the net-zero mitigation targets, but in any case, low-carbon onshore sources (mainly onshore wind and solar PV) are still dominant even in scenarios with over 300 GW of OWPPs deployed in the North Sea.

Via sensitivity analysis, we identified that the social acceptability of onshore wind has huge implications on the cost-effectiveness of the NSOG. Under stringent scenarios of low onshore wind acceptance (i.e. 20%-40% of maximum onshore wind potential available, limiting to 130-260 GW the onshore wind capacity potential in the whole NSR), the benefits of investing in the NSOG are more evident. In these cases, the absence of a NOSG increases the system costs by 29.2-31.4 bn€, representing a 11.6-11.8% corrected increase.

We also evaluated the role of imported hydrogen from outside the NSR at different prices. Results show that at prices over 4 €/kg, imported hydrogen is not competitive, and it does not penetrate in the energy system. At 2-3 €/kg its penetration in the energy system

 doi:10.20944/preprints202205.0043.v1

increases, minimizing the benefits of the NSOG and alleviating the need for low-carbon electricity. At 2 €/kg the import levels are so high that the NSOG does not play a role, and the investments in hub-connected OWPPs are marginal.

Overall, the main conclusion of this study is the need for coordination between NSR countries. As we saw, the NSOG concept requires the deployment of a vast energy infrastructure. Most of this infrastructure (e.g. HVDC interconnectors, offshore hubs or offshore electrolysers) is shared between different countries, and permits to increase the interconnectivity among them. Thus, coordinated policy making should take place, in order to create a stable legislative framework and to facilitate the required investments.

Acknowledgements

This work is part of the ENSYSTRA project, which was funded by the European Union's Horizon 2020 research and innovation programme under the Marie Skłodowska-Curie grant agreement No: 765515. The article reflects only the authors' view and the Research Executive Agency is not responsible for any use that may be made of the information it contains.

Preprints (www.preprints.org) | NOT PEER-REVIEWED | Posted: 5 May 2022 doi:10.20944/preprints202205.0043.v1

Appendix A: spatial clustering methodology

GIS spatial data

The activities considered for the GIS spatial analysis of this paper include telecommunication cables, pipelines, shipping routes, military areas, extraction of sand and gravel, oil and gas installations, marine protected areas, valuable and vulnerable marine areas, operational wind areas, scoping wind areas and fishing areas. All data sources, coverages and references are plotted in *Table 9*.

Table 9: offshore activities considered in the study and data sources, derived from [9]

Activity	Data source	Coverage
Telecommunication cables	EMODnet	North Sea
	Rijkswaterstaat geo-services	The Netherlands
	CONTIS BSH	Germany
	Marine Scotland NMP	Scotland
Pipelines	EMODnet	North Sea
Shipping - IMO	Rijkswaterstaat geo-services	The Netherlands
	CONTIS BSH	Germany
	Norwegian Coastal Administration	Norway
Shipping – Important shipping routes	EMODnet	North Sea
Military areas	Rijkswaterstaat geo-services	The Netherlands
	CONTIS BSH	Germany
	Marine Scotland NMP	Scotland
	UK Military Airfields Guide	UK
Aggregate extraction (sand, gravel)	EMODnet	North Sea
	Rijkswaterstaat geo-services	The Netherlands
	The Crown Estate	UK
	INSPIRE	Denmark
Oil and Gas installations	OSPAR	North Sea
	Oil and Gas Authoruty	UK
	NLOG	The Netherlands
Marine protected areas – Natura 2000	European Environmental Agency	North Sea
Valuable and vulnerable marine areas	Norwegian Environmental Agency	Norway
	Policy document on the North Sea 2016-2021	The Netherlands
	Marine Scotland NMPI	Scotland
Wind areas – operationals and authorised	OSPAR	North Sea
	Rijkswaterstaat geo-services	The Netherlands
	Marine Scotland NMPI	Scotland
Wind scoping areas	OSPAR	North Sea
	Rijkswaterstaat geo-services	The Netherlands
	Marine Scotland NMPI	Scotland
	Danish Energy Agency	Denmark
	Kartverket	Norway

Preprints (www.preprints.org) | NOT PEER-REVIEWED | Posted: 5 May 2022 doi:10.20944/preprints202205.0043.v1

Fishing intensity	OSPAR	North Sea
	Academic documentation	South of the North Sea

With the data derived from the sources of *Table 9* we can calculate the available area for new OWPP deployment, and the areas that are currently used for other purposes. But with that data we cannot estimate the share of space of these used areas that could be used for OWPPs deployment via multi-use of space. In [9], Gusatu et al. analysed the potential for multi-use between offshore wind farms and other marine uses per country, quantifying the capacity of OWPPs that could be deployed under different multi-use scenarios. *Table 10* shows the qualitative potential that [9] found for multi-use between offshore wind and different activities in the NSR countries. These estimations, together with the spatial data calculated from the *Table 9* data sources are combined to quantify the available space for OWPP deployment in different scenarios.

Table 10: potential for multi-use of space between offshore wind farms and other marine uses, derived from [9]

Multi-Use with Offshore Wind Farms	**The Netherlands**	**Germany**	**Denmark**	**Sweden**	**Norway**	**UK**
Fisheries	Medium	Low	Medium	Low	Low	High
Marine protected areas	Medium	Low	Medium	Low	Low	High
Military areas	Low	Low	Medium	Low	Low	Medium
Shipping – local routes	Medium	Medium	Low	Medium	Low	Medium
O&G	Medium	Low	Low	Low	Medium	Medium

Clustering algorithms for spatial data

The use of clustering algorithms applied to spatial data has gained momentum in recent years, as seen in [11]. Some of them are summarized in *Table 11*. The two most popular ones used in energy system models are k-means and max-p. Both algorithms are explained in detail in the following subsection of this Appendix. In short, max-p is more effective when clustering data that is geographically distributed across a territory, and when multiple parameters are considered. For example, in [33] Fleischer used the max-p algorithm to create homogeneous regions across Europe, using population data, solar and wind potential data and pumped-hydro storage capacity data. In that type of regionalization, where different parameters want to be clustered while ensuring contiguity, max-p has been proven to be more reliable than k-means [34]. In contrast, k-means is more effective when clustering purely geographical data. For example, in [35] Brown et al. clustered an European power network dataset (including 5586 HVAC lines, 26 HVDC lines and 4653 substations) using the geographical coordinate of each data point. Additionally, k-means works better with large amounts of data, and it is considerably faster than max-p.

Preprints (www.preprints.org) | NOT PEER-REVIEWED | Posted: 5 May 2022 doi:10.20944/preprints202205.0043.v1

Table 11: summary of relevant spatial data clustering algorithms, derived from [11]

Clustering method	Contiguity	Number of nodes	Data tractability	Comments and additional information
K-means	Not ensured	User defined	High	There are multiple heuristics to solve it, and it is overall pretty reliable and fast. However, resulting regions are not ensured to be contiguous.
Spatially constrained k-means	Ensured	User defined	High	If the contiguity constraint is very hard the homogeneity does not participate in the cluster definition, and therefore clusters are purely geographical.
Max-p	Ensured	Algorithm defined	Medium	It ensures contiguity and data homogeneity, but with large datasets the problem becomes intractable.
K-means++ with max-p	Ensured	Algorithm defined	High	It needs multiple steps and links between k-means++ and max-p, and it is challenging to automatize it.

K-means description

K-means is a very popular algorithm in data science. It was first introduced in [36], and in the last decades multiple variations and improvements have been built on top of it. Formally, the traditional k-means method can be described as a minimization problem, as described in Equation 1.

$$\min_{S} \sum_{i=1}^{k} \sum_{x \in S_i} |x - \mu_i|^2 \qquad \text{Eq. 1}$$

Being k the (desired) number of clusters, S_i each cluster, $x \in S_i$ each observation x included in a cluster S and μ_i the mean of the observations in S_i.

The main benefit of k-means is that, although it is considered a computationally difficult problem (NP-hard), it can manage large amounts of data and converge relatively quickly, due to the fact that multiple algorithms to solve it have been developed in the past. Another advantage is that it has been used extensively and there is a large literature about it, and therefore it can be considered a reliable method.

As k-means is not an algorithm designed explicitly for spatial clustering, there are different shortcomings when defining regions using it. The most relevant one is that the regions delivered from the standard k-means (i.e. Equation 1) do not ensure contiguity. For example, if k-means is used with a dataset of solar potentials across Europe, it will group together the

Preprints (www.preprints.org) | NOT PEER-REVIEWED | Posted: 5 May 2022 doi:10.20944/preprints202205.0043.v1

data values that are more similar to each other, in order to have homogeneous clusters (that is, in Equation 1, every solar potential $\boldsymbol{x}$ will be included in a cluster where the mean of solar potential data $\boldsymbol{\mu_i}$ is as similar as possible). One alternative to ensure contiguity between regions using k-means is the one applied in [35], where the data used for the clustering stage is purely geographical. In [35] Brown et al. clustered a European power network dataset (including 5586 HVAC lines, 26 HVDC lines and 4653 substations) using the geographical coordinate of each data point. As a consequence, it is ensured that every point will belong to the nearest cluster. The drawback of this approach is that the resulting clusters only consider geographical data, so other features of the dataset are not taken into account, and therefore the homogeneity of the resulting clusters is not considered.

Another alternative to ensure contiguity with k-means is to include a contiguity constraint in the minimization problem (for instance penalizing distance in the objective function). In this case, clusters are defined according to a certain parameter (for instance, solar potential, as mentioned before) while ensuring spatial contiguity. However, the fact of enforcing this spatial contiguity might lessen the homogeneity of each cluster (in other words, the penalty in the objective function would affect more than the parameter itself), and it is in general not recommended [37].

Other problem with k-means is that, due to the fact that It is a NP-hard problem and convergence to the global optimum is never guaranteed, it might provide results that are arbitrarily bad compared to the optimal clustering. In order to improve that, Arthur et al. [38] proposed a variation, named k-means++, in which the initial values for the iteration are chosen following a methodology.

Max-p description

The max-p regions problem was introduced by Duque et al. in [38]. According to the authors, the max-p problem entails the aggregation of a number of areas into a certain number of homogeneous regions, ensuring that each of the resulting regions satisfies a minimum threshold value, like for instance the energy demand per region. In this method, the resulting number of regions (clusters) is not defined by the user. The max-p problem is presented in [38] as a minimization problem. The objective function is shown in Equation 2.

$$\min \; \boldsymbol{Z} = \left(-\sum_{\boldsymbol{k}=\boldsymbol{1}}^{\boldsymbol{n}} \sum_{\boldsymbol{i}=\boldsymbol{1}}^{\boldsymbol{n}} \boldsymbol{x_i^{k0}} \right) \times \boldsymbol{10^h} + \sum_{\boldsymbol{i}} \sum_{\boldsymbol{j}|\boldsymbol{j}>\boldsymbol{i}} \boldsymbol{d_{ij} t_{ij}} \qquad \text{Eq. 2}$$

Where $\boldsymbol{k}$ is the index of potential regions, $\boldsymbol{i}$ is the index of areas, $\boldsymbol{x}$ and $\boldsymbol{t}$ are decision variables, $\boldsymbol{d}$ is a dissimilarity relationship between areas and $\boldsymbol{h}$ is a parameter calculated from $\boldsymbol{d}$. The max-p problem is completed with a set of 7 constraints, more information and details of the formulation, parameters, variables and heuristics to solve it can be found in [38].

One of the problems of the p-max algorithm is that the number of resultant regions is not defined by the user, as it is delivered by the algorithm. However, the number of regions is highly correlated with the minimum threshold, and this threshold is an input to the model. Therefore, a wise choice of the threshold values can permit to constrain and estimate the number of regions that the algorithm will deliver. Another drawback is that max-p cannot handle large amounts of data. As described in [38] the formulation of max-p is a mixed integer

Preprints (www.preprints.org) | NOT PEER-REVIEWED | Posted: 5 May 2022 doi:10.20944/preprints202205.0043.v1

problem (MIP) with $3n + (n-1)n^2 + n\frac{n^2-n}{2}$ constraints and $(n-1)n^2 + \frac{n^2-n}{2}$ variables, and therefore when the number of areas n increases the problem becomes computationally intractable.

The max-p algorithm is very effective when clustering data that is geographically distributed across a territory. For example, in [34] Getman et al. compared the performance of k-means and max-p when clustering a large spatiotemporal dataset of solar resource data in Colorado. The dataset had a resolution of 10x10 km2. The clusters provided by both approaches where assessed calculating two measures of consistency: sum of squares within (SSW), and R2. According to these metrics max-p performed better than k-means. The reason is that k-means considered only the geographical coordinates of each data point, and therefore resulting clusters did not take into account the homogeneity of the solar resource within the cluster. Additionally, due to the fact that contiguity was not hardly imposed, some clusters included disconnected data points. The main conclusion that can be inferred from this study is that, with datasets that are spatially continuous, like solar or wind potentials, max-p is preferable over k-means if the computational complexity of the problem is tractable. K-means is therefore more suitable for discrete datasets, where there is no continuity and where geographical distances are more important than data homogeneity within the cluster[9].

Combination of K-means++ and max-p

As mentioned before, both k-means and max-p have been successfully applied for spatial clustering, but they have different strengths and weaknesses. In [37] Siala et al. propose a methodology in which both of them are combined, so their strengths are combined and their weaknesses are diluted.

The methodology is designed for cases in which contiguity between clusters and homogeneity within clusters is required, and the input dataset is too large, so that p-max cannot handle it. Therefore, what is proposed is to apply k-means++ and max-p sequentially. The complete methodology is fully described in [37], and the open source implementation can be found in [39]. In a simple way, the methodology first divides the input data in smaller, then applies the k-means++ algorithm to every cell, to finally apply the max-p method. After that, the resulting clusters of every cell are put together, and if necessary another max-p clustering can be applied to the whole map in order to get a more reduced number of clusters.

Other methods

The literature of spatial clustering methods is extensive, and it is not the intention of this paper to review every single methodology in detail. For a more detailed review the reader is forwarded to [40] where 26 spatial data clustering methods are described.

Out of the methods not covered in this section, there are two that deserve a highlight: Skater, which stands for Spatial 'K'luster Analysis by Tree Edge Removal, and it was presented by Assunção et al. in [41], and Redcap, which stands for REgionalization with Dynamically Constrained Agglomerative Clustering And Partitioning, and was presented by Guo in [41].

[9] For example, a dataset of operating windfarms is not continuous, it is formed by discrete points with certain coordinates. When clustering, we most likely want to group wind farms that are close to each other rather than clustering wind farms that are far away but are similar in certain features.

Preprints (www.preprints.org) | NOT PEER-REVIEWED | Posted: 5 May 2022 doi:10.20944/preprints202205.0043.v1

Clustering methods used in available spatial data analysis software

In the previous subsections we mentioned some of the methods used in the literature for spatial data clustering. However, there are some available software and tools that already incorporate some of these methods within their toolboxes. In this subsections we will discuss which methods are used in geographic information system (GIS) software and in the GeoDa tool[10], an open source spatial data analysis tool.

GIS analyses have been applied for the last 60 years to multiple types of fields, like mapping, urban planning, environmental impact analysis or disaster management and mitigation. The application of GIS in energy system modelling can be beneficial to understand geospatial challenges, but as of today, as described in detail in [41][11], this interaction is in an early phase and should be further developed.

There are multiple GIS tools which are widely used nowadays, like ArcGIS[11] or QGIS[12]. GIS tools usually include within their features clustering options that are useful to process large spatial datasets. Most of these clustering methods can be divided in two categories: density based clustering, and multivariate clustering.

Density based clustering methods are exclusively based on spatial distribution. The aim is to detect areas where points are concentrated, separated by areas with no (or low) data points. Points within the search distance of every cluster are included, while points outside are considered noise. ArcGIS includes this method named “density-based clustering”, and it uses three different algorithms: DBSCAN, HDBSCAN and OPTICA. QGIS includes it named “DBSCAN clustering”, and it uses the algorithm DBSCAN.

Multivariate clustering methods generate the clusters according to user-defined features. The number of clusters to create is also given by the user, and the algorithm will provide a solution in which the features within a cluster are as homogeneous as possible, and each cluster is as different to the others as possible. Both ArcGIS and QGIS have multivariate clustering methods within their tools, in both cases based on the k-means algorithm. One of the main drawbacks is that the resulting clusters do not ensure contiguity, as the attributes used to generate the clusters do not necessarily include geographical data. If contiguity is required the k-means algorithm can be spatially constrained, as mentioned in the k-means subsection. Both ArcGIS and QGIS include in their toolbox spatially constrained versions of the multivariate clustering method, in the case of ArcGIS using Skater instead of k-means.

The GeoDa tool is one of the most popular software for spatial data analysis and geovisualization, having more than 300,000 users as of August 2019. It is open source and it includes multiple cluster techniques: non-spatially constrained methods, like k-means or hierarchical clustering; and spatially-constrained methods, like spatially-constrained k-means, skater and max-p.

The GeoDa tool has a very complete and comprehensive open documentation , including description of all their algorithms, codes used and a step-by-step user guide, so for more information and details the reader is forwarded to the GitHub repository of GeoDa in [42].

[10] geodacenter.github.io
[11] Arcgis.com
[12] Qgis.org

Preprints (www.preprints.org) | NOT PEER-REVIEWED | Posted: 5 May 2022 doi:10.20944/preprints202205.0043.v1

Comparison of methods and tools

Table 12 and *Table 13* summarize the information provided during this section, comparing different clustering methods according to their features, and assessing which algorithms are present in different available spatial analysis software.

Table 12: Comparison of features of selected spatial data clustering methods. *Although it is not possible to define the number of clusters beforehand, a wise choice of the minimum threshold is a good indicator

Clustering method	Contiguity	Number of nodes	Data tractability	Comments and additional information
K-means	Not ensured	User defined	High	There are multiple heuristics to solve it, and it is overall pretty reliable and fast. However, resulting regions are not ensured to be contiguous.
Spatially constrained k-means	Ensured	User defined	High	If the contiguity constraint is very hard the homogeneity does not participate in the cluster definition, and therefore clusters are purely geographical.
Max-p	Ensured	Algorithm defined*	Medium	It ensures contiguity and data homogeneity, but with large datasets the problem becomes intractable.
K-means++ with max-p	Ensured	Algorithm defined*	High	It needs multiple steps and links between k-means++ and max-p, and it is challenging to automatize it.

Table 13: Comparison of features of selected spatial data tools. **ArcGIS includes a "density based clustering" which provides similar results

Software	k-means	Spatially constrained k-means	Max-p	K means with max-p	SKATER	Redcap
ArcGIS	Included as "multivariate clustering"	Not included**	Not included	Not included	Included as "spatially constrained multivariate clustering"	Not included
QGIS	Included as "attribute based clustering"	Not included	Not included	Not included	Not included	Not included
GeoDa	Included	Included	Included	Included	Included	Included

Choice of the number of offshore nodes: elbow method and 80 km heuristic

As mentioned, in the k-means algorithm the number of nodes is an user-defined input. Finding a proper value for the number of clusters with k-means is not straightforward. Therefore, it is necessary to find certain heuristics to find the appropriate number.

In this paper, we use two different heuristics to find the proper number of nodes. The first one is the popular elbow method, exemplified in *Figure 24*. In the elbow method, the k-means algorithm is run with a wide range of target nodes. When plotting the average dispersion versus the number of nodes, there is usually an inflexion point (elbow) were increasing the number of nodes does not entail a notorious reduction of the dispersion. Therefore, the elbow represents an 'optimal' point were increasing the system resolution (in our case, the spatial resolution of the NSR) does not entail a large improvement of the clusters dispersion (in our case, a reduction of distances from the offshore wind farms to the central hubs).

Preprints (www.preprints.org) | NOT PEER-REVIEWED | Posted: 5 May 2022 doi:10.20944/preprints202205.0043.v1

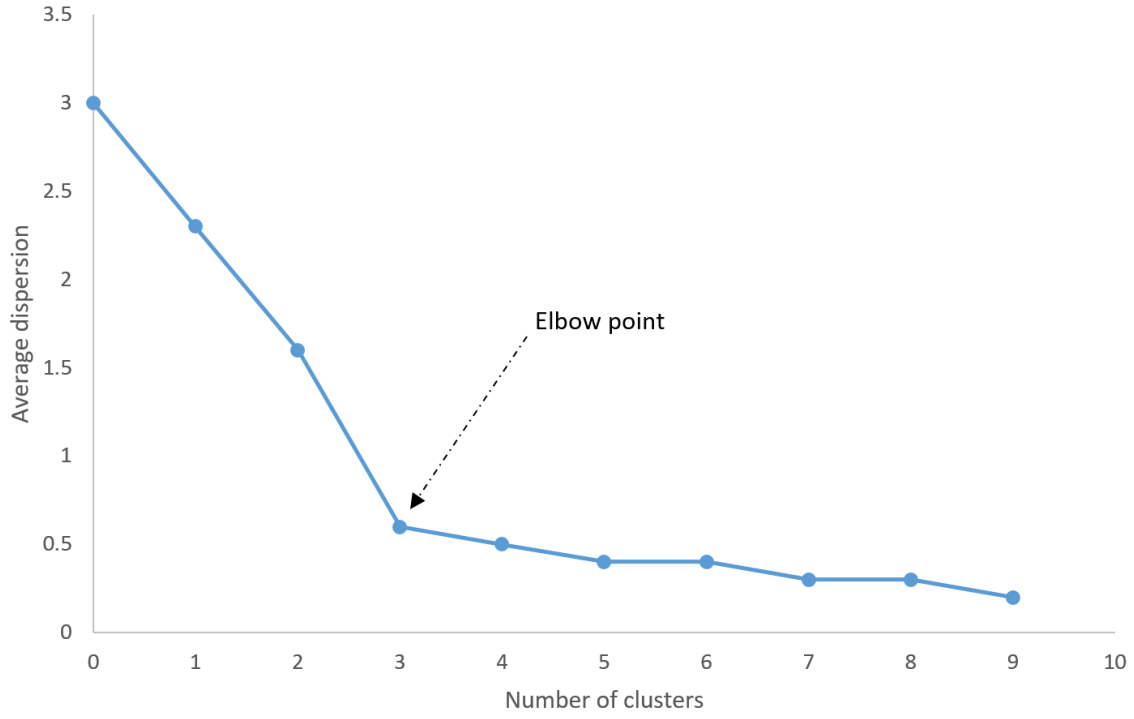

Figure 24: elbow method representation

The second heuristic that we use in this paper is the '80 km' heuristic. In the related literature, 80 km is usually the tipping point were HVDC interconnectors are more cost-effective than the HVAC ones. As said before, the main idea behind the 'best cluster configuration' is to represent offshore hubs, connected via HVDC to different countries. The offshore wind farms surrounding these hubs should naturally be connected to them via HVAC, and therefore it should be desirable that each cluster groups offshore wind farms closer than 80 km. Therefore, this heuristic -similarly to the elbow method- plots, for every number of nodes, the number of offshore wind farms that fall further than 80 km to the cluster centroid.

Appendix B: IESA-NS model description

The IESA-NS model has been developed based on the IESA-Opt framework, which was thoroughly described in [21]. The IESA-Opt model was initially developed to cover in detail the energy system of the Netherlands, filling multiple knowledge gaps that most integrated energy system models in the literature present [23]. For the purpose of this paper, the IESA-Opt model is enhanced, in order to cover the whole NSR with a high level of detail, including a detailed representation of the energy system of the Netherlands, Germany, Denmark, Sweden, Norway, the United Kingdom and Belgium.

Additional information and more details about assumptions, background and relevant sources can be found in the IESA-Opt methodological publication [43][21]. The goal of this section is to summarize the main capabilities of the new-built IESA-NS and to briefly describe its data inputs and outputs.

Preprints (www.preprints.org) | NOT PEER-REVIEWED | Posted: 5 May 2022 doi:10.20944/preprints202205.0043.v1

The IESA-NS model is a cost-optimization model, formulated as a linear problem (LP), that, in short, optimizes the long term investment planning and short term operation of the NSR energy system. The model can optimize multiple periods simultaneously (and therefore can be used to analyse single year optimization scenarios or transition pathways towards 2050), accounts for all the national GHG emissions and includes a thorough representation of all the sectors of the energy system.

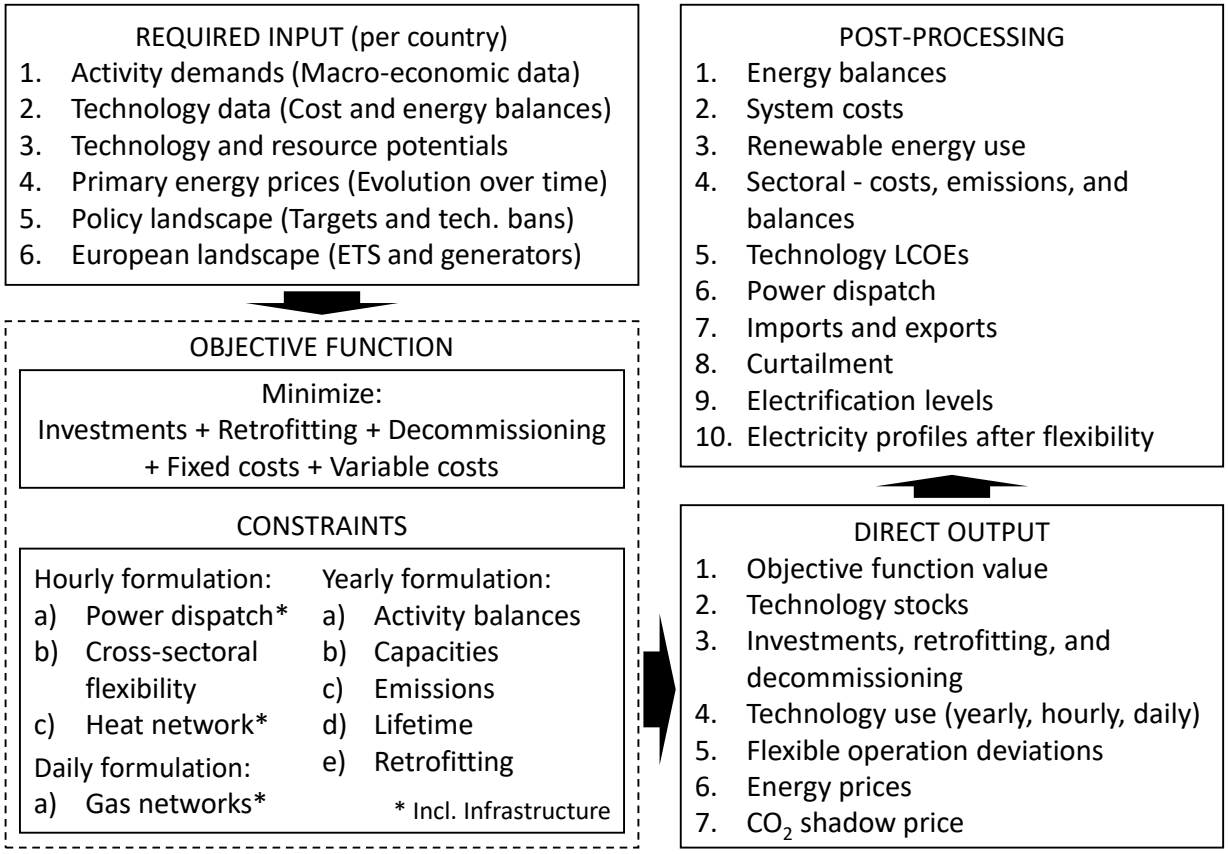

Figure 25: Methodological elements in the IESA-NS framework

Figure 25 shows a brief flowchart summarizing the methodological elements and steps followed by the IESA-NS model. As seen, there are mainly 6 different required inputs: activity demands, driven by macro-economic data; technology data in order to create the technology portfolio; available potentials of multiple resources and technologies; primary energy prices; national mitigation targets and specific technology bans; and finally data for the European power system, which is also endogenously represented in the system.

As mentioned, the IESA-NS model is formulated as an LP, whose objective function comprises the minimization of investments, retrofitting costs, decommissioning costs and both fixed and variable operation costs. The formulation presents a wide range of constraints to ensure that the optimal system configuration is feasible and respects different physical and theoretical boundaries.

One of the interesting features of the IESA-NS model is that its formulation includes different temporal resolutions. The power sector and the heat networks are optimized with hourly resolution, allowing to properly capture the intermittency of variable renewable sources, and

Preprints (www.preprints.org) | NOT PEER-REVIEWED | Posted: 5 May 2022 doi:10.20944/preprints202205.0043.v1

the dynamics of short and long term energy storage, among others. The multiple cross-sectoral flexibility options that the model includes (e.g. demand shedding, load shifting, flexible CHPs) are also formulated with hourly resolution. The gas and hydrogen network are modelled using daily resolution. Finally, some other constrains are formulated with yearly resolution, like the activity balance (i.e. the system should satisfy all the exogenous demands driven my macro-economic trends), certain system capacities, retrofitting decisions or the technology lifetimes.

The optimization process provides a plethora of direct results, like the optimal objective function value, all the technology stocks and their operation levels, the investment, retrofitting and decommissioning decisions, the operation of the flexible technologies, including their deviation from their reference profiles, the different energy prices, and all the CO2 shadow prices. Moreover, the IESA-NS model includes a thorough post processing that permits to analyse, among others, the energy balances, system costs, use of renewables, emissions, levelized costs of electricity (LCOE), hourly power dispatch in every node of the system, imports and exports dynamics, curtailment and electrification levels, and many more. All the data can be visualized in the tailor-made online user interface of the model [27].

As mentioned, the IESA-NS model is defined by activities and technologies. The activities are exogenous parameters, linked to macro-economic data and estimations, while the technologies are the tools that the model has to satisfy these activities. The whole list of activities and technologies can be found in the different databases attached as supplementary material or in [27].

Figure 26 describes the list of activities that is part of each country of the NSR in the IESA-NS model. The driver activities are the exogenous demand volumes corresponding to the residential, services, agriculture, industry and transport sector, together with aggregated emissions not fully contained in the energy system (and modelled with MACC curves). The model, with these demand volumes, decides which of the available technologies should be used to satisfy these demands. The use of technologies entails (sometimes) direct CO2 emissions, and certain energy requirements (either primary energy or processed energy). This processed energy has to be provided by endogenous energy activities, and the model has also to select which process is optimal to do so. For example: if there is an exogenous transport demand, and the model decides to satisfy it with an electric car, there will be an endogenous demand for electricity to power this car. Therefore, the model has to decide which process is optimal in order to supply this electricity.

Preprints (www.preprints.org) | NOT PEER-REVIEWED | Posted: 5 May 2022 doi:10.20944/preprints202205.0043.v1

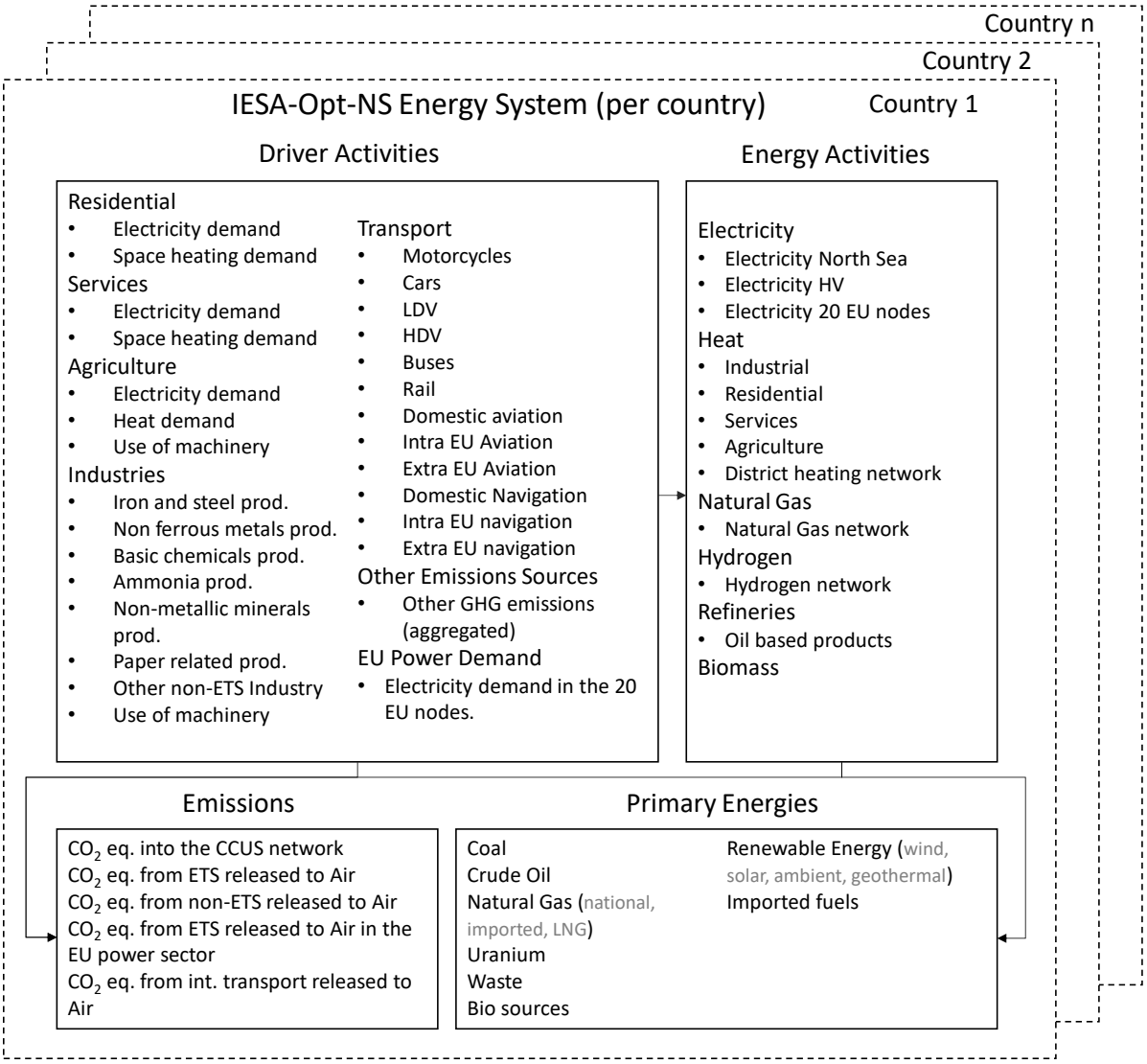

Figure 26: Energy system representation of activities considered within the IESA-NS framework

The IESA-NS model has been calibrated following multiple different reliable sources, in order to align the outcomes of the base year (2020) with real data. Data sources used for calibration included the IEA and the Eurostat energy balance sheets. The latest calibration of the IESA-NS model took place in spring 2021, with realized data from 2019.

Appendix C: Model formulation

Nomenclature of the model

Indexes

Symbol	Description
p	Index of the set conformed by all the modelled periods
h	Index of the set conformed by all the hours in a year
d	Index of the set conformed by all the days in a year
n	Index of the set conformed by all the nodes representing integrated energy systems
a	Index of the activities set

Preprints (www.preprints.org) | NOT PEER-REVIEWED | Posted: 5 May 2022 doi:10.20944/preprints202205.0043.v1

$Symbol$	Description
ae	Index electricity related activities subset, A^e
ah	Index of the national heat related activities subset, A^h
ag	Index of the gas related activities subset, A^g
t, t_i, t_j	Indexes of the technologies set
te	Index of the technologies representing air released emissions in the considered target scope.
td	Index of the dispatchable technologies subset
tp	Index of the operation technologies subset
tf	Index of the flexible technologies subset
tf_b	Index of the flexible technologies of the battery type subset
tc	Index of the flexible CHP technologies subset
ts	Index of the shedding technologies subset
ti	Index of the infrastructure technologies subset

Parameters

$Symbol$	Description
$VC_{t,p}$	The variable cost of a technology in a period
α_t	Annuity factor of a technology (or in this case the inverse)
$IC_{t,p}$	Investment cost of a technology in a period
DF_t	Fraction of the capital cost of a technology that remains after premature decom
$RC_{t_i,t_j,p}$	Retrofitting cost from one technology to another
$FC_{t,p}$	Fixed operational cost of a technology in a period
$AP_{t,a,p}$	Activities inputs and outputs profile of a technology
$V_{a,p}$	Exogenous required activity volumes in a period
Γ_t	Available use of a technology per unit of capacity
E_p	Absolute CO_2 emission target in a certain period.
RM_{t_i,t_j}	Binary matrix specifying which technologies can be retrofitted into others
$S^{min}{}_{t,p}, S^{max}{}_{t,p}$	Minimum and maximum allowed installed capacities of a technology in a year
$P_{h,tp}$	Hourly availability or reference operational profile of a technology
$AE_{t,a}$	Binary parameter indicating the hourly electricity activities of a technology
$R^{dw}_{td,p}, R^{up}_{td,p}$	Ramping up and down limits of hourly dispatchable technologies
η_{tc}	Only-heat reference efficiency of a flexible CHP
ε_{tc}	Only-power reference efficiency of a flexible CHP
SC_{ts}	Power shedding of a technology per unit of capacity
$UtP_{ts,p}$	Use-to-power ratio of a shedding technology in a period
SF_{ts}	Maximum allowed shedding fraction of a shedding technology
$AG_{tf,a}$	Binary parameter indicating the gas activities of a technology
FC_{tf}	Flexibility capacity in terms of the impact on the corresponding network of a technology.

Preprints (www.preprints.org) | NOT PEER-REVIEWED | Posted: 5 May 2022 doi:10.20944/preprints202205.0043.v1

$Symbol$	Description
NN_{tf}	Non-negotiable load of flexible technologies.
CC_{tf}	Charging (or discharging) capacity of a storage technology.
CT_{tf}	Charging time of a storage technology.
VU_{tf}	Hourly profile of the usage of a flexible vehicle (not connected to the grid).
AS_{tf}	Average speed of a flexible vehicle.

Variables

$Symbol$	Description
$u_{t,p}$	Use of a technology in a period
$i_{t,p}$	Investments in a technology in a period
$d^{pre}{}_{t,p}$	Premature decommissioning of a technology in a period
$r_{t^i,t^j,p}$	Retrofitting from one technology to another in a period
$s_{t,p}$	Stock (installed capacity) of a technology in a period
$d^{cum}{}_{t,p}$	Cumulative decommissioning of a technology in a period
$d^{lt}{}_{t,p}$	Decommissioning of a technology in a period due to lifetime expiry
$u_{h,td,p}$	Hourly use of a dispatchable technology in a period
$\Delta q^{up}{}_{h,tf,p}$	Increase in electricity demand from a flexible technology in an hour in a period
$\Delta q^{dw}{}_{h,tf,p}$	Decrease in electricity demand from a flexible technology in an hour in a period
$\Delta u_{h,tc,p}$	Deviation in use of a flexible CHP technology in an hour in a period
$\Delta p_{h,tc,p}$	Deviation in power output of a CHP technology in an hour in a period
$\Delta u_{h,ts,p}$	Decrease in use of a shedding technology in an hour in a period
$l_{h,tf,p}$	Losses from deviations in use of flexible technologies in an hour in a period
$\Delta q^{max}{}_{h,tf,p}$	Maximum increase limit of power demand of a flexible technology in an hour
$\Delta q^{min}{}_{h,tf,p}$	Maximum decrease limit of power demand of a flexible technology in an hour
$v^{max}{}_{h,tf,p}$	Upper saturation limit from shifted volume in an hour in a period
$v^{min}{}_{h,tf,p}$	Lower saturation limit from shifted volume in an hour in a period
$u_{d,td,p}$	Daily use of a dispatchable technology in a period
$\Delta q^{up}{}_{d,tg,p}$	Upwards deviation in use of a daily storage technology in a period
$\Delta q^{dw}{}_{d,tg,p}$	Downwards deviation in use of a daily storage technology in a period

Sectoral integrated cost-optimized energy system towards decarbonisation targets

As described in the IESA-NS conceptual framework, sectoral integration in IESA-NS turns around two main axes, activities and technologies (analogously to the commodities and processes nomenclature in TIMES). Thus, under a richly described technological landscape, there are many technology use combinations able to satisfy a desired volume of activities. From such a broad domain, the model simultaneously determines the optimal configuration

Preprints (www.preprints.org) | NOT PEER-REVIEWED | Posted: 5 May 2022 doi:10.20944/preprints202205.0043.v1

and use of technologies to satisfy the required activities' volumes. It does so by minimizing system costs resulting from the set of decision variables confirmed by use, investments, decommissioning, and retrofitting of technologies accordingly with the following expression.

$$\min \left[\sum_{t,p} u_{t,p} VC_{t,p} + i_{t,p} \alpha_t IC_{t,p} + d^{pre}{}_{t,p} DF_t \alpha_t IC_{t,p} + r_{t_i,t_j,p} \alpha_{t_j} RC_{t_i,t_j,p} + s_{t,p} FC_{t,p} \right] \qquad eq.(1)$$

Subject to ensure that the use of technologies meets at least the required exogenous activities drivers, as described by

$$\sum_{t} u_{t,p} AP_{t,a,p} \geq V_{a,p} \qquad eq.(2)$$

Also subject, as shown in (3), to the available installed capacities of the technologies and the particular activity-to-capacity ratio for each technology, Γ_t.

$$u_{t,p} \leq s_{t,p} \Gamma_t \qquad eq.(3)$$

Every single technology can affect one of the five accounts of emissions considered as activities: CCUS network, national ETS, national non-ETS, external ETS, and international transport emissions. Most technologies increase the net volume of the emitting activity and some technologies decrease it (such as carbon capture and direct air capture). To keep the emission activities balanced there are four 'technologies' who match their net account, which are named: CO2 released to air in the national ETS, national non-ETS, external ETS and international transport accounts. The emission constraint is therefore enforced by ensuring that the CO2 released to air in the national ETS and non-ETS accounts does not exceed the national targets of each node defined for the different periods as described by the following constraint:

$$\sum_{te} u_{te,p,n} \leq E_{p,n} \qquad eq.(4)$$

Nevertheless, it is important to mention that not all the sources of emissions considered within the scope of the targets are included within the activities that are covered by IESA-NS. To be precise roughly 85% of the emissions considered within the national inventories of NSR countries are covered by the activities included in the energy system framework, then for the remaining 15% (mostly agricultural activities), a less detailed approach is used. Here, the emissions resulting from activities such as enteric fermentation, manure management, use of fertilizers and use of refrigeration fluids are input to the model as driving activities, and their potential reductions and costs are addressed with MACC curves (extracted from the IMAGE model database).

Next to the previous formulation, other aspects must be included to better represent the feasible operation of the energy system. These aspects are an adequate multi-year transitional path representation, the hourly representation of the European power system dispatch, including the flexibility representation and technical limits in the operation of flexible demand and generation technologies, the consideration of gaseous networks

Preprints (www.preprints.org) | NOT PEER-REVIEWED | Posted: 5 May 2022 doi:10.20944/preprints202205.0043.v1

operation and the impact of available infrastructure in the intra-year operation of technologies.

Transition path

The transitional capability of the model derives from the fact that it can plan for the optimal system configuration for the different periods covered in the transition, at the same time that it determines the optimal intra-year operation of the stocks. The transitional elements are described by the investment, premature decommissioning, and retrofitting decisions that give shape to the technological stock accordingly with the following formulation:

$$s_{t,p} = s_{t,p-1} + i_{t,p} + r_{t^i,t,p} - r_{t,t^i,p} - (d^{cum}{}_{t,p} - d^{cum}{}_{t,p-1}) \qquad eq.(5)$$

being:

$$d^{cum}{}_{t,p} = d^{cum}{}_{t,p-1} + d^{pre}{}_{t,p} + d^{lt}{}_{t,p} \qquad eq.(6)$$

It is important to ensure that premature decommissioning can freely happen at any period if convenient, but to avoid that decommissioned technologies cannot be decommissioned in a year and recommissioned back in a subsequent period. Simultaneously, the model must be able to address the costs of premature decommissioning. For this purpose, the following constraint together with (5) and (6) ensure both requirements to be satisfied:

$$d^{cum}{}_{t,p} \geq d^{cum}{}_{t,p-1} \qquad eq.(7)$$

Also, as part of the scenario descriptions, some technologies are defined within a certain bandwidth of deployment. This same constraint, depicted in (8), is used to set the adoption potentials for technologies and to cap system emissions.

$$S^{min}{}_{t,p} \leq s_{t,p} \leq S^{max}{}_{t,p} \qquad eq.(8)$$

Lastly, the retrofitting of technologies is constrained by the available stocks of the original technology, and by an input binary parameter which determines which are the possible retrofitting relations. This results in the following formulation:

$$r_{t_i,t_j,p} \leq s_{t,p-1} RM_{t_i,t_j} \qquad eq.(9)$$

European hourly power sector dispatch

Modelling power dispatch within ESMs asks for choices to be made to avoid enormous computational requirements. To start with, the study [44] concluded that considering poor temporal resolutions negatively affects outcomes reliability for scenarios with moderate and high presence of VRES, and greatly recommend to prioritize using at least hourly resolution. Also, adopting a sequential description of the power dispatch enables to retain the chronological order in the variability of the events, which is key for short and long term storage technologies. Thus, IESA-NS adopted an hourly resolution of the complete year operation (8760 sequential points per year).

Furthermore, the same study [44] also mentions that operational detailing, namely unit commitment, increases reliability as the presence of VRES start to increase. However, it also states that adopting unit commitment loses relevance after a certain level of VRES penetration, as fewer thermal units affect the system dynamics. This observation is further reinforced by another study which states that MIP unit commitment performs better in

Preprints (www.preprints.org) | NOT PEER-REVIEWED | Posted: 5 May 2022 doi:10.20944/preprints202205.0043.v1

scenarios with low presence of VRES, but for scenarios with high levels of VRES an LP approach suffices to provide reliable results [45]. Also, there is plenty of evidence that increasing the geographical scope of the model to consider European cross-border interactions has a significant impact on the outcome reliability of the models [46]. Therefore, in this model we exclude the unit commitment formulation (MIP) and rather include the whole European power system represented in 20 nodes. This penalizes the ability of the model to reliably analyze low VRES scenarios with a high presence of thermal generators (as unit commitment is excluded), but keeping the convenient LP formulation enables IESA-NS to simultaneously solve the EU power dispatch and the integrated national energy system within the same formulation while considering a high temporal resolution and a moderate and high presence of VRES. Thanks to such modelling choice it is possible to analyze the interaction of storage, flexible demand technologies, VRES, and cross-border interconnection within the sector-coupled energy system of the Netherlands.

The following linear formulation is used to include the previously described concepts within the IESA-Opt framework. First, the fundamental constraint that supply and demand of electricity must remain balanced at every hour is included. For this purpose, we divide technologies into five main groups: dispatching technologies, t_d, technologies with flexible, t_{pf}, and non-flexible operation, t_{pn}, flexible CHPs, t_c, and shedders, t_s. For each of the 24 different electricity networks considered in the model, conforming the set A^e, the hourly balance is represented with the following constraint:

$$u_{h,td,p} AP_{td,a,p} = u_{t_p,p} P_{h,tp} AP_{tp,a,p} + (\Delta q^{up}{}_{h,tf,p} + \Delta q^{dw}{}_{h,tf,p}) AE_{tf,a} + (u_{tc,p} P_{h,tc} + \Delta u_{h,tc,p}) AP_{tc,a,p} + \Delta p_{h,tc,p} AE_{tc,a} + (u_{ts,p} P_{h,ts} + \Delta u_{h,ts,p}) AP_{ts,a,p} \quad \forall\, a \mid a \in A^e \qquad eq.(10)$$

This equation can be read as supply is equal to reference hourly demand, plus flexible demand variations ($\Delta q^{up}{}_{h,tf,p}$ and $\Delta q^{dw}{}_{h,tf,p}$), plus the bi-dimensional CHP flexibility variations ($\Delta u_{h,tc,p}$ and $\Delta p_{h,t_c,p}$), and plus the shedding demand variations ($\Delta u_{h,ts,p}$), for each interconnected node.

Another major determinant for the dispatch of electricity is resource availability, and this turns relevant for two reasons: the installed capacities of generation technologies and the intermittency of renewable energy sources. Every single technology in the model is described with an hourly operation $P_{h,t}$. For the dispatching technologies, this profile represents the hourly availability of the resource, and for the other technologies, it represents the hourly reference operation[13]. The following constraint ensures that supply occurs accordingly with

[13] The profiles are normalized and extracted from historical datasets such as the wind and solar availability in the NSR countries and the other 20 considered EU regions; the load profile of the NSR and EU regions; reference EV charging and connection profiles; temperature profiles; and a flat profile. Due to availability of data, so far only 84 hourly profiles have been included, but every technology is assigned to one of them, which means that many technologies share profiles. However, if more data becomes available the model is already enhanced to easily include it into the database, and would not result in increased computational times.

Preprints (www.preprints.org) | NOT PEER-REVIEWED | Posted: 5 May 2022 doi:10.20944/preprints202205.0043.v1

the existent installed capacity and to the extent at which the hourly resource availability allows it:

$$u_{h,td,p} \leq s_{td,p}\Gamma_{td}P_{h,td} \qquad eq.(11)$$

Also, ramping constraints are considered for dispatchable generation accordingly with the following constraint:

$$-R_{td,p}^{dw} \leq \left(u_{h,td,p} - u_{h-1,td,p}\right) \leq R_{td,p}^{up} \qquad eq.(12)$$

Lastly, the European representation, the dispatch architecture, the data on profiles and operational parameters are strongly based on the same modelling structure used as input by COMPETES model [47].

Hourly flexible operation in coupled sectors

Next to the power dispatch description, the representation of possible deviations from reference hourly operation profiles are paramount for the dispatch and to adequately represent sector coupling. With this aim, IESA-NS considers three different types of intra-year operational decisions: flexible CHPs, shedding technologies, and demand technologies with flexible operation.

Flexible CHPs

CHPs are modelled as operation technologies, which means that their hourly operation profile is fixed, and the changes in their use affect such profiles proportionally. However, some CHPs, known as extraction-condensing steam turbines, can extract a fraction of the condensed steam before (or during) the expansion phase (the power turbine) to be used to provide heat [48]. Such enhancement allows these turbines to adjust their power-to-heat ratio, which in combination with the amount of steam generated before the expansion, gives the technology a huge potential to modify its power and heat outputs and fuel inputs to adapt to electricity price events (among other externalities [49]. The resulting bi-dimensional flexibility (the fuel inputted into the boiler, and the extraction flow of the condensed steam) is considered by IESA-NS using a convenient LP simplification (resembling other ESMs [50]).

In a linear representation of a flexible CHP, the fuel requirement, F, is assumed to be determined by the heat and power outputs, H and P, accordingly with $F = {}^{H}/_{\eta} + {}^{P}/_{\varepsilon}$. Where η and ε represent the CHPs' efficiencies when producing only heat and power respectively. For this, IESA-NS considers two dimensions in which flexibility takes place: the hourly deviations in the fuel input representing the deviations in use, $\Delta u_{h,t_c,p}$; and the hourly deviations in the power output, $\Delta p_{h,t_c,p}$. This leads to the following constraint to ensure satisfying heat the heat demand provided by the CHP, in a specific time window:

$$\sum_{h \in TW_{tc}} \left[(u_{tc,p}P_{h,tc} + \Delta u_{h,tc,p})AP_{tc,a,p} - {}^{\eta_{tc}}/_{\varepsilon_{tc}}\Delta p_{h,tc,p}\right] = \sum_{h \in TW_{tc}} u_{tc,p}P_{h,tc}AP_{tc,a,p} \qquad eq.(13)$$

As the model distinguish from different temperature levels and different sectors, A^h represents the set of activities corresponding to the different heat forms that can be produced by the different CHPs in the model.

Preprints (www.preprints.org) | NOT PEER-REVIEWED | Posted: 5 May 2022 doi:10.20944/preprints202205.0043.v1

Shedding technologies

The upcoming energy transition will deliver a set of technologies that could provide sector coupling via the conversion of electricity into other energy forms (such as heat [51], hydrogen [52], methanol [53], methane [54], hydrocarbons [55], chlorine [56], ammonia [57], and other chemicals [58]) via the means of technologies such as heat pumps or electrolyzers. We use the word shedding to refer to the action taken by abovementioned technologies of cutting down operations in a critical hour to decrease electricity consumption and help to alleviate the system. This opens the door to foreseeable scenarios where these type of technologies could be interruptedly operated to avoid high electricity price events and decrease their operational costs [58]. However, extra capacity must be installed to be able to satisfy demand while sacrificing operational times [59]. Summarizing, shedding technologies in IESA-NS can selectively operate in specific hours in exchange for overinvestments.

The representation of these technologies in the model assumes they can shed their hourly activities by the means of an hourly decision variable which represents the decrease in use for each hour. This variable is capped by the installed capacity of the technology, as shown below:

$$\Delta u_{h,ts,p} \leq s_{ts,p} SC_{ts} UtP_{ts,p} \qquad eq.(14)$$

Because, as stated in (2), the model must ensure sufficiency in the activities balances, it will determine the required technological stock, determining in this way the necessary excess capacity to cope with such shedding.

Furthermore, technologies might not have a flat operational profile and might be subject to specific sectoral dynamics, or perhaps a certain technology may require a minimum level of operation. For these cases the following constraint is imposed:

$$\Delta u_{h,ts,p} \leq u_{ts,p} P_{h,ts} SF_{ts} \qquad eq.(15)$$

where SF_{t_s} represents the assumed potential shedding fraction of each shedding technology. And the profile is flat for technologies without specific sectoral dynamics.

Conservative flexibility

The last element presented here consists of the formulation used for technologies that allow for deviations in the reference profile without compromising the technology output and with or without paying an efficiency penalty. We call these options here as conservative flexibility, as all the up or down flexibility must be eventually recovered with an action in the opposite direction. Some examples of these technologies are some residential and services appliances such as dishwashers, washing machines, fridges or freezers [60][61]; electric heating appliances with active or passive storage [62][63][64]; electric vehicles with smart charging or vehicle-to-grid enhancements [65]; industrial processes with opportunities for flexible programming of their operations [60][66][67][68]; and all sort of different kind of batteries and storage technologies [69][70][71].

To be able to model such a vast group of technologies, they were grouped into 4 different archetypes[14]: load shifting for typical demand response and active thermal storage; smart

[14] There is a fifth archetype considered by the model: load recovery for passive or latent thermal storage [65][83]. However, as it plays no role in the results obtained in this scenario, it was excluded from this description.

Preprints (www.preprints.org) | NOT PEER-REVIEWED | Posted: 5 May 2022 doi:10.20944/preprints202205.0043.v1

charging of electric vehicles; vehicle-to-grid; and storage technologies. Each of these groups is represented under a specific formulation in the model and can be applied to all of the technologies considered under each category. However, all of the formulations share three elements in common: a balance constraint, a capacity constraint, and a saturation constraint, and each of the elements is interpreted differently for each archetype.

The energy balance states that the net energy demand should remain constant for the considered time window, and the use of time windows is adopted to maintain a linear formulation of the balance. This implies that the net balance of the upwards and downwards gross shifted load within the time window should be equal to the corresponding losses if any, as follows:

$$\sum_{h \in TW_{tf}} \Delta q^{up}{}_{h,tf,p} + \sum_{h \in TW_{tf}} \Delta q^{dw}{}_{h,tf,p} = \sum_{h \in TW_{tf}} l_{h,tf,p} \qquad eq.(16)$$

Both upward and downward shifts are subject to a physical capacity constraint determining the minimum and maximum boundaries of the feasible rescheduling capacity. For instance, this constraint in flexible heat-pumps sets the maximum available upward shift equal to the difference between reference profile and heat-pump's maximum capacity. These limits can be asymmetrical to each other and can be hourly variables. This second element is illustrated in the two following equations:

$$\Delta q^{up}{}_{h,tfp} \leq \Delta q^{max}{}_{h,tf,p} \qquad eq.(17)$$

$$\Delta q^{dw}{}_{h,tf,p} \geq \Delta q^{min}{}_{h,tf,p} \qquad eq.(18)$$

Finally, a saturation constraint ensures that the shifted volume does not violate a feasible operational limit, such as the storage capacity of an active storage unit or a latent heat requirement of a built environment system. These saturation limits can be either fix or represented by a combination of parameters and variables depending on the archetype involved, therefore the third type of constraints follow the below structure:

$$v^{min}{}_{h,tf,p} \leq \sum_{h \in TW_{tf}} \left[B^{up} \Delta q^{up}{}_{h,tf,p} + B^{dw} \Delta q^{dw}{}_{h,tf,p} \right] \leq v^{max}{}_{h,tf,p} \qquad eq.(19)$$

B^{up} and B^{dw} are two conceptual binary parameters used to illustrate that the saturation constraint can be imposed independently on both shift directions.

The interpretation of these three forms of constraints is presented below for all the 4 presented archetypes.

Demand Response

This form of flexibility assumes that the application of flexibility is capped by the installed capacity of the technology [72]. This directly affects the capacity constraint interpretation stating that the maximum upward deviation available is given by the difference between the installed capacity and the use of the technology determined by the hourly profile in the following way:

$$\Delta q^{up}{}_{h,tf,p} \leq (s_{tf,p} FC_{tf} - u_{tf,p} P_{h,tf}) AE_{tf,a} \qquad eq.(20)$$

Preprints (www.preprints.org) | NOT PEER-REVIEWED | Posted: 5 May 2022 doi:10.20944/preprints202205.0043.v1

and the maximum upward deviation is given by the ability of the technology to decrease it's reference hourly consumption given by

$$\Delta q^{dw}{}_{h,tf,p} \leq (1 - NN_{tf}) u_{tf,p} P_{h,tf} AE_{tf,a} \qquad eq.(21)$$

The volume constraint ensures that the reallocated energy consumption within a time window does not exceed the original total consumption of the time window, nor upwards nor downwards as shown below.

$$\sum_{h \in TW_{tf}} \Delta q_{h,tf,p} \leq \sum_{h \in TW_{tf}} u_{tf,p} P_{h,tf} AE_{tf,a} \qquad eq.(22)$$

Storage

The interpretation of the capacity constraint for storage is given by the (dis)charging capacity. The maximum amount of flexibility that any storage technology can provide is determined by the following constraint:

$$\Delta q_{h,tf,p} \leq s_{tf,p} CC_{tf} \qquad eq.(23)$$

The interpretation of the volume constraint for storage is marked by the storage capacity as described by the theoretical charging time of a battery accordingly with the following constraint.

$$\sum_{i \leq h} \Delta q_{i,tf,p} \leq s_{tf,p} CC_{tf} CT_{tf} \qquad eq.(24)$$

Smart Charging and Vehicle-to-Grid

The main characteristic of these forms of flexibility is that they are dependent on the number of vehicles connected to the grid in a given moment. Thus, the upward capacity is capped by the difference between the charging capacity of connected EV's and the reference charging profile as given by:

$$\Delta q^{up}{}_{h,tf,p} \leq CC_{tf} \left(s_{tf,p} - \frac{u_{tf,p} VU_{h,tf}}{AS_{tf}} \right) - u_{tf,p} P_{h,tf} AE_{tf,a} \qquad eq.(25)$$

While the downwards flexibility is constrained by the reference consumption and the non-negotiable load for smart charging:

$$\Delta q^{dw}{}_{h,tf,p} \leq (1 - NN_{tf}) u_{tf,p} P_{h,tf} AE_{tf,a} \qquad eq.(26)$$

And by the discharging capacity of connected vehicles for vehicle-to-grid flexibility:

$$\Delta q^{dw}{}_{h,tf,p} \leq DC_{tf} \left(s_{tf,p} - \frac{u_{tf,p} VU_{h,tf}}{AS_{tf}} \right) \qquad eq.(27)$$

The volume constraint for both Smart Charging and V-to-G is given similar to the storage, where the cumulative application of flexibility cannot exceed the difference between the available storage capacity of connected vehicles and the minimum required stored energy for the journeys of the vehicles departing in that hour given by:

$$\sum_{i \le h} \Delta q_{i,tf,p} \le CC_{tf} CT_{tf} \left(s_{tf,p} - \frac{u_{tf,p} VU_{h,tf}}{AS_{tf}} \right) - \sum_{h \le i \le h+AJ} u_{tf,p} P_{i,tf} AE_{tf,a} \qquad eq.(28)$$

Operation of gaseous networks

Integrated electricity and gas models usually focus on designing a proper nodal representation of the network based on pressure tolerances and Bernoulli equations, intending to provide detailed planning and operation optimization [73]. Because of the large scope of the problem and specific goals of the methodology, IEM often ignores any type of detailed description of the gas system. However, because we aim to address seasonality, buffer opportunities, and infrastructure costs, IESA-NS includes a simplified representation of gaseous networks operation based on a daily balance dispatch approach. This representation is presented below.

Gas networks, as transporters of a compressible fluid, are inherently provided with a buffer which allows for damping (i.e. the temporal discoordination between the input and output flows to the gas network) [74]. However, operation of the network must occur within safety pressure boundaries, meaning that the size of the buffer has limits (and regions), thus requiring intra-day balancing actions to keep networks functional[15]. There is no specific balancing period in this scheme. The imbalances are corrected when the magnitude of the imbalance reaches a certain predefined level [75].

A daily balancing approach was selected for activities distributed by the network of gaseous pipelines. This approach was selected first due to the previously described damping characteristic, and second, due to a typical daily flat price profile resulting from models with the hourly balancing of gas dispatch [76]. Such modelling choice allows for dispatching national wells and imports, considering the daily operation of the buffers (e.g., gas storage chambers), and describing other generation processes with particular sectoral dynamics such as fermentation, (bio)gasification, and methanation[16]. However, this representation cannot provide network planning or operation of circulating compressors. Finally, the same approach is used for all the gases transported in pipelines, namely, natural gas, hydrogen, and sequestered carbon dioxide for CCUS.

Similar to the electric balancing description, the gas dispatch is described for each day accordingly with:

$$u_{d,td,p} AP_{td,a,p} = u_{tp,p} P_{d,tp} AP_{tp,a,p} + (\Delta q^{up}{}_{d,tg,p} + \Delta q^{dw}{}_{d,tg,p}) AG_{tg,a} \qquad eq.(29)$$

Also, the daily dispatch technologies, analogously to the power dispatch, are bounded by their daily availability profiles and installed capacities accordingly with:

$$u_{d,td,p} \le s_{td,p} \Gamma_{td} P_{d,td} \qquad eq.(30)$$

Infrastructure description

[15] There are different types of balancing actions designed accordingly with the size of the imbalance. As reference of the magnitude, no balancing action is required for hourly imbalances of ~2% of the daily market volume. In average, 3 balancing actions per day were required between November 5th 2019 and December 4th 2019 (high demand season) [74].

[16] Methanation, as an electricity consumer, is already subject to hourly shedding constraints. Thus, the daily gas dispatch formulation further restricts its operation.

Preprints (www.preprints.org) | NOT PEER-REVIEWED | Posted: 5 May 2022 doi:10.20944/preprints202205.0043.v1

The infrastructure imposes a limitation to the system in terms of the extent an activity can be carried out within a certain time-frame and geographical area. This restriction provides an extra incentive for flexibility as it can avoid network reinforcement costs [73]. Furthermore, infrastructure descriptions help to provide a better representation of the expected transitional costs, as the energy system must adapt to enable the deployment of infrastructure intensive technologies, such as CCUS, hydrogen, and district heating.

The activities constrained by available infrastructure are described with daily and hourly timeframes. For the hourly ones, infrastructure limits the volumes of the activity in a time frame accordingly with:

$$(u_{t,p}P_{h,t} + \Delta u_{h,ts,p})AP_{t,a,p} + (\Delta q^{up}{}_{h,tf,p} + \Delta q^{dw}{}_{h,tf \mid tf \neq tf_b,p})AE_{tf,a} \leq s_{ti_h,p}\Gamma_{ti_h}$$
$$\forall\, a \mid a \in A^e \;\&\; \forall\, t \mid AP_{t,a,p} > 0 \qquad eq.(31)$$

Very similarly, the model considers the following constraint for the daily described infrastructure technologies, t_{i_d}:

$$(u_{tp,p}P_{d,tp} + \Delta u_{h,tc,p} + \Delta u_{h,ts,p})AP_{tp,a,p} + (\Delta q^{up}{}_{d,tf,p})AG_{tf,a} \leq s_{ti_d,p}\Gamma_{ti_d}$$
$$\forall\, a \mid a \in A^g \;\&\; \forall\, t \mid AP_{t,a,p} > 0 \qquad eq.(32)$$

Other elements of the energy infrastructure, such as transformers and buffers, are considered as operational technologies. Thus, both their investment and operational costs are determined as for any other operational technology within the model. Therefore, the formulation presented in this section only refers to infrastructure which exerts no action other than enabling the flow of an activity to a certain volume.

Appendix D: Reference scenario definition

In the reference scenario all the NSR countries must meet their net-zero GHG emission targets. Most of the data for the energy drivers and some cost assumptions are derived from the JRC POTEnCIA Central scenario for all the NSR countries. The POTEnCIA Central scenario assumes a business as usual economic development, with the European GDP growing accordingly to the '2018 Ageing report' (i.e. around 1.38% growth per year until 2050), a growth of population and households based on EUROSTAT data, and projections of industry based on the sectoral Gross Value Added (GVA) values. Therefore, the impact of different demographic projections in the future energy demand is not considered in the set of scenarios of this paper, as it does not fall within the scope of the paper. Future research should address this topic, as the impact in the modelling outcomes can be relevant. All the input data used for the reference scenario (i.e. drivers for energy demand, techno-economic parameters and commodity costs disaggregated per country) can be consulted in [27] together with the whole database of the model.

Figure 27 shows some relevant input data of the reference scenario aggregated for the whole NSR. All the industry production volumes (*Figure 27* top left) are increased during the period 2020-2050, except the ammonia production, which is assumed to remain constant. The production of non-metallic minerals increases by around 40%, the production of iron and steel increases by 10%, while the production of basic chemicals, paper related industry, non-ferrous metals and other industrial products is increased around 25%. Regarding electricity

Preprints (www.preprints.org) | NOT PEER-REVIEWED | Posted: 5 May 2022 doi:10.20944/preprints202205.0043.v1

demand[17] (Figure 27 top right) there is a steady growth in the residential and services sector (around 6% growth) and in the agriculture sector (roughly 21%). Regarding heat demand (*Figure 27* bottom left), the POTEnCIA central scenario assumes a 25% increase of the demand in the agriculture sector. In order to estimate the space heating demands for residential and services sector, a methodology is developed. The scenario assumes a steady growth of housing stock in the NSR, and a high increase of efficiency and better insulations from 2030, resulting in a slow increase of the heating demand from 2020-2035, and a decline from 2035 until 2050, where both heat demands are reduced around 3% compared to 2020 levels. The transport sector also increases its volume (*Figure 27* bottom right), with motorcycles and light-duty vehicles increasing around 70% their kilometres served, while trains, buses heavy-duty vehicles and passenger cars increase their volume between 10 and 30% in 2050.

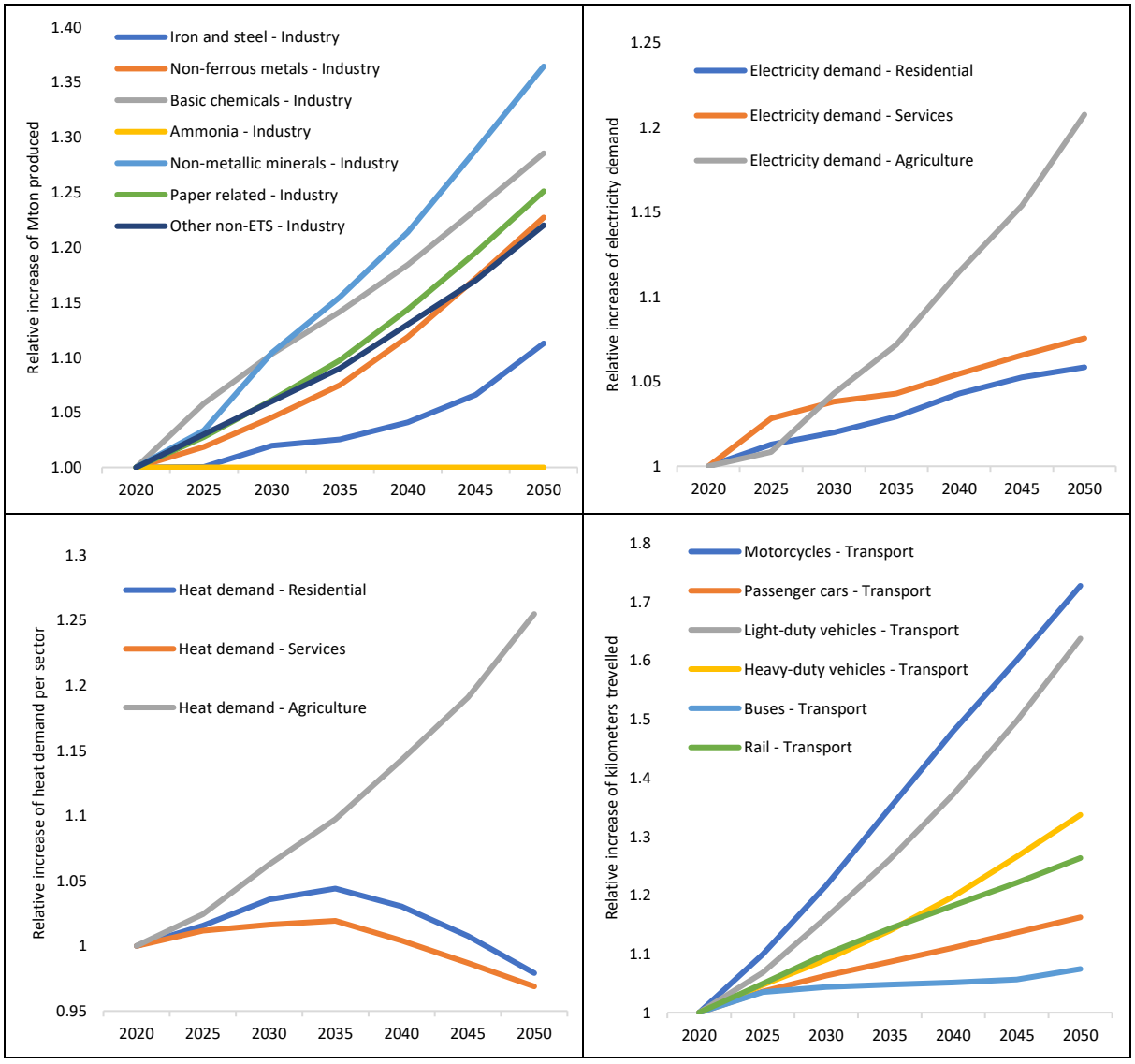

Figure 27: evolution of different input data compared to 2020 levels: industry production volumes (top left), electricity demand per sector (top right), heat demand per sector (bottom left), kilometres per type of transport (bottom right)

[17] Note that here electricity demand includes only appliances and electric devices of the residential, services and agriculture sector, i.e. end-uses that can only be satisfied by electricity. Electricity used for other end uses, e.g. space heating or industrial processes is not quantified here.

Preprints (www.preprints.org) | NOT PEER-REVIEWED | Posted: 5 May 2022 doi:10.20944/preprints202205.0043.v1

The input data related to fuel and commodity costs are based on multiple sources, mainly the POTEnCIA central scenario, the ENSPRESO database and different TNO factsheets. *Table 14* shows values of a selection of key parameters and their evolution during the transition 2020-2050. Note that some of the values are common to the whole NSR (e.g. coal or crude oil), while others are country dependent (e.g. biomass, in which each country has different biomass sources and therefore different costs). Additionally, extra costs of import/export of fuels are not considered in these figures (e.g. tariffs or infrastructure costs when importing natural gas from abroad).

Table 14: price projections of different commodities considered in IESA-NS

Commodity	**Units**	**Values**				**Source**
		2020	2030	2040	2050	
Coal	[€$_{2019}$/GJ]	3.0	3.7	4.1	4.4	[43][21]
Crude oil	[€$_{2019}$/GJ]	11.6	17.0	18.8	19.6	[43][21]
Natural gas	[€$_{2019}$/GJ]	6	8.74	9.64	10	[43][21]
Liquefied natural gas (LNG)	[€$_{2019}$/GJ]	7	8	8.5	9	[43][21]
Uranium	[€$_{2019}$/GJ]	0.8	0.8	0.8	0.8	[43][21]
Waste	[€$_{2019}$/GJ]	6.9	7.0	7.0	7.0	[43][21]
National biomass[18]	[€$_{2019}$/GJ]	6.9	6.6	6.2	5.7	[77]

The IESA-NS includes around 250 technologies per country, in order to provide multiple alternatives to supply the activity demands per sector. Each technology requires, among others, techno economic data (i.e. CAPEX, fixed and variable O&M costs and lifetimes), operation and flexibility profiles, and energy balances (i.e. energy inputs and outputs of each technology). The techno-economic data of selected technologies is shown in *Table 15*. Data related to additional technologies can be consulted in the database of the model.

Table 15: Techno-economic data of selected technologies

Technology	Investment cost, 2050	Fixed operational cost, 2050	Variable operational cost, 2050	Technical lifetime	Source
Fixed bottom offshore wind	2100	47	0.1	25	[20]
Floating wind	2760	47	0.1	25	[20]
Offshore electrolyser	10	0.3	0	20	[18]
Onshore wind	1100	17	0.4	20	[12]
Solar PV	280	2	0.1	20	[12]

[18] Average value of all the NSR countries. The disaggregated values per country can be found in the model database [27]

Preprints (www.preprints.org) | NOT PEER-REVIEWED | Posted: 5 May 2022 doi:10.20944/preprints202205.0043.v1

Regarding wind and solar PV energy, all the relevant technological data is extracted from the JRC technical report 'Cost development of low carbon energy technologies'. The scenario used is the 'ProRES', in which the world moves towards decarbonisation reducing fossil fuel use, renewables account for 93% of electricity demand, and as a consequence the learning process in renewable technologies is moderate. Regarding offshore interconnectors, it is assumed that HVDC becomes competitive beyond 100 km from shore, which is in line with most studies in the literature [78]. Therefore, offshore wind potential in areas beyond 100 km is allocated to the offshore nodes of the system, which are connected to shore via HVDC. The cost for the HVDC lines is calculated following the methodology of [79]. Offshore wind potential in areas up to 100 km are directly connected to shore via cheaper HVAC interconnectors.

Most of the remaining data is compiled from the ENSYSI model, and certain specific technologies are based on data from POTEnCIA, JRC and TNO factsheets. The input data of all the technologies included in the reference scenario can be consulted in [27].

The wind, solar and biomass potentials of the reference scenario are taken from the ENSPRESO reference scenario. Regarding onshore wind, the ENSPRESO scenario assumes that current legal requirements for exclusion zones and setback distances are respected. This results in a potential of 4710 GW from the EU, and 634 GW for the NSR, excluding Norway[19]. Regarding offshore wind, ENSPRESO assumes that current legal requirements for exclusion zones are maintained, offshore can only be installed in zones with a depth of 50 meters or lower, and the shipping density is assumed to be lower than 1000 ships per year. This results in 324.2 GW for the whole EU, and 239.4 GW for the NSR, excluding Norway. For solar PV, the ENSPRESO scenario selected assumes a density of 170 MW/km2, with a 3% of the non-artificial areas available for PV deployment. This results in a potential of 10127 GWe for the whole EU, and of 2213 GWe for the NSR, excluding Norway. Biomass potentials are also derived from the ENSPRESO medium scenario, which includes more than 30 different types of biomass feedstocks.

Regarding CO_2 storage, in the NSR there are multiple studies at national and multinational level assessing the total storage potential. For this reference scenario, we use the numbers from the EU GeoCapacity project, in which 66 GtCO2 storage availability are estimated using deep saline aquifers, hydrocarbon fields and coal fields in the NSR [80]. Other studies in the literature present more ambitious and optimistic potentials (e.g. [81] where 264 GtCO2 are estimated for the NSR). However, the conservative value is included in the reference scenario because: 1) there is not a clear common roadmap around CCUS in the NSR. 2) there are different political attitudes in the NSR countries (e.g. Sweden, Norway, UK and Netherlands have a negative view around onshore storage [81]). The yearly availability of CO2 storage is assumed to be 1% (i.e. 100 years of availability at maximum yearly injection rate) of the total storage capacity, in order to prevent that in 2050 the systems are heavily dependent on CCUS and the storage availability is scarce.

[19] The JRC POTEnCIA database excludes Norway. Therefore, in all the cases where Norway data is not available, we use the data from the well-known TIMES-NORWAY model [84].

Preprints (www.preprints.org) | NOT PEER-REVIEWED | Posted: 5 May 2022 doi:10.20944/preprints202205.0043.v1

Although the idea of the reference scenario is remain as unconstrained as possible, there are two exogenous constraints related that are imposed to the power generation sector. First, coal power generation is banned in all the NSR countries from 2030. Most NSR countries have policies and regulations in order to phase out coal generators from 2025 to 2030, and seems likely that these efforts will continue in the near future. Regarding nuclear generation, Germany and Belgium are not allowed to invest in additional capacity or to extend the lifetime of their operating plants, due to the fact that both countries have a clear political agenda in order to phase out nuclear power generators during the 2020 decade.

As mentioned in the methodological section, the IESA-NS model dispatches the power sector of the whole Europe with a hourly resolution, but the model does not optimize the capacity expansion or the capacity mix. For this scenario, the EU projections of European capacities from 2020-2050 are derived from the Ten Year Network Development Plan (TYNDP) from ENTSOE.

Appendix E: Techno-economic data of the NSOG infrastructure (power and hydrogen)

Geographic distances of the NSOG optimal configuration

Table 16 shows the distance between the clusters of the NSOG configuration used in the paper. The distance is calculated using the ArcGIS software, measuring the shortest distance between cluster centroids. Only distances between clusters that can be effectively connected as shown in *Figure 11* are presented, non-suitable interconnectors are not measured (e.g. 'n/a' in *Table 16*).

Table 16: distance (km) between the centroids in the NSOG configuration used in this paper

Distance (km)	Cluster 0	Cluster 1	Cluster 2	Cluster 3	Cluster 4	Cluster 5	Cluster 6	Cluster 7
Cluster 0	-	n/a	n/a	190	129	n/a	185	n/a
Cluster 1	xx	-	n/a	n/a	n/a	275	n/a	175
Cluster 2	xx	xx	-	178	n/a	144	193	n/a
Cluster 3	xx	xx	xx	-	n/a	n/a	127	n/a
Cluster 4	xx	xx	xx	xx	-	n/a	150	170
Cluster 5	xx	xx	xx	xx	xx	-	150	155
Cluster 6	xx	xx	xx	xx	xx	xx	-	141
Cluster 7	xx	xx	xx	xx	xx	xx	xx	-

Table 17 shows the distance between the onshore connection points and the clusters of the NSOG configuration used in this paper. Note that cluster 6, as per *Figure 11* is not connected directly to shore. The distance is calculated using the ArcGIS software, measuring the shortest distance between cluster centroids and their nearest onshore connection point.

Table 17: distance (km) between the onshore connection points and the centroids in the NSOG configuration used in this paper

Distance (km)	Netherlands	Germany	Great Britain	Denmark	Norway
Cluster 0	162	xx	212	xx	xx
Cluster 1	xx	xx	200	xx	425

Preprints (www.preprints.org) | NOT PEER-REVIEWED | Posted: 5 May 2022 doi:10.20944/preprints202205.0043.v1

Cluster 2	xx	xx	xx	122	200
Cluster 3	170	224	xx	xx	xx
Cluster 4	xx	xx	174	xx	xx
Cluster 5	xx	xx	xx	xx	229
Cluster 6	xx	xx	xx	xx	xx
Cluster 7	xx	xx	240	xx	xx

HVDC costs

HVDC costs in this paper are calculated based on the cost assumptions of [18], which estimates the CAPEX of hub-to-hub HVDC interconnectors to 1.1 €/MW/m; and the CAPEX of hub-to-shore HVDC interconnectors to 1.4 €/MW/m. Thus, costs of HVDC interconnectors in the NSOG architecture used in this paper are shown in *Table 18* and *Table 19*.

Table 18: CAPEX of hub-to-hub HVDC interconnectors

Cost (M€/GW)	Cluster 0	Cluster 1	Cluster 2	Cluster 3	Cluster 4	Cluster 5	Cluster 6	Cluster 7
Cluster 0	-	0	0	209	141.9	0	203.5	0
Cluster 1	xx	-	0	0	0	302.5	0	192.5
Cluster 2	xx	xx	-	195.8	0	158.4	212.3	0
Cluster 3	xx	xx	xx	-	0	0	139.7	0
Cluster 4	xx	xx	xx	xx	-	0	165	187
Cluster 5	xx	xx	xx	xx	xx	-	165	170.5
Cluster 6	xx	xx	xx	xx	xx	xx	-	155.1
Cluster 7	xx	xx	xx	xx	xx	xx	xx	-

Table 19: CAPEX of hub-to-shore HVDC interconnectors

Cost (M€/GW)	Netherlands	Germany	Great Britain	Denmark	Norway
Cluster 0	226.8	xx	296.8	xx	xx
Cluster 1	xx	xx	280	xx	595
Cluster 2	xx	xx	xx	170.8	280
Cluster 3	238	313.6	xx	xx	xx
Cluster 4	xx	xx	517.54	xx	xx
Cluster 5	xx	xx	xx	xx	320.6
Cluster 6	xx	xx	xx	xx	xx
Cluster 7	xx	xx	336	xx	xx

New hydrogen pipeline costs

Regarding new hydrogen pipelines, also in [18] their CAPEX is linearized to 0.4 €/MW/m. Thus, costs of hub-to-hub and hub-to-shore hydrogen pipelines are shown in *Table 20* and *Table 21*.

Table 20: CAPEX of hub-to-hub hydrogen pipelines

Cost (M€/GW)	Cluster 0	Cluster 1	Cluster 2	Cluster 3	Cluster 4	Cluster 5	Cluster 6	Cluster 7

Preprints (www.preprints.org) | NOT PEER-REVIEWED | Posted: 5 May 2022 doi:10.20944/preprints202205.0043.v1

Cluster 0	-	0	0	76	51.6	0	74	0
Cluster 1	xx	-	0	0	0	110	0	70
Cluster 2	xx	xx	-	71.2	0	57.6	77.2	0
Cluster 3	xx	xx	xx	-	0	0	50.8	0
Cluster 4	xx	xx	xx	xx	-	0	60	68
Cluster 5	xx	xx	xx	xx	xx	-	60	62
Cluster 6	xx	xx	xx	xx	xx	xx	-	56.4
Cluster 7	xx	xx	xx	xx	xx	xx	xx	-

Table 21: CAPEX of hub-to-shore hydrogen pipelines

Cost (M€/GW)	Netherlands	Germany	Great Britain	Denmark	Norway
Cluster 0	64.8	xx	84.8	xx	xx
Cluster 1	xx	xx	80	xx	170
Cluster 2	xx	xx	xx	48.8	80
Cluster 3	68	89.6	xx	xx	xx
Cluster 4	xx	xx	69.6	xx	xx
Cluster 5	xx	xx	xx	xx	91.6
Cluster 6	xx	xx	xx	xx	xx
Cluster 7	xx	xx	96	xx	xx

Retrofitted hydrogen pipelines

We identify existing natural gas pipelines in the North Sea, using the Global Fossil Infrastructure Tracker, developed by the Global Energy Monitor [29] and the ENTSOG natural gas maps [30]. Suitable candidate pipelines 1) were operative in 2021 and 2) cross any of the buffer areas of the offshore hub locations (i.e. *Figure 10*). The cost of a retrofitted pipeline, in line with recent literature (e.g. [82]) is set to a 10% of the cost of an equivalent new hydrogen pipeline. *Table 22* shows the natural gas pipelines that can be retrofitted to transport hydrogen. Each pipeline is ultimately connected to one country and one cluster. We assume an operating pressure of 80 bars in all cases. We assume an standard size of 30 inches for the pipelines with unavailable size data.

Table 22: candidate natural gas pipelines to be retrofitted, derived from [29]

Name	Connected country	Cluster	Diameter (inches)	Capacity (PJ/y)
Sean Gas Field–Bacton Pipeline	United Kingdom	0	30	160
Statpipe Gas pipeline	Norway	6	30	160
CATS	United Kingdom	7	36	250
Trent Field–Bacton Gas Pipeline	United Kingdom	0	24	130
Fulmar Field–St. Fergus Gas Pipeline	United Kingdom	1	20	80

Preprints (www.preprints.org) | NOT PEER-REVIEWED | Posted: 5 May 2022 doi:10.20944/preprints202205.0043.v1

Elgin and Franklin Gas Fields–Bacton Pipeline	United Kigdom	4	34	240
Murdoch Field–Theddlethorpe Gas Pipeline	United Kingdom	4	26	140
Baltic pipe	Denmark	2	n/a	160
Nogat	Netherlands	6	n/a	160
Tyra	Denmark	2	n/a	160
Norpipe	Germany	6	36	250
NGT	Netherlands	0	n/a	160

Table 23: Sean Gas Field-Bacton Pipeline (left) and Statpipe Gas pipeline (right), taken from [29]

Table 24: CATS pipeline (left) and Fulmar Field-St. Fergus Gas pipeline (right), taken from [29]

Preprints (www.preprints.org) | NOT PEER-REVIEWED | Posted: 5 May 2022 doi:10.20944/preprints202205.0043.v1

Table 25: Elgin and Franklin Gas Fields-Bacton pipeline (left) and Murdoch Field Gas pipeline (right), taken from [29]

Table 26: Baltic pipeline (left) and Nogat pipeline (right), taken from [29]

Table 27: Norpipe pipeline, taken from [29]

[1] Paris Agreement. United nations framework convention on climate change. Paris, Fr 2015. https://doi.org/10.1017/s0020782900004253.

[2] Federal Ministry for Environment Nature Conservation. Climate Action Plan 2050 - Principles and goals of the German government's climate policy. Germany 2016:92.

[3] Danish Energy Agency. Denmark's Climate and Energy Outlook 2020 2020:1–65.

[4] Ministry of the environment, Government offices of Sweden. Sweden's long-term strategy for reducing greenhouse gas emissions. Unfccc 2020.

[5] HM Government. The Ten Point Plan for a Green Industrial Revolution 2020:14–6.

[6] Gușatu LF, Menegon S, Depellegrin D, Zuidema C, Faaij A, Yamu C. Spatial and temporal analysis of cumulative environmental effects of offshore wind farms in the North Sea basin. Sci Rep 2021;11:10125. https://doi.org/10.1038/s41598-021-89537-1.

[7] Freeman K, Frost C, Hundleby G, Roberts A, Valpy B, Holttinen H, et al. Our Energy Our Future 2019:78.

[8] Ruijgrok PhD EC., van Druten MSc E., Bulder MSc B. Cost Evaluation of North Sea Offshore Wind Post 2030 2019.

[9] Gusatu LF, Yamu C, Zuidema C, Faaij A. A spatial analysis of the potentials for offshore wind farm locations in the North Sea region: Challenges and opportunities. ISPRS Int J Geo-Information 2020;9. https://doi.org/10.3390/ijgi9020096.

[10] Gorenstein Dedecca J, Hakvoort RA. A review of the North Seas offshore grid modeling: Current and future research. Renew Sustain Energy Rev 2016;60:129–43. https://doi.org/10.1016/j.rser.2016.01.112.

[11] Martínez-Gordón R, Morales-España G, Sijm J, Faaij APC. A review of the role of spatial resolution in energy systems modelling: Lessons learned and applicability to the North Sea region. Renew Sustain Energy Rev 2021;141. https://doi.org/10.1016/j.rser.2021.110857.

[12] Martínez-Gordón R, Sánchez-Diéguez M, Fattahi A, Morales-España G, Sijm J, Faaij AP. Modelling a highly decarbonised North Sea energy system in 2050: a multinational approach. Adv Appl Energy 2021:100080. https://doi.org/10.1016/J.ADAPEN.2021.100080.

[13] Singlitico A, Østergaard J, Chatzivasileiadis S. Onshore, offshore or in-turbine electrolysis? Techno-economic overview of alternative integration designs for green hydrogen production into Offshore Wind Power Hubs. Renew Sustain Energy Transit 2021;1:100005. https://doi.org/10.1016/j.rset.2021.100005.

[14] Jiang Y, Huang W, Yang G. ScienceDirect Electrolysis plant size optimization and benefit analysis of a far offshore wind-hydrogen system based on information gap decision theory and chance constraints programming. Int J Hydrogen Energy 2021. https://doi.org/10.1016/j.ijhydene.2021.11.211.

[15] Yan Y, Zhang H, Liao Q, Liang Y, Yan J. Roadmap to hybrid offshore system with

hydrogen and power co-generation. Energy Convers Manag 2021;247:114690. https://doi.org/10.1016/j.enconman.2021.114690.

[16] Wu Y, Liu F, Wu J, He J, Xu M, Zhou J. Barrier identification and analysis framework to the development of offshore wind-to-hydrogen projects. Energy 2022;239:122077. https://doi.org/10.1016/j.energy.2021.122077.

[17] Dinh VN, Leahy P, McKeogh E, Murphy J, Cummins V. Development of a viability assessment model for hydrogen production from dedicated offshore wind farms. Int J Hydrogen Energy 2021;46:24620–31. https://doi.org/10.1016/j.ijhydene.2020.04.232.

[18] Gea-Bermúdez J, Bramstoft R, Koivisto M, Kitzing L, Ramos A. Going offshore or not: Where to generate hydrogen in future integrated energy systems? 2021. https://doi.org/10.36227/techrxiv.14806647.v2.

[19] Ramirez Camargo L, Stoeglehner G. Spatiotemporal modelling for integrated spatial and energy planning. Energy Sustain Soc 2018;8:1–29. https://doi.org/10.1186/s13705-018-0174-z.

[20] Santhakumar S, Heuberger-Austin C, Meerman H, Faaij A. Technological learning potential of offshore wind technology and underlying cost drivers. 2022.

[21] Sánchez Diéguez M, Fattahi A, Sijm J, Morales España G, Faaij A. Modelling of decarbonisation transition in national integrated energy system with hourly operational resolution. Adv Appl Energy 2021;3:100043. https://doi.org/10.1016/j.adapen.2021.100043.

[22] Fattahi A, Sijm J, Van Den Broek M, Martinez Gordon R, Sanchez Dieguez M, Faaij A. Analyzing the techno-economic role of nuclear power in the transition to the net-zero energy system of the Netherlands using the IESA-Opt-N model 2022:1–38. https://doi.org/10.20944/preprints202204.0122.v1.

[23] Fattahi A, Sijm J, Faaij A. A systemic approach to analyze integrated energy system modeling tools: A review of national models. Renew Sustain Energy Rev 2020;133:110195. https://doi.org/10.1016/j.rser.2020.110195.

[24] Entso-e. Completing the map – Power system needs in 2030 and 2040 2021.

[25] Mantzos L, Wiesenthal T, Neuwahl F, Rózsai M. The POTEnCIA Central scenario: An EU energy outlook to 2050. EUR 29881 EN, Publ Off Eur Union, Luxemb 2019, ISBN 978-92-76-12010-0 n.d. https://doi.org/10.2760/78212.

[26] European Commission. The 2018 Ageing Report: economic and budgetary projections for the EU Member States (2016-2070). vol. 079. 2018. https://doi.org/10.2765/615631.

[27] IESA-Opt-NS model repository n.d. https://github.com/IESA-Opt/IESA-NS/.

[28] Emodnet n.d. https://www.emodnet-humanactivities.eu/view-data.php (accessed August 4, 2020).

[29] Global Energy Monitor n.d. https://globalenergymonitor.org/ (accessed February 16,

2022).

[30] ENTSOG. ENTSOG maps n.d. Karsten Braasch (accessed March 28, 2022).

[31] Caglayan DG, Weber N, Heinrichs HU, Linßen J, Robinius M, Kukla PA, et al. Technical potential of salt caverns for hydrogen storage in Europe. Int J Hydrogen Energy 2020;45:6793–805. https://doi.org/10.1016/j.ijhydene.2019.12.161.

[32] Gușatu LF, Menegon S, Depellegrin D, Zuidema C, Faaij A, Yamu C. Spatial and temporal analysis of cumulative environmental effects of offshore wind farms in the North Sea basin. Sci Rep 2021;11:1–18. https://doi.org/10.1038/s41598-021-89537-1.

[33] Fleischer CE. Minimising the effects of spatial scale reduction on power system models. Energy Strateg Rev 2020;32:100563. https://doi.org/10.1016/j.esr.2020.100563.

[34] Getman D, Lopez A, Mai T, Dyson M, Getman D, Lopez A, et al. Methodology for Clustering High-Resolution Spatiotemporal Solar Resource Data. Natl Renew Energy Lab(NREL), Golden, CO (United States) 2015.

[35] Horsch J, Brown T. The role of spatial scale in joint optimisations of generation and transmission for European highly renewable scenarios. Int Conf Eur Energy Mark EEM 2017:1–8. https://doi.org/10.1109/EEM.2017.7982024.

[36] Lloyd SP. Least Squares Quantization in PCM. IEEE Trans Inf Theory 1982;28:129–37. https://doi.org/10.1109/TIT.1982.1056489.

[37] Siala K, Mahfouz MY. Impact of the choice of regions on energy system models. Energy Strateg Rev 2019;25:75–85. https://doi.org/10.1016/j.esr.2019.100362.

[38] Arthur D, Vassilvitskii S. K-Means++: The Advantages of Careful Seeding. Proc Annu ACM-SIAM Symp Discret Algorithms n.d. https://doi.org/10.1145/1283383.1283494.

[39] python Clustering of Lines And RAsters: pyCLARA n.d. https://github.com/tum-ens/pyCLARA (accessed May 3, 2020).

[40] Bindiya M Varghese UAPJ. Spatial Clustering Algorithms - an Overview. Asian J Comput Sci Inf Technol 2013;3.

[41] Assunção RM, Neves MC, Câmara G, Da Costa Freitas C. Efficient regionalization techniques for socio-economic geographical units using minimum spanning trees. Int J Geogr Inf Sci 2006;20:797–811. https://doi.org/10.1080/13658810600665111.

[42] GeoDa gothub repository n.d.

[43] Fattahi A, Sánchez Diéguez M, Sijm J, Morales España G, Faaij A. Measuring accuracy and computational capacity trade-offs in an hourly integrated energy system model. Adv Appl Energy 2021;1:100009. https://doi.org/10.1016/j.adapen.2021.100009.

[44] Poncelet K, Delarue E, Six D, Duerinck J, D'haeseleer W. Impact of the level of temporal and operational detail in energy-system planning models. Appl Energy 2016;162:631–43. https://doi.org/10.1016/j.apenergy.2015.10.100.

[45] Cebulla F, Fichter T. Merit order or unit-commitment: How does thermal power plant

modeling affect storage demand in energy system models? Renew Energy 2017;105:117–32. https://doi.org/10.1016/j.renene.2016.12.043.

[46] Mertens T, Poncelet K, Duerinck J, Delarue E. Representing cross-border trade of electricity in long-term energy-system optimization models with a limited geographical scope. Appl Energy 2020;261:114376. https://doi.org/10.1016/j.apenergy.2019.114376.

[47] Özdemir Ö, Hobbs BF, van Hout M, Koutstaal PR. Capacity vs energy subsidies for promoting renewable investment: Benefits and costs for the EU power market. Energy Policy 2020;137. https://doi.org/10.1016/j.enpol.2019.111166.

[48] Wang J, You S, Zong Y, Cai H, Træholt C, Dong ZY. Investigation of real-time flexibility of combined heat and power plants in district heating applications. Appl Energy 2019;237:196–209. https://doi.org/10.1016/j.apenergy.2019.01.017.

[49] Romanchenko D, Odenberger M, Göransson L, Johnsson F. Impact of electricity price fluctuations on the operation of district heating systems: A case study of district heating in GÖteborg, Sweden. Appl Energy 2017;204:16–30. https://doi.org/10.1016/j.apenergy.2017.06.092.

[50] Brown T, Schlachtberger D, Kies A, Schramm S, Greiner M. Synergies of sector coupling and transmission reinforcement in a cost-optimised, highly renewable European energy system. Energy 2018;160:720–39. https://doi.org/10.1016/j.energy.2018.06.222.

[51] Bloess A, Schill WP, Zerrahn A. Power-to-heat for renewable energy integration: A review of technologies, modeling approaches, and flexibility potentials. Appl Energy 2018;212:1611–26. https://doi.org/10.1016/j.apenergy.2017.12.073.

[52] Glenk G, Reichelstein S. Economics of converting renewable power to hydrogen. Nat Energy 2019;4:216–22. https://doi.org/10.1038/s41560-019-0326-1.

[53] Andika R, Nandiyanto ABD, Putra ZA, Bilad MR, Kim Y, Yun CM, et al. Co-electrolysis for power-to-methanol applications. Renew Sustain Energy Rev 2018;95:227–41. https://doi.org/10.1016/j.rser.2018.07.030.

[54] Blanco H, Nijs W, Ruf J, Faaij A. Potential of Power-to-Methane in the EU energy transition to a low carbon system using cost optimization. Appl Energy 2018;232:323–40. https://doi.org/10.1016/j.apenergy.2018.08.027.

[55] Blanco H, Nijs W, Ruf J, Faaij A. Potential for hydrogen and Power-to-Liquid in a low-carbon EU energy system using cost optimization. Appl Energy 2018;232:617–39. https://doi.org/10.1016/j.apenergy.2018.09.216.

[56] Roh K, Brée LC, Perrey K, Bulan A, Mitsos A. Flexible operation of switchable chlor-alkali electrolysis for demand side management. Appl Energy 2019;255:113880. https://doi.org/10.1016/j.apenergy.2019.113880.

[57] Ikäheimo J, Kiviluoma J, Weiss R, Holttinen H. Power-to-ammonia in future North European 100 % renewable power and heat system. Int J Hydrogen Energy 2018;43:17295–308. https://doi.org/10.1016/j.ijhydene.2018.06.121.

[58] Schack D, Rihko-Struckmann L, Sundmacher K. Structure optimization of power-to-chemicals (P2C) networks by linear programming for the economic utilization of renewable surplus energy. vol. 38. Elsevier Masson SAS; 2016. https://doi.org/10.1016/B978-0-444-63428-3.50263-0.

[59] Roh K, Brée LC, Perrey K, Bulan A, Mitsos A. Optimal Oversizing and Operation of the Switchable Chlor-Alkali Electrolyzer for Demand Side Management. Comput Aided Chem Eng 2019;46:1771–6. https://doi.org/10.1016/B978-0-12-818634-3.50296-4.

[60] Lund PD, Lindgren J, Mikkola J, Salpakari J. Review of energy system flexibility measures to enable high levels of variable renewable electricity. Renew Sustain Energy Rev 2015;45:785–807. https://doi.org/10.1016/j.rser.2015.01.057.

[61] Staats MR, de Boer-Meulman PDM, van Sark WGJHM. Experimental determination of demand side management potential of wet appliances in the Netherlands. Sustain Energy, Grids Networks 2017;9:80–94. https://doi.org/10.1016/j.segan.2016.12.004.

[62] Lizana J, Friedrich D, Renaldi R, Chacartegui R. Energy flexible building through smart demand-side management and latent heat storage. Appl Energy 2018;230:471–85. https://doi.org/10.1016/j.apenergy.2018.08.065.

[63] Luo XJ, Fong KF. Development of integrated demand and supply side management strategy of multi-energy system for residential building application. Appl Energy 2019;242:570–87. https://doi.org/10.1016/j.apenergy.2019.03.149.

[64] Patteeuw D, Bruninx K, Arteconi A, Delarue E, D'haeseleer W, Helsen L. Integrated modeling of active demand response with electric heating systems coupled to thermal energy storage systems. Appl Energy 2015;151:306–19. https://doi.org/10.1016/j.apenergy.2015.04.014.

[65] van der Kam M, van Sark W. Smart charging of electric vehicles with photovoltaic power and vehicle-to-grid technology in a microgrid; a case study. Appl Energy 2015;152:20–30. https://doi.org/10.1016/j.apenergy.2015.04.092.

[66] Shoreh MH, Siano P, Shafie-khah M, Loia V, Catalão JPS. A survey of industrial applications of Demand Response. Electr Power Syst Res 2016;141:31–49. https://doi.org/10.1016/j.epsr.2016.07.008.

[67] Samad T, Kiliccote S. Smart grid technologies and applications for the industrial sector. Comput Chem Eng 2012;47:76–84. https://doi.org/10.1016/j.compchemeng.2012.07.006.

[68] Paulus M, Borggrefe F. The potential of demand-side management in energy-intensive industries for electricity markets in Germany. Appl Energy 2011;88:432–41. https://doi.org/10.1016/j.apenergy.2010.03.017.

[69] Aneke M, Wang M. Energy storage technologies and real life applications – A state of the art review. Appl Energy 2016;179:350–77. https://doi.org/10.1016/j.apenergy.2016.06.097.

[70] Zakeri B, Syri S. Electrical energy storage systems: A comparative life cycle cost analysis. Renew Sustain Energy Rev 2015;42:569–96. https://doi.org/10.1016/j.rser.2014.10.011.

[71] Wang G, Konstantinou G, Townsend CD, Pou J, Vazquez S, Demetriades GD, et al. A review of power electronics for grid connection of utility-scale battery energy storage systems. IEEE Trans Sustain Energy 2016;7:1778–90. https://doi.org/10.1109/TSTE.2016.2586941.

[72] Morales-España G, Martínez-Gordón R, Sijm J. Classifying and modelling demand response in power systems. Energy 2021:122544. https://doi.org/10.1016/j.energy.2021.122544.

[73] Klyapovskiy S, You S, Michiorri A, Kariniotakis G, Bindner HW. Incorporating flexibility options into distribution grid reinforcement planning: A techno-economic framework approach. Appl Energy 2019;254:113662. https://doi.org/10.1016/j.apenergy.2019.113662.

[74] Damping, Gasunie Transport Services 2021. https://www.gasunietransportservices.nl/en/shippers/balancing-regime/damping (accessed November 3, 2021).

[75] Balancing regime, Gasunie Transport Services, 2021 n.d. https://www.gasunietransportservices.nl/en/shippers/balancing-regime (accessed November 3, 2021).

[76] Zheng JH, Wu QH, Jing ZX. Coordinated scheduling strategy to optimize conflicting benefits for daily operation of integrated electricity and gas networks. Appl Energy 2017;192:370–81. https://doi.org/10.1016/j.apenergy.2016.08.146.

[77] Ruiz P, Nijs W, Tarvydas D, Sgobbi A, Zucker A, Pilli R, et al. ENSPRESO - an open, EU-28 wide, transparent and coherent database of wind, solar and biomass energy potentials. Energy Strateg Rev 2019;26:100379. https://doi.org/10.1016/j.esr.2019.100379.

[78] ACER. Electricity Infrastructure Unit Investment Cost Indicators. Acer 2015:1–17.

[79] Koivisto M, Gea-Bermudez J. NSON-DK energy system scenarios – Edition 2 Department of Wind Energy E Report 2018. 2018.

[80] Final P, Report A. Project no . SES6-518318 EU GeoCapacity Assessing European Capacity for Geological Storage of Carbon Dioxide 2008.

[81] IOGP, European Commission. The potential for CCS and CCU in Europe 2019:1–47.

[82] Mckenna R, Andrea MD, Garzón M. Advances in Applied Energy Analysing long-term opportunities for offshore energy system integration in the Danish North Sea. Adv Appl Energy 2021;4:100067. https://doi.org/10.1016/j.adapen.2021.100067.

[83] Gils HC. Assessment of the theoretical demand response potential in Europe. Energy 2014;67:1–18. https://doi.org/10.1016/j.energy.2014.02.019.

[84] Lind A. The Impact of Climate Change on the Renewable Energy Production in Norway - National and Regional Analyses The Impact of Climate Change on the Renewable Energy Production in Norway – National and Regional Analyses 2014.